Scale-up in twin-screw wet granulation

Inaugural-Dissertation

zur Erlangung des Doktorgrades
der Mathematisch-Naturwissenschaftlichen Fakultät
der Heinrich-Heine-Universität Düsseldorf

vorgelegt von

Marcel Franke

aus Wetzlar

Düsseldorf, Dezember 2023

aus dem Institut für Pharmazeutische Technologie und Biopharmazie
der Heinrich-Heine-Universität Düsseldorf

Gedruckt mit der Genehmigung der
Mathematisch-Naturwissenschaftlichen Fakultät der
Heinrich-Heine-Universität Düsseldorf

Berichterstatter:

1. Prof. Dr. Dr. h.c. Peter Kleinebudde

2. Prof. Dr. Jörg Breitkreutz

Tag der mündlichen Prüfung: 08.03.2024

Für meine Oma

(*27.11.1938 - † 03.12.2022)

List of publications and contributions

Parts of this thesis have already been published in a peer reviewed journal or presented at conferences.

Original manuscripts

Research Paper

Franke, M., Riedel, T., Meier, R., Schmidt, C., Kleinebudde, P., 2023. Comparison of scale-up strategies in twin-screw wet granulation. International Journal of Pharmaceutics, 641, 123052.

DOI: 10.1016/j.ijpharm.2023.123052

Personal contribution: 65 % - MF planned and performed all related trials. He completed most of the subsequent data analysis, wrote the main body of the manuscript independently, and illustrated all graphs and figures. He contributed to the idea and design of the project.

Franke, M., Riedel, T., Meier, R., Schmidt, C., Kleinebudde, P., 2023, Scale-up in Twin-screw wet granulation: Impact of formulation properties. Pharmaceutical Development and Technology, 28, 948-963.

DOI: 10.1080/10837450.2023.2276791

Personal contribution: 70 % - MF planned and performed all related trials. He completed most of the subsequent data analysis, wrote the main body of the manuscript independently, and illustrated all graphs and figures. He contributed to the idea and design of the project.

Conference contributions

Poster presentations

Franke, M., Riedel, T., Meier, R., Kleinebudde, P., *Measuring residence time distributions on a continuous twin screw wet granulation line,* DPhG Jahrestagung 2021, Online

Franke, M., Riedel, T., Meier, R., Schmidt, C., Kleinebudde, P., *Comparison of scale-up strategies for twin-screw granulation,* 13th PBP World Meeting, Rotterdam

Other contributions

Oral presentation during APV Taskforce "*Continuous Manufacturing"* meeting at Merck KGaA in Darmstadt, June 2023

List of abbreviations

API	Active pharmaceutical ingredient
BFD	Barrel fill density
CCS	Croscarmellose sodium
CE	Conveying elements
CM	Continuous manufacturing
CP	Center point
CS	Circumferential speed
CV	Coefficient of variation
DME	Distributive mixing element
DoE	Design of experiments
DT	Drying temperature
EMD	Earth Mover's Distance
FBU	Feeding & blending unit
FC	Fully continuous
ffc	Flow function coefficient
GSD	Granule size distribution
HSWG	High-shear wet granulation
ICH	International Council for Harmonisation of Technical Requirements for Pharmaceuticals for Human Use
KE	Kneading element
L/D	Length-to-diameter
LOD	Loss on drying
L/S	Liquid-to-solid
LFR	Liquid feed rate
MAN	Mannitol
MCC	Microcrystalline cellulose
MgSt	Magnesium stearate
MP	Manual processing
MRT	Mean residence time
PAT	Process analytical technology
PFR	Powder feed rate
Ph. Eur.	European Pharmacopeia
PVP	Polyvinylpyrrolidone

QbD	Quality by design
R	Reference run
RRMSE	Relative root mean square error
RTD	Residence time distribution
RTRT	Real time release testing
S1-3	Strategy 1-3
SD	Standard deviation
SS	Screw speed
t_{Max}	Time until highest color signal
TS(W)G	Twin-screw (wet) granulation
VFBD	Vibrating fluid bed drier
Vib. Acc.	Vibrational acceleration

Table of contents

1 Introduction

1.1 Drug development - from powder to tablet

There are numerous application routes and drug products to meet the specific requirements imposed by e.g., the active pharmaceutical ingredient (API). Things to consider during drug development are bioavailability, pharmacokinetics and -dynamics, and other factors, such as the site of action or the patients age and ability to swallow. However, solid oral dosage forms and especially tablets are still the preferred dosage form among patients, physicians, and manufacturers due to their ease of use by simple oral administration, relatively low production cost, ability to provide accurate dosing that fits the need for a variety of drugs and the usually long shelf-life. Tablets as a dosage form allow for individual and precise dosing of drug substances in a broad range of concentrations. Furthermore, by adding various excipients they can be designed to e.g., release the API only in the intestine or controlled over a duration of multiple hours to overcome different clinical challenges and increase patient compliance [1]–[3].

To gain access to the markets, pharmaceutical manufacturers must ensure patient safety and high product quality and thus meet many requirements and specifications imposed by various national and international organizations, pharmacopoeias, and regulatory authorities worldwide. These may include various criteria, such as the uniformity of mass and content, suitable disintegration and/or dissolution times depending on the intended release profile and dosing of the API, sufficient resistance to breaking and a low friability [4]. In most cases the available APIs cannot be compressed into tablets on their own due to the many challenges that arise from e.g., extremely low dosing or limitations in the processability caused by physicochemical properties, such as a poor flowability that prevents accurate dosing or a low tabletability of the API when no additional excipients are added. Many of these challenges can be overcome by adding various excipients e.g., glidants to increase the flowability of powders, disintegrants to achieve a shorter disintegration time, dry or liquid binders to increase the tensile strength of tablets, [5], [6] and adding different and oftentimes essential processing steps along the way, such as milling, blending, granulation, drying and coating [2], [3], [7], [8].

Based on the “Biopharmaceutics Classification System” [9], which is widely used as a framework to predict the *in vivo* performance of drugs, Leane et al. [10] have suggested an initial “Manufacturing Classification System” to create a guide for risk assessment for different manufacturing routes of oral solid dosage forms based on the API properties. They differentiate between three classical manufacturing routes (direct compression, dry granulation and wet granulation) and one additional category for other technologies to account for more specific challenges of an API, such as low bioavailability, extremely high potency, quick degradation or moisture sensitivity of a high drug-load API that was not suitable for direct compression or dry granulation.

Each of the three classical manufacturing routes comes with its own challenges and benefits:

1. Direct compression is usually the fastest and least complex manufacturing route as the process involves only blending and compression processes. While this makes direct compression economically desirable, it also comes with the highest requirements regarding material attributes of API and excipients. Especially in early development the batch-to-batch variability of the API can oftentimes be high, which increases the potential risk of this manufacturing route [11], [12].
2. Dry granulation can be used as an additional processing step especially for APIs that are sensitive to moisture or heat and thus cannot be used in wet granulation processes. It is performed to improve the handling during compression by e.g., improving powder flowability and increasing particle size. However, this has oftentimes been observed to come with the cost of a decreased tabletability of the resulting powder after roll compaction especially when high compaction pressures were applied during roll compaction [13], [14].
3. Wet granulation is still a widely used technique in drug manufacturing as it improves both flow and compression properties and helps facilitate uniform distribution of the API within the granules, which leads to a good content uniformity. High-shear wet granulation and fluid bed granulation are still the most used techniques in traditional manufacturing even though over the last decades twin-screw wet granulation (TSWG) has gained increasing attention as an alternative technology with the potential to be fully continuous [15]–[17].

The “Manufacturing Classification System” suggests various parameters including physical and mechanical properties (e.g., particle size distributions, powder flow and compressibility) of the powder blend, but also moisture and heat sensitivity to evaluate which of these manufacturing routes is most suitable to produce tablets for a selected API to fulfill the high quality standards in this industry and enable a robust process at production scale.

1.2 Batch manufacturing – the traditional route

Whereas some of these processes, such as roll compaction or tableting are inherently continuous with a constant in- and outflow of material that is being processed, many other processes are still traditionally performed batch-wise, meaning starting materials are introduced at the beginning of the process and then kept within the process until the (intermediate) product is collected afterwards [18].

Despite fast implementation of (fully) continuous processes in other industries (e.g., bulk chemicals or food), batch-processing and manufacturing has long been the prevailing established operating procedure in the production of solid oral dosage forms [19], [20]. For complex manufacturing processes with multiple processing steps involved (blending, granulation, drying, milling, blending, tableting etc.) this results in long development and production times for a batch as the next processing step can only be initiated after the previous one is finished. Furthermore, as the decision of whether to release or reject a final product is highly dependent on the analysis of critical quality attributes (CQAs) that have to meet the pre-defined specifications and quality standards this can lead to the rejection and consecutively destruction of whole batches that were previously produced over days or even weeks. Furthermore, oftentimes additional testing of the intermediary products between processes have to be performed due to potential batch-to-batch variabilities and the additional need to store those intermediary products at varying storage conditions and timeframes.

However, over the last decades many new technologies and regulatory guidelines emerged that made a transition from batch-manufacturing to fully continuous production lines much more attractive even in such highly regulated environment as the pharmaceutical industry.

1.3 Continuous manufacturing (CM) – challenges and benefits

The desire for transition to CM and the advantages it offers is caused by multiple factors, such as economic considerations, potentially improved quality as well as continuous progress both on the regulatory and the technological side [18], [21]. Therefore, this chapter serves the purpose of giving a short introduction to some of the economic, technological and regulatory advancements made over the last two decades, benefits that arose from implementing CM-lines and novel challenges that had to be faced and overcome.

One of the main factors to drive change among all industries is the desire to save resources by reducing cost and time. At first the transition to CM requires a high initial investment in both time and monetary resources in order to build new lines and train the operators on these novel technologies. However, on the other hand CM offers much more flexible batch sizes and the potential to drastically reduce cost and development times in drug product development. Fully continuous lines usually require significantly less space due to the direct connection between the processing steps. Furthermore, they enable much more flexible batch sizes, which can be adjusted by the runtime of a continuous process instead of operating each process in isolation with a fixed batch size and then storing the intermediary product somewhere or even shipping it to a different site for further processing. This flexible approach, scaled by runtime, also comes with the advantage that lower amounts of API, which can be extremely costly in early-stage development, are required to gain a good process understanding and investigate the effect of more changes in process parameters in a shorter period of time. Furthermore, condensing many previously isolated batch-processes to a CM line comes with significant savings in development and production times. This offers a reduced time to market and thus enables a more flexible and demand-driven approach to the production of drug products. Additionally fewer trained operators are required to perform all the necessary processes and supervise the machines involved on a CM-line compared to performing every step batch-wise in isolation. The potential for cost-reduction by switching from batch-manufacturing to CM has been a trending subject among industry and academia over the last two decades [22]–[26].

Despite a high interest in implementing CM in the pharmaceutical industry, many open questions regarding the strict regulatory frameworks all over the world have to be answered in order to mitigate the risk of being shut down by authorities after implementing these novel technologies. The implementation of guidelines that encouraged a risk-based approach based on “Quality by Design” (QbD) principles [27] by the International Council for Harmonisation of Technical Requirements for Pharmaceuticals for Human Use (ICH), representing regulatory bodies in Europe, the US and Japan, could be considered one of the first major milestones, as it acknowledged that quality cannot be enforced by additional testing but it must be built into the product. Over the years the guidelines ICH Q8 (R2) (Pharmaceutical development), ICH Q9 (Quality Risk Management), ICH Q10 (Pharmaceutical Quality Systems) and ICH Q11 (Development and Manufacture of Drug Substance) have been published and offer guidance on the implementation of QbD in the pharmaceutical industry [28]–[31]. In 2012 the US FDA published their “Perspective on Continuous Manufacturing” [32], which was followed two years later by their Keynote on “Modernizing Pharmaceutical Manufacturing – Continuous Manufacturing as a Key Enabler” [33]. This emphasizes the increased interest from regulatory bodies to push CM in the pharmaceutical industry as the potential for increased quality and fewer defects was acknowledged [34]. Several working groups among regulatory agencies from Europe, the US and Japan have been established as correspondents for pharmaceutical manufacturers interested in applying emerging technologies [35]. While this can be considered as a starting point for the implementation of more advanced control strategies and an overall more science-based approach, many questions in regard to the correct implementation of CM, such as the definition of a batch, the application of sampling or control strategies in CM and the criteria to assess how (much) product should be rejected when the specifications are not met are still not fully answered [36]. These questions have been addressed in more detail only recently (2023) in the ICH Q13 guidelines (Continuous Manufacturing of Drug Substances and Drug Products) [37] where a clear guidance regarding the batch definition in CM was given and defined by “one of the following:

- Quantity of output material
- Quantitiy of input material
- Run time at a defined mass flow rate”

Furthermore, they wrote that “other approaches to define batch size are possible, if scientifically justified based on the characteristics of the CM process and Good Manufacturing Practice. A batch size can also be defined as a range. For example, a batch size range can be established by defining a minimum and maximum run time.”, which leaves some leeway for different approaches.

Starting with Orkambi® in 2015, several continuously manufactured solid oral dosage form products by Vertex, Johnson & Johnson, Pfizer and Eli Lilly have been approved by multiple regulatory authorities in different global regions [21]. However, considering the strong push for CM by regulators and the expected benefits, the overall adoption into the industry is still relatively low as these advantages are tempered by the high initial monetary investment but also more importantly by the necessary advances in knowledge and experience regarding these novel technologies, which require time and effort [38].

In that regard many technological and scientific advances have been made within the same time-period, but there are also still many open questions and challenges that have to be overcome until CM might be used on a broad scale:

To be able to implement feasible control strategies and to advance the process understanding from powder to tablet, many novel technologies and applications for existing technologies to e.g., monitor the moisture content, blend quality, content uniformity, particle size distribution or residence time distributions (RTD) in line, have emerged as part of various process analytical technologies (PAT) [21], [39]–[46]. Even though developing and implementing these methods oftentimes requires a significant amount of time and resources, they are a major step towards building the necessary foundation for QbD and a thorough process understanding, and take further steps towards real time release testing (RTRT) as a major milestone in reducing time to market of a finalized batch. To achieve RTRT, pharmaceutical manufacturers need to provide convincing documentation and justification of all the tools, models, data collection and processing steps that are used to predict or monitor the CQAs of the final product [47].

PAT tools for CM that have been used and further developed for different purposes include probes utilizing high-speed cameras or spatial filtering to determine the size

distribution of powders and granules, NIR and Raman spectroscopy for the prediction of various granule and tablet properties, such as content uniformity or residual moisture, and more recently terahertz time-domain spectroscopy to determine the porosity of tablets non-destructively [21], [40], [48]–[51]. However, implementing feasible control strategies based on PAT can be challenging as a representative and continuous sample presentation needs to be ensured and predictive models can usually not simply be applied to new processes or formulations but oftentimes require new relevant experimental data to be collected. Another obstacle in the implementation of feasible control strategies can be building and maintaining the infrastructure to store and monitor the large datasets collected from monitoring and determining in- and output parameters during CM and to then build, apply and validate feasible models and control strategies in a GMP environment. While some of these challenges would have been difficult or even impossible to overcome even a decade ago, the continuous exponential growth of computational resources has greatly augmented the capabilities for prediction and data collection.

Over the same time period, advances in upstream processes such as drug substance development based on e.g., crystal engineering were made, novel co-processed excipients for direct compression to mitigate insufficient processability of APIs were introduced, new concepts for continuous granulation and drying, such as twin-screw dry granulation, continuous fluid-bed drying or in-barrel drying were developed and multiple fully continuous manufacturing lines were supplied from different vendors, such as GEA Pharma systems, L.B. Bohle, or Glatt [21], [52]–[58]. However, which of the many technologies and manufacturing routes for continuous manufacturing work best when facing the challenges of drug product development especially in the early phase is still subject to further investigation and an open discussion among industry peers and academia and various systems are being evaluated and implemented at different companies and manufacturing sites in the pharmaceutical industry. As the aim of this work lies in the scale-up and process transfer of a continuous twin screw wet granulation and consecutive continuous drying process, this will be the focus of the following chapter.

1.4 Twin-screw wet granulation

1.4.1 General

Twin-screw extrusion as a concept dates back to a basic patent by Meskat and Erdmenger that was granted in 1953 and consequently emerged in the chemical industry first, followed by other industries, such as the food, rubber and more recently the pharmaceutical industry. The basic concept is relatively simple: Material is fed onto a cylindrical barrel and then transported by co- or counter-rotation of two embedded intermeshing screws. Among different industries and use-cases there are several ways to adapt the process e.g., by changes in the screw-design and configuration, the addition of different barrel zones for heating and cooling, adding a die plate at the end of the barrel during extrusion, or by implementing an additional liquid port that can be used for wet granulation.

Readers interested in a detailed history of twin-screw extruders, different design parameters and other use-cases than wet granulation in the pharmaceutical industry are referred to a detailed book on co-rotating twin-screw extruders by Klemens Kohlgrüber [59].

In the pharmaceutical industry, the first experiments on a twin-screw extruder were performed by Lindberg et al. [60], who performed a set of experiments for effervescent granulation. However, the concept of twin-screw wet granulation (TSWG) has only gained increased attention after 15 more years when it was applied by Schroeder and Steffens in 2002 [61] followed by Keleb et al., who were the first to introduce changes to the screw configuration and evaluate their effect on the granule properties in 2004 [17]. Since then, TSWG has witnessed significant contributions from various authors and working groups that greatly enhanced our understanding of the underlying process parameters, led to the implementation of various pilot projects within the pharmaceutical industry and the application of novel drying concepts that could seamlessly integrate with the constant discharge of wet granules.

1.4.2 Process overview

An overview of a typical twin-screw granulation module for TSWG in the pharmaceutical industry is depicted in Figure 1.

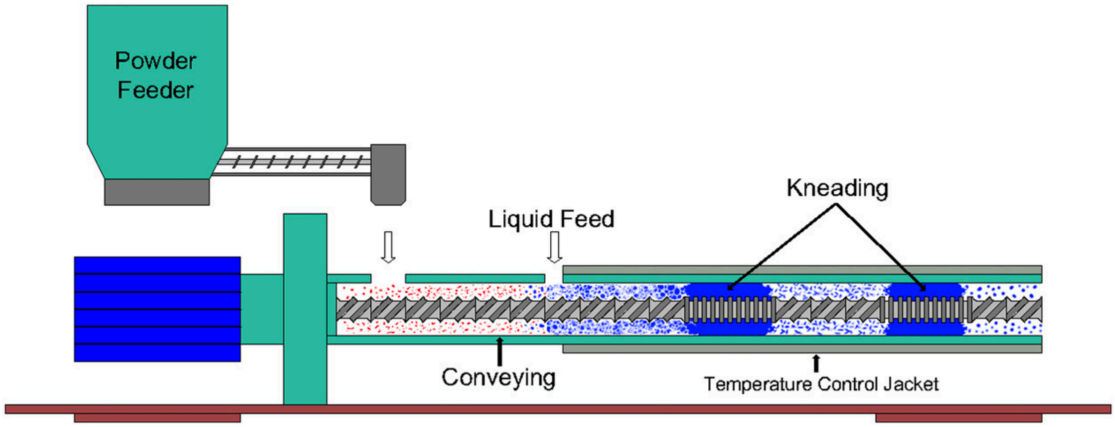

Figure 1 Components of a typical twin-screw granulation module as published by Seem et al. [62] - used with permission of Powder Technology, Elsevier.

1.4.2.1 Powder feeder

Most commonly a powder blend, which was either pre-mixed batch-wise in a container or fully continuously in an automated process step, is continuously fed into the continuous granulator by a loss-in-weight feeder. Many studies were conducted on this first processing step, which is sensitive to physicochemical properties of the initial powder blend (such as flowability) and thus needs to be adapted to e.g., the flow properties of the different powder blends, to ensure a constant and robust powder flow at all times [63]–[67]. Furthermore, to build a foundation for feasible control strategies and divert powder or granules during continuous production in general, the occurrence of potential segregation effects, which are occasionally described in batch-manufacturing, and the RTD for different powder blends during this processing step have been thoroughly examined [68]–[72]. Additionally, the effects of the powder feed rate (PFR) on other process parameters, such as the fill level and the RTD, and on CQAs of the manufactured granules and tablets have been investigated in various studies [73]–[76].

1.4.2.2 Granulator

The granulator into which the powder is fed, usually consists of modular co-rotating twin-screws, one or multiple ports for liquid addition, and a temperature control jacket. The temperature control jacket ensures constant process temperature by either cooling down the barrel and thus removing the heat that is constantly generated during the running process, or by heating the barrel either for in-barrel drying or as a means of process control based on e.g., changing binder solubility (Figure 1).

The modularity of the twin-screws can be a great advantage in early development for different drug products as it adds the ability to further control process variables, such as the shear stress (e.g., by adding kneading elements) or the transportation speed along the granulator. At the same time, it is a parameter, which cannot be changed or adapted during the running process and adds a high level of complexity that can impact how other process parameters (such as the PFR) affect the final or intermediary products. Most commonly used in TSWG are conveying elements (CEs), kneading elements (KEs) and distributive mixing elements (DMEs), which are also known as comb mixing elements (Figure 2).

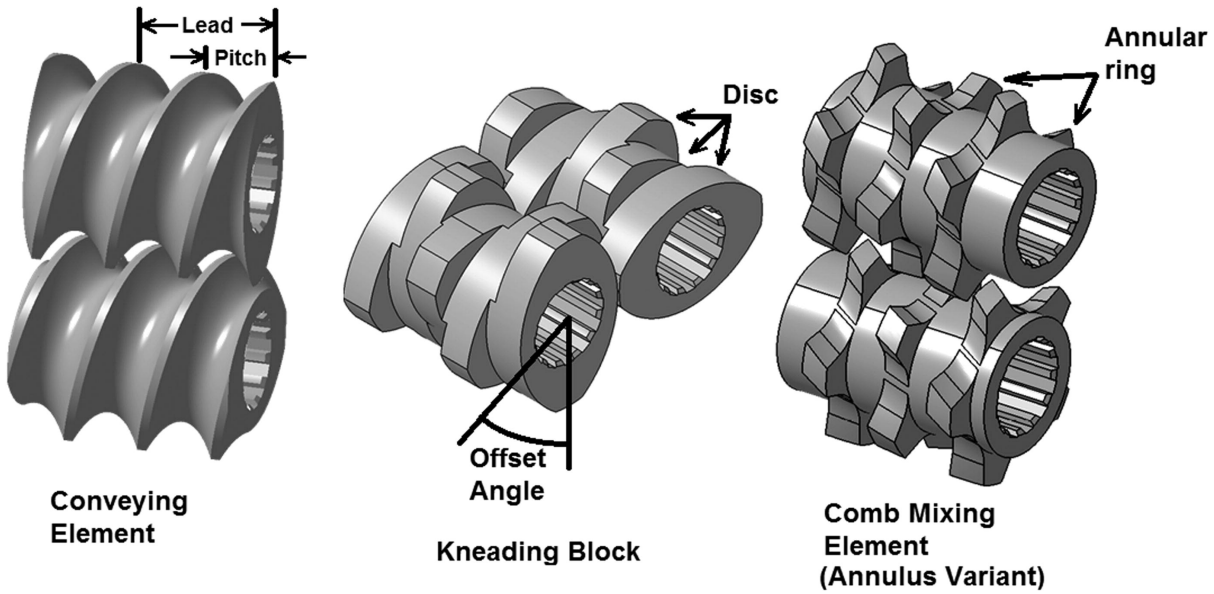

Figure 2 as published in [77] (© 2015): Drawings of the three common screw elements used in twin-screw granulators in their side-by-side arrangement, showing a conveying element, kneading block and comb mixing element - reprinted by permission of Informa UK Limited, trading as Taylor & Taylor & Francis Group, http://www.tandfonline.com

Previous studies have shown that successful granulations and even a process scale-up could be performed using only CEs *[78]–[80]*, which generally possess the highest transport capacity but only apply low shear forces. Usually, additional KEs are embedded to increase granule density and reduce the amount of fines through these more shear-intensive zones *[78], [81]–[85]*, while DMEs were found to promote the occurrence of breakage and layering of granules during TSWG and were proposed as an option to remove the necessity of an additional milling step [86]. However, geometrical differences of the screws (such as the length-to-diameter-ratio (L/D-ratio), the pitch of CEs or the offset angles of the kneading discs in KEs) due to a lack of standardization are common among different manufacturers and have led to additional challenges in the process transfer from one device or scale to another [76], [87].

The impact of a varying number of kneading discs and different staggering angles on the RTD of granules during TSWG was also shown in a comprehensive study by Kumar et al. [88]. They showed an increase of the residence time of granules for kneading blocks consisting of 6 or more kneading discs, with increasing staggering angle and an increased material holdup that led to a higher torque. Furthermore, they observed a high decrease in mean residence time (MRT) with increased screw speed (SS), followed in effect strength by combinatorial effects of throughput and SS. Lastly they observed a significant reduction of the MRT by the throughput on its own at high overall channel fill levels or when the flow was constrained by a high staggering angle or a high number of kneading disks. As a result, they introduced the concept of a throughput force to describe the interplay of material throughput, screw speed, channel fill and restrictive forces. In a later study by Liu et al. [89] similar results regarding SS and PFR were found, and additionally they showed that the observed MRT increased substantially with increasing L/S-ratio (liquid to solid-ratio) and attributed it to a retardation of material flow at higher liquid contents. Due to the continuous nature of TSWG and the relatively high screw speeds in the range of 100+ rpm, the observed granule MRTs in general were relatively short (< 30s), which requires a sufficient distribution of the added liquid in a short period of time to promote the formation of granules but also leads to a high adaptability of the process and the option for quick-reacting control strategies without introducing too much delay [75], [88]–[90].

On the topic of liquid distribution, granule growth and homogeneity, several studies have been performed to investigate the effect of various input parameters related to the granulation liquid or the liquid addition method, such as the binder concentration,

properties and addition method, and the L/S-ratio, pump or nozzle diameter [79], [91]–[95]. Dhenge et al. examined the steps in granule growth at different positions of the twin-screw granulator and investigated the effect of different elements along the screws and various binder concentrations, types and viscosities on granule formation and growth [79], [93], [96]. The granule size increased with increasing L/S-ratio, in the kneading zones, and with increased amounts of binder. Vercruysse et al. [88] compared granulation runs using different nozzle sizes, pump types, L/S-ratios and numbers of liquid addition zones. The quality of liquid distribution was mainly impacted by the amount of liquid added and the number of kneading zones. The oftentimes described bimodal granule size distribution (GSD) persisted even when moisture uniformity was achieved. Obviously, this could not be caused by an insufficient mixing of powder and liquid during the short residence times observed in TSWG. Vandevivere et al. [94], [95] investigated different methods of binder addition (as a dry ingredient in the blend or dissolved in the granulation liquid) and compared the necessary L/S-ratio to create feasible granules using a highly and a poorly soluble model excipient. They showed that adding a dry binder led to a comparable or sometimes even higher granule quality, and that the poorly soluble model excipient required a significantly higher L/S-ratio to form similar granules.

The barrel temperature is another highly relevant process parameter during TSWG: A temperature control jacked for the barrel ensures that the excess frictional heat constantly generated by the continuous screw rotation and granule transportation does not affect the granulation process over time. Furthermore, it can be used to adjust the granulation temperature e.g., to increase the solubility of the binder and thus produce larger granules. Various research groups demonstrated the influence of barrel temperature on different granule properties after TSWG and showed that depending on the solubility (and its temperature-dependance) of the binder but also the ingredients in the blend, a change in temperature may affect the granule size distribution, granule shape and density more or less strongly [74], [97]–[99]. To illustrate this further, Vanhoorne et al. [98] showed that in a lactose/starch-mix with HPMC as a binder an increase in barrel temperature led to an increase in granule size while this effect was inversed when the starch was removed and only lactose was used as a filler at a slightly lower L/S-ratio (0.1 versus 0.08). Some more recent studies

showed that during TSWG drying can potentially be achieved inside the barrel, which would reduce the need for any subsequent drying process [57], [100], [101]. However, even when an additional vacuum was applied to improve the efficiency of the drying process, very high temperatures of 100°C or more were necessary to achieve a somewhat sufficient drying capacity during the very short residence time in the granulator, which introduces additional stress and risk for degradation or interactions of thermo-sensitive formulations. Furthermore, as the surface area and the residence time inside the granulator usually don't scale proportionally to the throughput in commercial devices, it is questionable how well a scale-up of this technology could be performed.

1.4.3 Continuous vibrating fluid bed drying

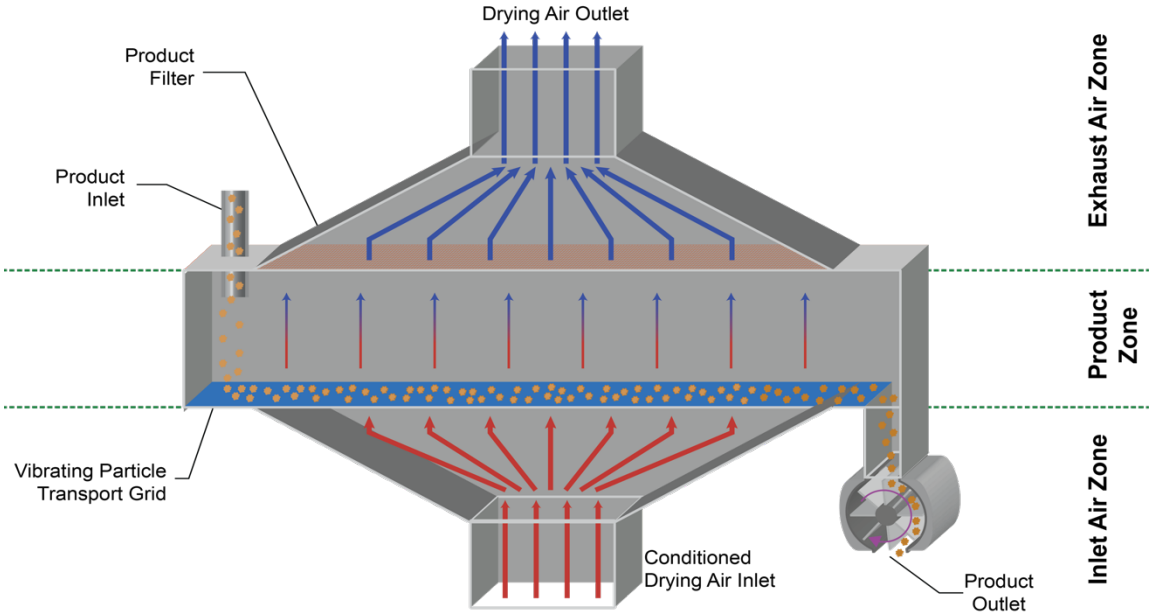

Figure 3 Schematic depiction of the continuous fluid bed dryer of the QbCon© used by courtesy of L.B. Bohle

In contrast to the segmented fluid bed dryers, which are currently predominant in continuous TSWG lines and work through a parallelization of multiple drying chambers and thus a sub-division in semi-batches, the vibrating fluid bed dryer (VFBD) developed by L.B. Bohle enables a fully continuous drying process of the wet granules produced during TSWG (Figure 3):

Granules that are discharged from the granulator fall directly through the product inlet of the VFBD and land on the vibrating particle transport grid. The particles are then transported from the product inlet to the product outlet by mechanical vibration, which promotes the destruction of larger lumps and gives the operator control over the RTD

within the drier. Hot and conditioned drying air enters through the inlet on the bottom of the dryer and streams through the mesh of the transport grid, removes moisture from the granules and then leaves through the drying air outlet. A product filter ensures that no powder particles leave the process and a low negative pressure is applied to direct the air stream and ensure it does not affect the granulation process. Depending on formulation, throughput and drying parameters, granules that were produced at L/S-ratios around 0.3 could successfully be dried to a resulting loss on drying (LOD) of around 1 % during relatively short MRTs between 0.5 and 3 minutes [102]–[105].

Fülöp et al. [105] used a horizontal VFBD produced by Quick 2000 Kft and investigated the effect of different process parameters during the drying process on the LOD of granules. Subsequently, they performed first feasibility studies on the scale-up of the drying process. They successfully dried granules produced at L/S-ratios of 0.07 – 0.16 down to a LOD of around 1 – 1.3 % at a throughput of 1 kg/h, and showed that similar results could be obtained at a throughput of 3 kg/h (LOD 1.5 %). At a throughput of 10 kg/h at similar drying parameters, a lot of residual moisture remained in the granules (LOD 3.7 %), which could be improved by increasing the airflow and -temperature (LOD 2.25 %). However, even though they identified the vibration intensity as a critical mechanical parameter for the drying process, no attempt was made at adjusting it further.

Kiricenko and Kleinebudde [102] performed a design of experiments (DoE) with a central composite circumscribed design to examine the effects of drying temperature, airflow and vibration acceleration on the MRT, the GSD and the LOD during VFBD using two different formulations. The GSD was not impacted by the drying parameters as long as the granules were sufficiently dried (LOD <2 %) and no excess moisture remained after drying. This could be achieved by either increasing the temperature or airflow, or by decreasing the vibration acceleration. The MRT and thus the drying time was most strongly affected by the vibration acceleration but also some impact of the airflow was identified.

1.5 Scale-up and process-transfer

1.5.1 Scale-out in high-shear wet granulation

To reduce time to market for a promising drug candidate, the early development usually starts as soon as possible with the limited amounts of API that are available. Thus, one major challenge in early drug product development with a novel API is the scarcity of drug substance available to conduct experiments and manufacture first dosage form prototypes for clinical trials. Thus, much smaller devices for e.g., granulation and tableting are used in research and development or clinical trial supply where the demand and the availability of the API is usually much lower than later during commercial manufacturing. This holds especially true for traditional batch manufacturing, where batch sizes cannot significantly be increased on the same device due to physical restrictions of the devices in contrary to CM technologies, where a scale-up of the production size can be achieved by simply increasing the throughput or the runtime of the process [19], which is sometimes also referred to as scale-out. However, as the demand between different stages of clinical trials and especially commercial availability can increase by several orders of magnitude, it is unrealistic to cover the full range of batch sizes from research to commercial on the same device scale even with the added flexibility of a CM process. Therefore, developing a thorough process understanding on the small scale as well as finding feasible scale-up frameworks or models is essential to reduce material and time consumption during a transfer to a larger scale.

1.5.2 Scale-up in high-shear wet granulation

Despite being one of the most widely applied and investigated technologies for pharmaceutical granule production, the scale-up of high-shear wet granulation (HSWG) is still considered one of the most complex pharmaceutical processes [106]. As the focus of this work lies in scale-up and process transfer of TSWG, an in-depth analysis of all process parameters and research findings for HSWG would go beyond the scope of this thesis. Therefore, this following chapter is intended to showcase only some of the parallels in both technologies and identify scale-up approaches, that could potentially be transferred or adapted from HSWG to TSWG. Several research groups have looked into TSWG as a fully continuous alternative to HSWG for its overall

process similarity (inducing particle agglomeration by shearing a wetted powder blend) and the advantages a CM process offers (added flexibility, smaller manufacturing footprint, implementation of real-time control strategies, etc..) [107]–[112].

Equipment design

Similar to TSWG, where the screw configuration and dimensions can vary greatly, HSWG offers a large variety of adaptions in e.g., the material and design of the mixing bowls or the number, design, angles of inclination or width of the impeller blades. This poses an additional challenge for the scale-up of vastly different devices and can oftentimes reduce the applicability of certain scale-up rules to devices of comparable equipment design and geometries.

Fill level

One of the more trivial parameters in batch manufacturing processes, such as HSWG is the fill level during the process as it can be estimated and scaled more easily by the fraction of the total volume inside the granulator that is occupied by the powder blend instead of relying on surrogates, such as the powder feed number (PFN, see Eq. (3)), which was used by Osorio et al. [113] in TSWG. As a parameter that affects the flow pattern of the blend and the binder distribution, it is usually kept constant among different scales to avoid overloading or underloading which might affect the granulation process [114].

Impeller Speed

When it comes to scale-up considerations for the impeller speed during HSWG there are three more commonly described approaches based on a power law correlation as shown in Eq. (1):

$$\frac{\omega_1}{\omega_2} = \left(\frac{D_1}{D_2} \right)^n \qquad (1)$$

where ω_1 and ω_2 are the impeller speeds in revolutions per minute, and D_1 and D_2 are the impeller diameters in the two granulators, and n is the power law number.

Most commonly used values of n are 0.5 (constant Froude number (Fr)), 1 (constant tip speed) and 0.8, which was empirically found to result in a similar shear stress when applied to different scales [115], [116].

The *Fr* in a HSWG represents the ratio of angular acceleration to the gravitational acceleration (Eq. (2)) and was first used by Horsthuis et al. [117] where it was found to be proportional to the temperature rise caused by kinetic energy which is added during mixing in the HSWG process at different geometrically different granulators.

$$Fr = \frac{D\omega^2}{2g} \qquad (2)$$

where ω represents the revolutions per min, *D* the diameter of the impeller and *g* the gravitation constant.

All three rules (constant tip speed, constant Froude number and constant shear stress) have been used during scale-up in multiple studies with varying levels of success [116]–[119].

Power consumption or torque of the impeller

Both, the power consumption and the torque of the impeller during the granulation process have been investigated and reported to yield similar results as potential end-point markers for the HSWG-process and therefore found their way into several scale-up experiments and considerations [120]–[122]. However, while the detection of a plateau in power consumption during HSWG is used to select an endpoint for the granulation process and therefore used to reduce the batch-to-batch variability and potentially increase the yield, this is hardly possible in a continuous process such as TSWG where the power consumption should remain similar during steady state and is thus only monitored to determine when this steady-state inside the granulator might be reached [75].

Readers interested in a more in-depth analysis of the HSWG process and some of the highly complex scale-up considerations are referred to review articles by Kumar et al. [123] and Liu et al. [114].

1.5.3 Scale-up in TSWG and VFBD

Despite many research articles looking into TSWG as a promising technology for wet granulation in the pharmaceutical industry over the last two decades, there are still only a handful of investigations on scale-up and process transfer for this technology [76], [80], [82], [113].

Djuric et al. [87] attempted a process transfer from one twin-screw extruder with a screw diameter of 27 mm (K-CL-KT 20, K-Tron Soder, Switzerland) to a another twin-screw extruder with only 19 mm screw diameter (MP19 TC25, APV Baker, United Kingdom). Even though they tried to keep the screw configurations on both devices as similar as possible, the used screws were produced by different manufacturers and differed significantly in their L/D-ratio and the geometry of the available screw elements, such as the staggering angle and the length of kneading blocks used. Output variables, such as friability, flowability and the amount of fines and oversized granules were investigated in a full factorial design with two variables and three levels for two different formulations based on either dicalcium phosphate or lactose as filler. The extruder type had the highest impact on granule properties suggesting that more research work should be done with geometrically more similar extruders. What stands out in this work already is, that even with the strong differences in the extruder setup and without an additional milling process (size fractions between 125 µm and 1250 µm were used for tablet compression), no significant differences could be found in the tablet tensile strength and porosity for the lactose-based formulation. While there were significant differences in the dicalcium phosphate formulation, these could potentially be explained by the higher percentage of oversized granules on the larger scale, which were discarded prior to tableting.

Osorio et al. [113] developed potential scaling rules based on dimensional analysis of the process. They introduced the powder feed number as a surrogate for the barrel fill (see Eq. (3)) and inspired by its use in HSWG, examined whether the Fr could be used as a relevant scale-up parameter in TSWG.

$$PFN = \frac{\dot{m}}{\rho * \omega * D^3} \qquad (3)$$

where PFN is the dimensionless powder feed number, $\dot{m}$ is the PFR [kg/h, ρ is the bulk density [kg/m^3], ω is the angular velocity of the screw [s^{-1}] and D is the screw diameter [m].

They performed their experiments on granulators of three different sizes (11 mm diameter L/D-ratio of 40, 16 mm with a L/D-ratio of 25 and 24 mm with a L/D-ratio of

40) and evaluated the effect of similar L/S-ratios, Frs and PFNs on all scales at different levels. While unsurprisingly GSD and granule porosity were strongly affected by the L/S-ratio, they found only a minor effect of Fr and PFN on particle size of larger lumps (d_{90}) that would hold no practical relevance. Furthermore, even though particle size in general, and the occurrence of larger lumps specifically, increased significantly at larger granulator scales, the granule porosity was independent of the granulator scale and mostly impacted by the L/S-ratio. Thus, even though no further downstream processes, such as milling and tableting were performed in this study, it seems possible that similar granule and tablet properties could be achieved as the granule porosity, which would be harder to maintain in scale-up of HSWG, was not affected by the device scale and could play a significant role for downstream processing.

Menth et al. [80] compared several granule and tablet properties during a DoE they performed on three differently sized Modcos Systems (Glatt GmbH, Germany) lines (XS with 11 mm screw diameter, S-Line with 16 mm screw diameter and M-Line with 24 mm screw diameter). Differences in L/D-ratio on the three devices were compensated by matching the distance between the liquid inlet port and the outlet port of the granulator to the best of their ability (resulting in L/D-ratios from liquid inlet port to the granulator outlet of 21 for XS, 23 for S and 23 for M) and the screw configuration was built on only CEs during all their experiments. During their scale-up approaches the moisture level, which was calculated as the percentage of the liquid feed rate (LFR) in the total mass flow (LFR + PFR), the fill level, and thus also the PFN for the barrel, and the screw speed were kept at similar levels on all scales, which meant that the PFR was increased at larger scales to reach a similar fill level. All experiments were performed at three different levels of SS (250, 270 and 300 rpm) and thus the effect of slight variations in fill level, Fr and PFN could be investigated. However, the exponential fit given for the oversized granule fraction to the Fr during their experiment seems highly unexpected as nothing similar to the strong effect of these small differences in SS on the M-scale could be shown in any previous experiments. Furthermore, it should be noted that the data used for the presented fit for that correlation is very limited as no information is given regarding e.g., the residual moisture of the granules for the specific runs depicted and the exponential fit is mostly based on the observations on the M-line. Additionally, even though a milling step was performed prior to tableting, no further measurements of the GSD were done and thus it is not possible to evaluate how much the GSDs might have been modified through

milling. However, based on the investigated attributes, granules and tablets of similar quality could be produced successfully with a screw configuration based on only CEs on three different granulator scales when the moisture and fill level were kept constant during scale-up.

Other notable aspects, not specifically focused on scale-up in TSWG but process transfer in general, were investigated in the thesis of Sebastian Pohl [76]. However, as he was using the previous version of the QbCon© 1, which had a larger screw (25 mm diameter, L/D 20, similar to the QbCon© 25) and also used a Pharma 16 granulator (16 mm screw diameter, L/D 40), some of the findings might also be relevant for a process-scale up, even though screw geometries and configurations could not be kept identical among the different device manufacturers.

While an attempt to numerically represent different screw configurations based on a calculated shear stress value, failed, he also further examined another approach for fill level determination and its effect on granule and tablet parameters during TSWG and process transfer, as well as the impact of screw length and tip speed (comparable to the circumferential speed (CS), which is introduced in 3.2.2 later in this work and thus proportional to the screw speed). To better compare fill level of different granulators he proposed the barrel fill density (Eq. (4)) to adapt the specific feed load proposed by Kolter et al. [124] and added the free volume specific to device and screw-configuration.

$$\mathrm{BFD} = \frac{SFL}{V_{free}} = \frac{\dot{m}}{SS * V_{free}} \qquad (4)$$

where BFD is the barrel fill density in g/cm^3, SFL is the specific feed load in g, $\dot{m}$ is the throughput in g/min, SS is the screw speed in min^{-1} and V_{free} is the free volume of the granulator in cm^3 for the specific screw configuration.

During an initial DoE performed in these studies, the BFD was found to have a significant impact on the GSD, while the influence of the L/S-ratio was found to be not significant. However, this is likely caused by the levels set for the DoE, which varied only slightly for the L/S-ratio (0.177, 0.191 and 0.205) while the differences in BFD

reached up to 700 % (0.45, 1.87 and 3.29 g/cm^3) and therefore represented a substantial difference in fill levels of the granulator. In further studies, the tip speed of the screw was not found to impact the produced granules much during granulation when the BFD was kept similar. Furthermore, relatively comparable GSDs could be achieved during process transfer when the BFD was kept constant among different devices with an increase in oversized granules at higher screw diameters due to the larger critical granule size, which is in line with the results reported in previous scale-up studies.

2 Aims and outline of the thesis

Even though a number of excellent publications have already improved the process understanding of TSWG over the last two decades, there are still plenty of new studies being conducted on a multitude of aspects due to the complex nature of TSWG with its infinite options of potential screw configurations alone.

While the effects of relevant process parameters, such as screw configuration, L/S-ratio, PFR, SS, formulation properties, etc. have been thoroughly investigated by multiple working groups, only a few studies have looked into the scale-up of the twin-screw granulation process. In theory, the process could be scaled infinitely by simply increasing the runtime until a sufficient amount of granules is produced. However, as this is economically not feasible when requirements between laboratory scale and production can account for different orders of magnitude, the scale-up and transfer from one line to another is still necessary.

This thesis aims to contribute to the overall process understanding of TSWG with the focus on scale-up from a research & development scale to a production scale.

Therefore, different work packages are included to cover the following topics:

- Developing suitable scale-up strategies by acquiring a thorough process understanding on the small scale and identifying potentially relevant process parameters for the scale-up through dimensional analysis
- Application and evaluation of the developed scale-up strategies to potentially establish a scale-up model that enables a simple process transfer from laboratory scale to production scale
- Investigation of the scale-up behavior with different formulations to research the effect on formulation properties & sensitivity on the process transfer
- Comparing the outcome of standalone continuous granulation and drying with consecutive non-continuous granule processing and tableting to a fully continuous production from powder blend to tablets

3 Results and discussion

3.1 Experiments on the QbCon© 1

Parts of this section have already been published in the International Journal of Pharmaceutics [125].

Adaptions for this work include:

- Linguistic changes
- Extension of datasets
- Changes and additions in graphs, labels and legends

3.1.1 Introduction

As described earlier in 1.4, TSWG is a highly complex process with a nearly unlimited number of degrees of freedom, not only caused by different formulation properties but also by factors that are specific to this technology, such as possible variations in screw design and geometry, granulator dimensions, and other process parameters during granulation [62], [84], [126].

Previous studies have shown the high impact of many of these factors, which can be broken down into four different categories:

1. Directly adjustable parameters

These are factors that can be directly controlled on the device and easily adjusted even during a running process. Well researched adjustable process parameters with a potentially high impact on granule and tablet properties in TSWG are the L/S-ratio [84], [89], [92], [96], [127]–[130], barrel temperature [74], [97] and the PFR [73], while the SS .

2. Fixed parameters

Unlike the adjustable process parameters, these cannot easily be adjusted during a running process but are set in advance for each run. A relevant example for a fixed parameter of potentially high impact is the screw configuration, where the number, length and geometry of kneading blocks [82], [84], [131], [132] or the pitch and angle

of the screw elements [78], [82], [83] have to be decided on in advance and can drastically change the outcome. The nozzle and position for the liquid addition, as well as the formulation that is used [92], [128], [133] are also highly relevant parameters that can significantly impact the product properties.

3. Device specific parameters

While 1. and 2. are mostly independent of the device or line and could in theory be kept similar for a process on different devices, there are also plenty of factors that are intrinsic to the used device and cannot easily be changed. For TSWG that includes e.g., the dimensions of the granulator, the L/D-ratio of the screw and the drying process that is applied after granulation. The built-in devices for e.g., powder and liquid feeding or the consecutive drying process are usually specific to a manufacturer and therefore not easily interchangeable.

4. Resulting factors (dependent variables)

Some of the factors that are commonly investigated cannot (yet) be directly adjusted at the devices but are oftentimes the result of a combination of other factors from categories 1-3. While the barrel fill level will be directly impacted by the set screw speed, L/S-ratio and feed rate, it is also dependent on the granulator and screw dimensions, the density of the used formulation and the resulting free volume inside of the barrel. Another resulting factor that is oftentimes investigated is the RTD, which is also impacted by multiple process parameters, such as L/S-ratio, screw speed and even fill level of the barrel [88], [134] and could play a significant role in the implementation of control strategies.

Due to the high complexity of the process, it seems unreasonable to define one universal process guideline that fits all situations in TSWG. However, there are plenty of similarities in the findings of different research groups regarding the identification of critical process parameters.

Therefore, this initial work package focused on one pre-defined screw configuration and one formulation and aimed at identifying the main impact factors on granule and consecutively tablet properties as well as assessing the robustness of the process and trying a new approach of experimentally measuring the fill level during twin-screw granulation. The robustness and reproducibility were tested through repetitive runs on

the granulator on different days as well as at different points during a DoE, which was conducted to confirm critical process parameters for the used formulation. A full factorial design was selected to determine the impact of SS, PFR and L/S-ratio (2^3) with three additional center points to help estimate the variability.

3.1.2 Preparation of the DoE on the small scale

There are four main process parameters that can be directly adjusted on the device during the granulation process: SS, PFR, L/S-ratio and barrel temperature.

While SS, PFR and L/S-ratio can be adjusted with an almost instantaneous effect on the process, adjusting the barrel temperature is always subject to a response delay as it depends on an external tempering unit and e.g., the thermal conductivity of both the cooling liquid and the barrel material. Additionally, barrel temperature is a parameter that can easily be kept identical among different scales and devices and was therefore considered less relevant for later scale-up experiments. Thus, it was not included as a factor in the DoE und was instead kept at a constant 30°C.

As the impact of each of those three process parameters was to be investigated for the selected screw configuration and formulation, a full factorial DoE with three input parameters and thus 2^3 runs and three additional center points was planned (see Table 1 & 5.2.2.2).

To determine feasible high and low levels for each of the three input parameters (SS, PFR and L/S-ratio), preliminary runs were performed in advance to the DoE. For the PFR, 1 kg/h and 2 kg/h were considered to be realistic and appropriate throughput levels for the laboratory scale device. Higher throughput levels would have introduced additional restrictions for the settings of the L/S-ratio due to limitations in the drying capacity of the consecutive continuous fluid bed drier at high liquid feed rates (see 5.2.2.3 for the drying process). Furthermore, the setpoints for the PFR also introduce additional limitations for the feasible SS. For this formulation, a SS of 150 rpm was used as the lower limit to prevent material hold-back in the granulator at a PFR of 2 kg/h.

The setpoints for the L/S-ratio were then determined empirically by increasing the added water during the granulation process at constant SS and PFR and observing the overall appearance of the resulting granules and the transportation behavior within the VFBD. With the used formulation, first granules started to build around a L/S-ratio of 0.13 indicating that liquid bridges started to form between primary powder particles.

Up until 0.26 no limitations in the transportation within the drier could be observed, while at higher L/S-ratios, larger lumps started to form within the VFBD that led to disturbances in the transportation and overall flow of the process and an increased variability in LOD measurements at the exit of the drier.

Process parameters of the VFBD were also optimized during the preliminary runs to ensure that all produced granules would be sufficiently dried (LOD between 0.8 % and ~1.5 %). More information about process optimization and adjustments of the VFBD process can be found in 5.2.2.3.

3.1.3 Screening DoE & identification of main impact factors

A total of 11 runs were performed on the small-scale granulator during the full factorial DoE as can be seen in Table 1. All experiments were performed using Formulation 1 (see Table 14 in 5.2.2.1) and the respective screw configuration referenced in Table 16 of 5.2.2.2.

Table 1 Parameter Overview DoE QbCon© 1

Run	SS [rpm]	PFR [kg/h]	L/S-Ratio	Vib. Acc. [m/s²]	Airflow [Nm³/h]	Air Temp. [°C]	LOD [%]
N01	150	1	0.13	5	15	40	1.37
N02	300	1	0.13	5	15	40	1.40
N03	150	2	0.13	5	15	55	1.33
N04	300	2	0.13	5	15	55	1.08
N05	150	1	0.26	5	30	55	1.35
N06	300	1	0.26	5	30	55	1.39
N07	150	2	0.26	5	30	80	1.68
N08	300	2	0.26	5	30	80	1.39
N09	225	1.5	0.195	5	22.5	55	1.15
N10	225	1.5	0.195	5	22.5	55	0.80
N11	225	1.5	0.195	5	22.5	55	1.20

All runs were performed as described in 5.2.2.3 on the same day in a previously randomized order (the “Run” order in all tables is not equivalent to the performed granulation order, see Table 18 in the appendix).

An overview of the performed RTD measurements (see 5.2.1.2) can be found in Figure 39 in the appendix. The RTD of granules in the granulator was mainly driven by the applied screw speed and the L/S-ratio during granulation as both had a significant impact on the t_{Max} value of the color signal (the time at which the highest signal was measured), indicating that a high percentage of the added color dye was washed out of the granulator earlier with increased screw speed and slightly later with increased L/S-ratio. The model predictions for the MRT were less accurate (Q2 < 0.5 as can be seen in Table 2, however this might be caused by the way the MRT was determined by finding the time at which 0.5x the area under the curve was reached, which is sensitive to changes in measurement duration as the measured signal never constantly and fully returns to the baseline and thus a higher variation during measurements occurs. The impact of the screw speed could also be confirmed in additional experiments performed outside of the scope of the DoE, where the screw speed was increased from 100 rpm to 400 rpm in 25 rpm increments as can be seen in Figure 4. Similar effects of decreasing RTDs with increasing SSs in a twin-screw granulator are well documented in literature [88], [90], [135].

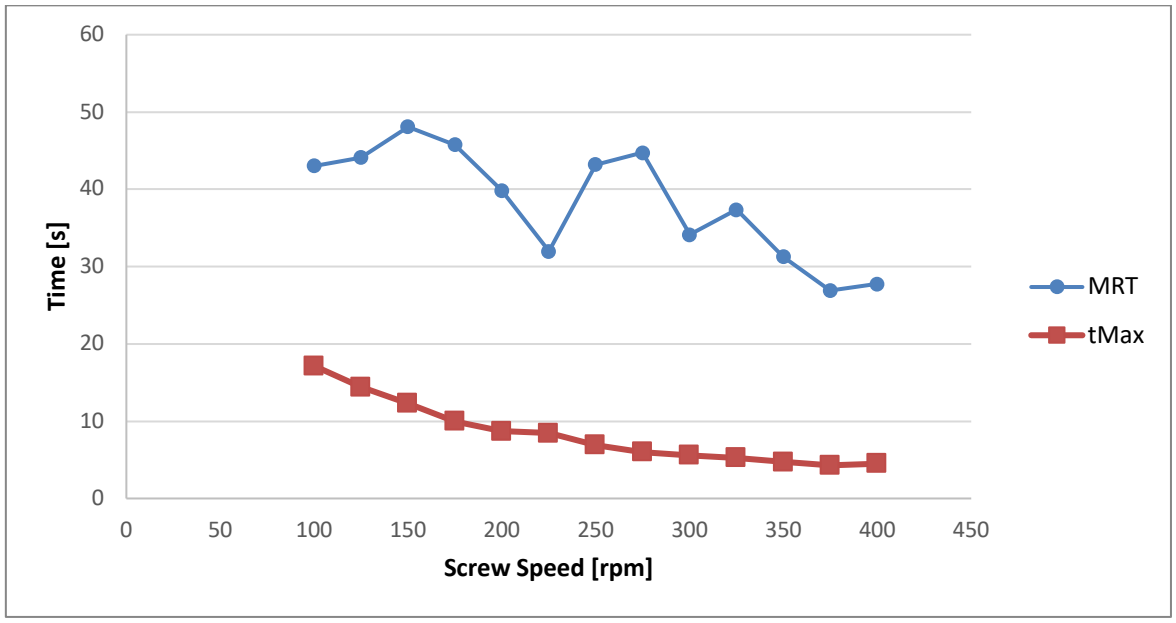

Figure 4 Residence Time measurements performed at different screw speeds between 100 and 400 rpm.

Table 2 Results from the DOE: power of the model (coefficient of determination (R^2)), coefficient of prediction (Q^2), model validity and reproducibility; coefficients for factors (SS, PFR, L/S-ratio and a constant) to the responses (coefficients ± CI, a = 0.05) and their respective p-values. Measured values are shown in *Table 18* in the appendix, quadratic interactions not shown as no significance was found.

	before milling		**after milling**						
Parameter/coefficient	d_{50} [µm]	d_{90} [µm]	d_{50} [µm]	d_{90} [µm]	Cohesive Strength [MPa]	Tensile Strength (150 MPa) [MPa]	Disintegration Time [s]	t_{Max} [s]	MRT [s]
R^2	0.96	0.52	0.97	0.95	0.95	0.96	0.87	0.91	0.88
Q^2	0.87	-0.67	0.92	0.85	0.84	0.91	0.55	0.77	0.49
Model Validity	0.26	-0.20	0.38	0.48	0.59	0.87	0.42	-1.9E-03	0.66
Reproducibility	0.996	0.997	0.994	0.987	0.98	0.942	0.996	0.996	0.92
SS [rpm]	-36.14	-64.17	-2.87	-5.42	-1.10E-03	2.50E-03	-2	-3.64	-4.85
p-value	0.10	0.28	0.79	0.59	0.98	0.89	0.91	1.90E-03	0.14
PFR [kg/h]	66.66	70.70	21.05	25.35	0.14	0.13	44.5	0.12	-4.01
p-value	0.01	0.24	0.08	0.03	0.02	1.30E-04	0.04	0.82	0.2
L/S-ratio	231.19	118.13	141.98	111.08	0.49	0.19	102.75	1.6	12.05
p-value	5,9E-06	6.8E-02	2.40E-06	8.70E-06	9.70E-06	1.20E-05	1.00E-03	0.03	0.01
Constant	599.42	1303.82	309.44	718.85	1.37	1.79	366.6	0	27.7
p-value	2,8E-09	1.9E-08	3.80E-09	7.00E-12	2.90E-09	0.01	3.80E-07	1.30E-05	3.50E-04

For the GSD a clear trend towards larger granules at higher L/S-ratios could be observed. As shown in Table 2, changes in e.g., d_{50} before and after milling and x_{90} after milling can be explained quite well by the model. The relatively low model validity there and for many other observations in this study can oftentimes be attributed to the very high reproducibility of measurements around 0.99. With increasing reproducibility, the estimated observational error in the model decreases and therefore even small differences between experimental and model data are associated with systematic errors and thus a decrease in model validity. This is also described in the user guide for Modde® [136].

Overall, as depicted in Figure *5*, there were distinct differences in the GSD curves based on the applied L/S-ratio. The number of fines was reduced significantly with increasing L/S-ratio while the percentage of larger granules increased. This observation was consistent before and after milling and clear distinctions between the three different settings for the L/S-ratio could be observed. This shift towards higher particle sizes with increasing granulation liquid is well described in literature and consistent among various research groups and experiments [84], [92], [96], [127]–[130]. PFR also had a significant impact on the median granule size prior to milling, while after milling only minor trends could still be observed. Furthermore, no correlation between the SS during granulation and the GSD was found.

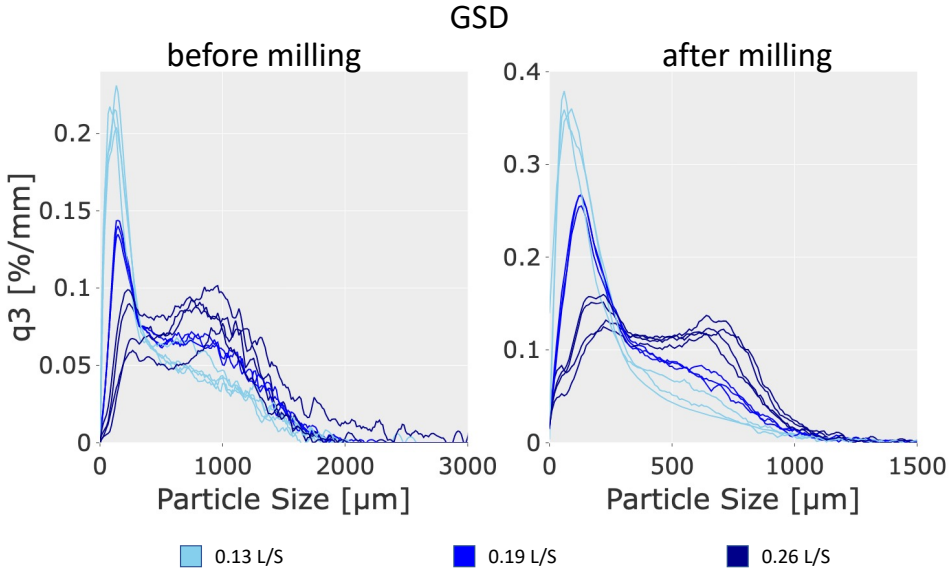

Figure 5 Granule size distributions of runs performed during the DoE; colors are based on the L/S-ratio used during granulation (0.13, 0.19 and 0.26)

Measured bulk and tapped density (Table 3) could not be sufficiently explained by the current model (R^2 and Q^2 both < 0.5, hence not shown in Table 2), however this is likely caused by the high overall similarity among all results with a coefficient of variation (CV) < 0.03 for both bulk and tapped density.

Despite these similarities, a trend towards lower Hausner ratios could be observed with increasing L/S ratio and feed rate ($p < 0.05$), which is likely correlated to the decrease in fine fractions in the GSD of those granules and the overall shift towards larger particles as powder flow properties are known to be impacted by particle size and shape [137].

Table 3 Results for bulk and tapped density and Hausner ratio for milled granules produced within the DoE

	Run	bulk density [g/mL]	tapped density [g/mL]	Hausner ratio
Low L/S	N01	0.49	0.62	1.26
	N02	0.49	0.62	1.26
	N03	0.47	0.58	1.23
	N04	0.48	0.60	1.24
Center points	N09	*0.41	*0.50	1.24
	N10	0.48	0.60	1.24
	N11	0.49	0.60	1.23
High L/S	N05	0.50	0.61	1.22
	N06	0.49	0.59	1.22
	N07	0.52	0.62	1.18
	N08	0.50	0.60	1.20

*is considered a potential outlier caused by erroneous measurement settings

Cohesive strength and failure load of granules were determined by uniaxial compression as described in 5.2.3.8. with the goal of investigating possible correlations between granule strength and tensile strength of tablets produced. Both cohesive strength and failure load were mainly impacted by the L/S-ratio applied during granulation with PFR also having a significant impact on the cohesive strength on granules especially at higher L/S-ratios (Figure 6).

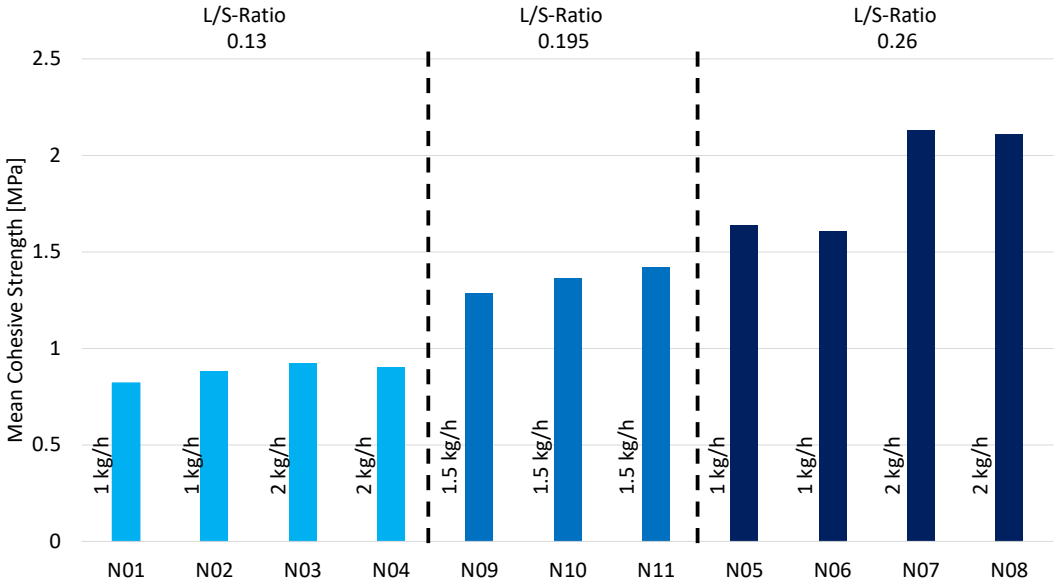

Figure 6 Mean cohesive strength of granules produced during the DoE grouped based on the applied L/S-ratio used during granulation. PFR of runs referenced left of the respective bars.

As in any wet granulation process, granules produced during TSWG are subject to different changes along the process: Wetting and nucleation, consolidation and growth, and breakage and attrition [138]. Which of those processes dominates during TSWG is highly dependent on the screw configuration, the water and binder addition and the current granule position within the granulator [139]–[141]. As the screw configuration and thus the overall process flow was kept constant for all runs while the water added was increased, wetting and nucleation as well as consolidation and growth were promoted as more liquid was present to interact with the dry powder bed and create interparticle bonds through liquid bridges. Consequently, more dense and stable particles were formed during the granulation process and fewer loosely bonded agglomerates. This was confirmed by comparing the cohesive strength and the mass percentage of the different fractions at different L/S-ratios (Table 4), where the mass percentage of finer granules (0-125 µm) decreased while the overall cohesive strength of all fractions increased drastically.

Table 4 Overview of mean cohesive strength and the respective mass percentage of granule fractions at different L/S-ratios

	Run	Cohesive Strength [MPa]				Mass percentage of fraction			
		0-125 µm	125-355 µm	355-500 µm	500-800 µm	0-125 µm	125-355 µm	355-500 µm	500-800 µm
0.13 L/S	N01	1.33	0.72	0.22	0.40	32 %	44 %	13 %	10 %
	N02	1.34	0.82	0.23	0.35	33 %	46 %	11 %	9 %
	N03	1.47	0.75	0.33	0.32	38 %	36 %	11 %	13 %
	N04	1.40	0.76	0.27	0.28	37 %	43 %	10 %	9 %
0.195 L/S	N09	2.61	1.05	0.59	0.72	23 %	44 %	15 %	17 %
	N10	2.48	1.19	0.64	0.79	25 %	42 %	14 %	17 %
	N11	2.53	1.38	0.57	0.61	25 %	43 %	14 %	17 %
0.26 L/S	N05	2.48	1.91	1.12	1.21	13 %	39 %	19 %	27 %
	N06	3.19	1.73	1.02	1.00	14 %	39 %	20 %	25 %
	N07	2.41	2.49	1.57	1.92	14 %	34 %	17 %	32 %
	N08	2.98	2.48	1.45	1.80	11 %	34 %	18 %	34 %

Even though tablet tensile strength was also mainly impacted by the L/S-ratio and the PFR, there was no strong correlation between the granule cohesive strength and the tablet tensile strength indicated by the low coefficient of determination (R^2 = 0.814) seen in Figure 7. While the effect of PFR was comparably strong on both cohesive strength and tensile strength of tablets (0.13 versus 0.14, Table 2), the effect of L/S-ratio was significantly higher on the granule strength than on the tablet strength (0.49 versus 0.19)

However, the process of analyzing granules though uniaxial compression took a few minutes for each cycle and required additional preparation steps for analyzing different granule fractions. Overall, this made it an equally time-consuming process as adding the extragranular excipients to the milled granules and making tablets to be tested afterwards. Thus, even though additional information regarding the granule strength of different size fractions could be gathered with this method, the additional expenditure of time and resources and the low accuracy in the prediction of tablet strength, made this method unfeasible for the scale-up experiments performed in subsequent chapters.

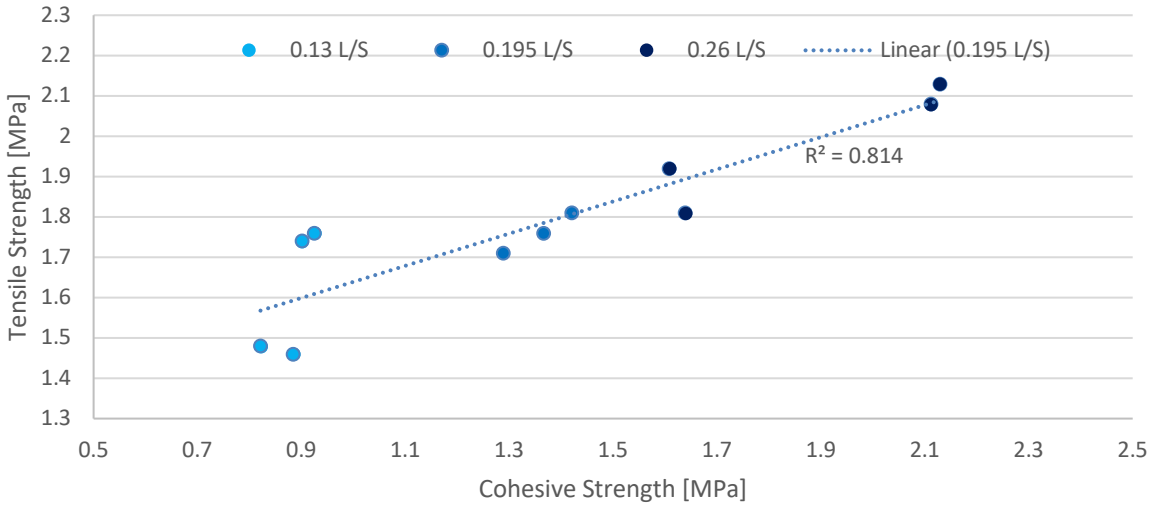

Figure 7 Tensile strength of tablets at 150 MPa compaction pressure versus cohesive strength of granules

The overall trend towards higher tensile strengths with increasing L/S-ratio and potentially LFR can be gathered from Figure 7. The highest tensile strength is reached for runs with an L/S-ratio of 0.26 and the lowest tensile strength for the runs at 0.13 L/S-ratio. Similar effects with even larger differences in the design space for the L/S-ratio have been observed by Liu et al. [89].

At lower compaction pressures, there were relevant differences in the friability of tablets based on the L/S-ratio during granulation. Tablets that were made with a compaction pressure of 90 MPa from granules produced at a L/S-ratio of 0.13 had a friability that in some cases not met the requirements of the European Pharmacopeia [4] (< 1.0 %). At higher compaction pressures a low friability for all tablets could be achieved and the differences between different runs became practically irrelevant and insignificant (Figure 8).

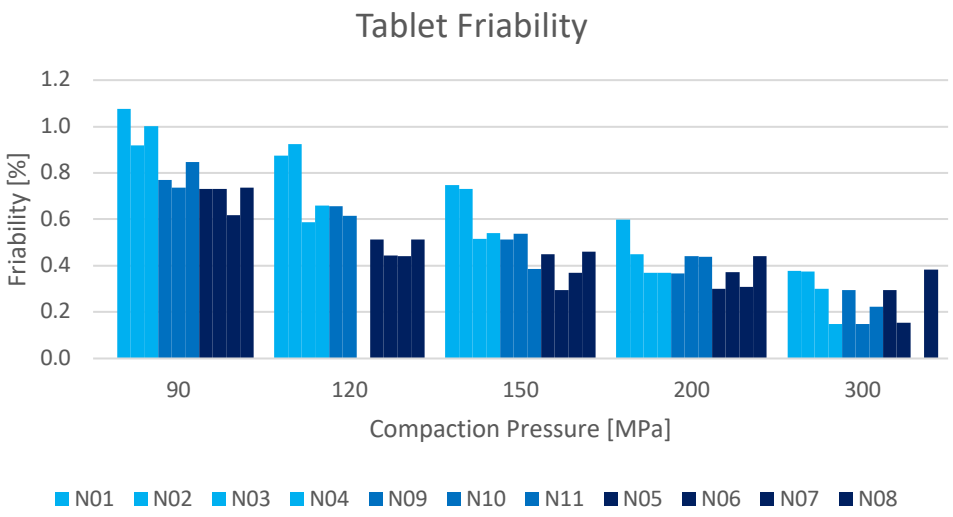

Figure 8 Overview of friability of tablets. Depicted order from left to right represented in the legend. L/S-ratios are represented by the color of the bars: Light blue – 0.13, blue – 0.195, dark blue – 0.26

As can be seen in Table 2, while both a higher L/S-ratio and an increased PFR had a positive effect on granule and tensile strength, it also came with the downside of an increased disintegration time for tablets. For this study and formulation all tablets made with a compaction pressure of 150 MPa were sufficiently resistant to breakage (tensile strength > 1.5 MPa) and disintegrated fast enough (< 15 minutes) and therefore this did not pose any practical issues. Nevertheless, in cases where either one of those parameters is not meeting the requirements, this possible trade-off should be kept in mind. However, there have also been contradicting results on the effect of L/S-ratio on e.g., the tensile strength of tablets where an increase in L/S-ratio lead to a reduced tensile strength with a high drug load formulation and a different screw configuration [142]. Therefore, whenever large changes to screw configuration or physicochemical properties of the used powder blends are introduced, some preliminary experiments on the effects of process parameters on product properties are recommended due to the highly complex nature of TSWG.

3.1.4 Reproducibility

The reproducibility of various granule and tablet properties for the center points during the DoE was very high (> 0.94) for all properties shown in Table 2. These observations were further confirmed in additional experiments, which were performed on three

separate days where the same granulation and drying parameters as in the CPs of the DoE were used each day. GSDs for all six runs performed either at different positions of the DoE or on one of the three additional days can be seen in Figure 9. Both the GSDs and their respective cumulative distribution curves show an extremely high overlap.

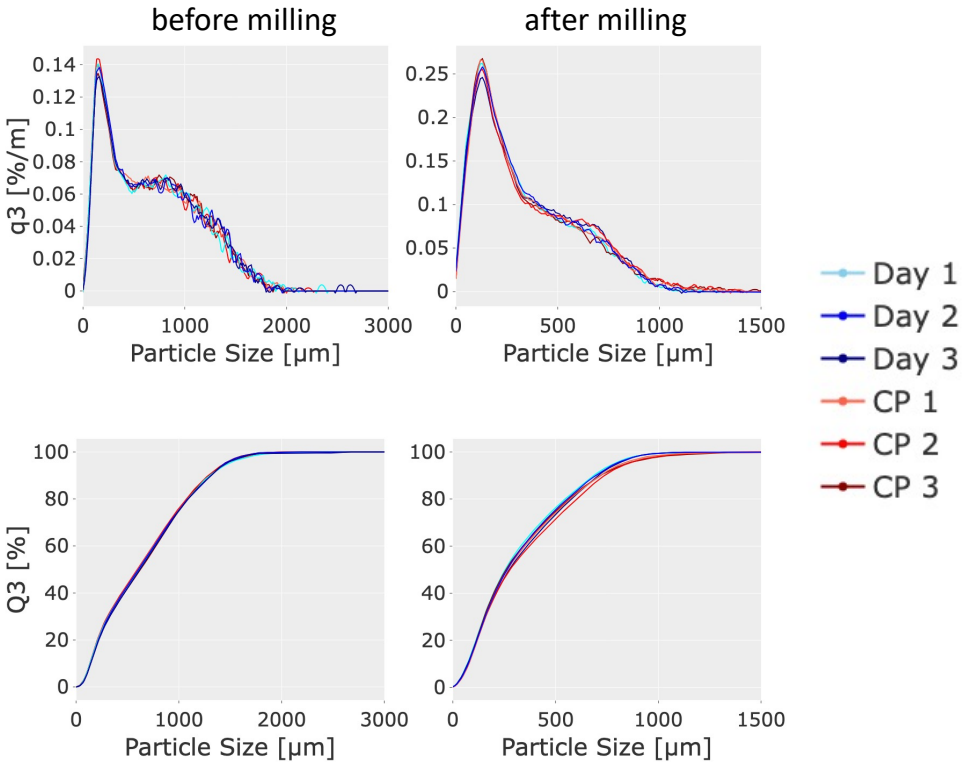

Figure 9 GSD and the respective cumulative distribution of granules produced on three different days (Day 1-3) and at three different time-points during the previous DoE (CP 1-3) with similar granulation parameters.

Similar results were obtained for the tabletability curves of tablets that were produced from those granules (Figure 10). The observed tabletability curves were almost congruent and no significant differences could be observed.

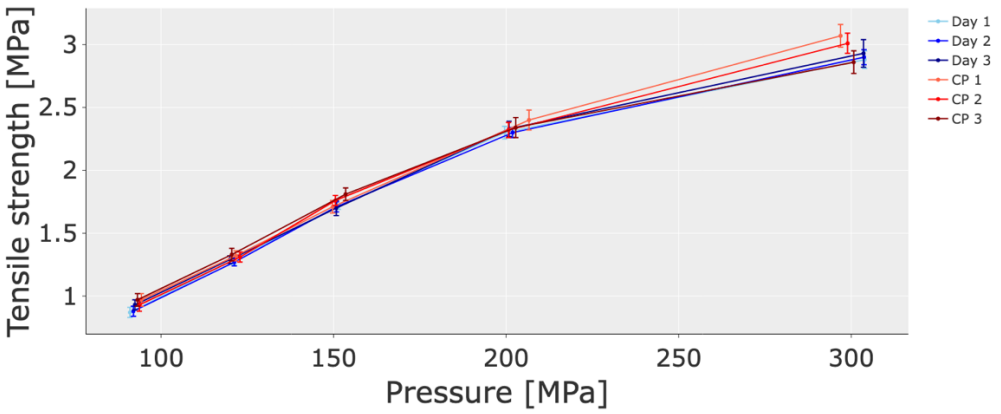

Figure 10 Tabletability of granules produced on three different days (Day 1-3) and at three different time-points during the previous DoE (CP 1-3) with similar granulation parameters. Mean ± standard deviation; n=20

As the Earth Mover's Distance (EMD) (referenced in 5.2.3.3) is later used to quantify differences in GSDs between scales and scale-up strategies and these repetitive runs showcase most likely the highest possible similarity, the EMD was also computed for these runs. The mean GSD of day 1-3 was used as a reference to compare all six runs individually through the EMD. As can be seen in Table 5, all computed EMDs were smaller than 25 µm, while the EMDs for Day 1-3, which were all used for the mean GSD used as reference, were smaller than 10 µm both before and after milling.

Table 5 EMD for GSDs of granules produced with the same parameters compared to the mean GSD curve of granules produced on three different days with similar parameters

		EMD [µm]					
Reference		Day 1	Day 2	Day 3	CP 1	CP 2	CP 3
Mean GSD Day 1-3	before milling	6	7	7	9	11	16
	after milling	9	2	9	11	24	11

As the computation of the EMD is very sensitive to the input data and the scales and spacing used for it, it cannot be used for direct comparison among different experiments, when different devices for GSD measurement are utilized or the input data is formatted or presented differently. Therefore, in this work all comparisons are carried out according to the procedure described in in 5.2.3.3.

3.1.5 Experimental fill level determination

Granulators in TSWG are generally made from metal and are thus opaque with no option of making any observations of the running process among the length of the screws. As TSWG is a complex and dynamic process, in which multiple variables, such as the L/S-ratio and the screw elements, heavily impact the resulting granules and all intermediary powder agglomerations, predicting the exact fill level of the granulator (i.e., the volume occupied by the powder bed in relation to the available volume in the granulator) also poses a challenge without any means of verification. As the dimensions of the granulator change during process scale-up, the available volume also changes and thus the fill level in the granulator at different PFRs and SSs.

Many attempts of accurately describing the channel fill level have been made by various research groups. Kolter et al. [124] first introduced the dimensional specific feed load as the mass flow divided by the screw speed, which was later used as input parameter by other research groups, that made differing observations regarding effects on the measured output parameters [75], [139]. Kohlgrüber et al. [59] introduced a dimensionless number to describe the barrel fill level by dividing the powder mass flow rate by the product of screw speed, screw diameter, and the material density. The approach of using a dimensionless input parameter was picked up by Osorio et al. [113] as they introduced the powder feed number (PFN) to describe the fill level inside three differently sized granulators.

As the fill level inside the granulator is naturally linked to the PFR and the screw speed, several other studies as well as the previously conducted DoE in this work have at least indirectly investigated the effects of varying fill levels on different product properties [73], [74], [143], [144]. The paradox of screw speed having a very low impact on CQAs in most studies, while the fill level, which is inversely linked to the screw speed, is oftentimes used to explain observations reported in literature, has been previously pointed out by Gorringe et al. [145]. However, they also acknowledged the complexity of TSWG processes and the possible differences in impact at varying screw configurations, L/S-ratios and levels of starvation within the granulator.

To increase the understanding of how the barrel fill level is impacted by different process parameters and during process scale-up, an experimental attempt on determining the fill level along the different screw segments was made.

The overall idea for this method was to stop and “freeze” the TSWG process after an appropriate start-up time and then create a mold from inside the granulator that could be used to determine the remaining free volume inside the granulator. The fill level would then be determined according to Eq. (5):

$$fill\ level = \frac{V_{free} - V_{mold}}{V_{free}} \quad (5)$$

Where V_{free} is the free volume inside of the granulator measured prior to the run in an empty granulator, and V_{mold} is the remaining free volume inside the granulator measured during the run. Ideally, this mold could even be segmented according to the screw configuration to observe possible differences in fill level along the process.

If a mold could be made that was sufficiently representative of volume changes within the granulator, the volume of this mold could be determined through e.g., water displacement method.

A two-component dental silicone mixture (LM Abform Silikon flüssig, Laurenz & Morgan GmbH, Germany) was used in preliminary trials to see whether sufficiently accurate molds of screw elements without the powder could be made, to investigate if the powder blend interacts with the silicone or possibly even dissolves in it, and if the molding material could be easily removed from the material. As these requirements were met in the preliminary trials, next a mold of the granulator was made directly after the granulation process was stopped.

Molding the upper half of the granulator and the screw posed to be a challenge, as the liquid could not be contained inside any granulator walls in the open barrel. The process is depicted in Figure 11.

However, as can be seen on the pictures, some parts of the mold had holes caused by e.g., air bubbles in the two-component mixture or possible tear-outs, which would significantly decrease the quality of the fill level determination. Furthermore, due to the challenging molding process especially for the upper half of the granulator, the accuracy of the mold volume in general was doubtful.

Figure 11 Pictures taken during the creation of the barrel mold: Makeshift walls were built around the granulator with playdough (1) to effectively overfill the bottom half of the granulator with the two-component mixture (2) and stop it from flowing out of the granulator. Afterwards it was let to rest until the polymerization process increased the viscosity enough to stay intact when the playdough was removed but not too much so it could still adapt its shape to the upper half of the barrel when it was closed (3) and create an accurate mold to determine the right volume. After an additional waiting period to ensure the polymerization process had concluded and the mold was finished, the barrel was opened again (4) and the mold inspected and removed.

As the focus laid on the scale-up experiments, and the first results in this regard (shown in the consecutive chapters) indicated a relatively low effect strength of the barrel fill level on various granule and product properties, no further experimental attempts of improving the method were pursued. However, if contrary to current results, a higher impact of the expected barrel fill was demonstrated, this method could potentially be further developed.

3.1.6 Summary

Aims of this work package were to acquire a sufficient understanding of the TSWG process using the selected formulation and screw configuration and find suitable parameter settings that could be applied on the small-scale granulator to produce granules with a sufficient flowability and consecutively tablets of high enough quality.

The attempt that was made on determining the fill level of the granulator by molding the barrel from the inside provided insufficient results, as an accurate mold of the upper part of the granulator could not be made and hence an accurate measurement of the free volume was not possible.

The TSWG process overall however, proved to be highly reproducible as was shown both, during the DoE as well as in consecutive experiments performed over the course of multiple days with no differences in relevant quality attributes, such as the tablet tensile strength or the GSD. The DoE confirmed L/S-ratio as main impact factor on different product properties, such as the GSD, granule and tablet strength, and disintegration time of tablets. PFR was also found to have an impact on most of these properties, even though at a much lower observed effect. Within the ranges applied in this experiment, the SS was not found to have any significant impact on the measured product properties, however, it had an impact on the RTDs of granules inside the granulator.

3.2 Scale-up from development to production scale

Parts of this section have already been published in the International Journal of Pharmaceutics [125].

Adaptions for this work include:

- Linguistic changes
- Extension of datasets
- Changes and additions in graphs, labels and legends

3.2.1 Introduction

Process scale-up is an essential part of drug development in the pharmaceutical industry. During early development phases, resources, such as the API are oftentimes still only available in very limited quantities and a much lower demand has to be met for the early stages of clinical trials than for the later phases or even the commercial launch [146]. With increasing demand and available resources, processes are usually transferred from smaller laboratory scales to production scales to meet the demand and save production costs. The challenge therein lies in ensuring that the CQAs of the product are still similar after the process transfer and meet the high safety and quality standards within the pharmaceutical industry.

As described in the previous chapters, many interactions and process parameters in TSWG have already been extensively investigated by various research groups. However, most publications are limited to one specific device and scale and the current knowledge about process transfer or scale-up in TSWG is still limited.

The high complexity and many impact factors of TSWG pose an additional challenge for scale-up and process transfer, as the amount of different screw configurations that could be used is almost limitless and even with similar screw configurations the geometry and dimensions might be different for twin-screw granulators constructed by different manufacturers.

Many of these challenges were already considered in the design process of the differently sized QbCon® lines by L.B. Bohle. Thus, the L/D-ratio as well as the geometry (e.g., the pitch of CE or the staggering angle and number of kneading discs in KEs of every individual screw element), can be kept similar during granulation on both lines.

To the authors best knowledge, no investigations on the effect of different, but geometrically similar scales of twin-screw granulators on the RTDs of granules have been published so far. None of the previously performed scale-up or process transfer studies for TSWG report any measurements of RTDs [76], [80], [87], [113].

Several investigations have helped to understand the impact of changes in screw configuration or process parameters on the RTD and even predicted or modeled RTD curves based on either an axial dispersion or the two compartment model for a specific screw configuration and formulation [64], [135], [147]–[149]. However, the process flow of particles in a twin-screw granulator is far too complex to be simulated with our current understanding and the computational resources available, as it is highly impacted by different design and process parameters. Therefore, the RTDs of all runs performed during process scale-up were determined experimentally as described in 5.2.1.2 to help better understand how the granulator scale impacts the effects of process parameters on the RTD during granulation.

Three different scale-up strategies based on previous investigations from other research groups' results (see 1.5.3) were developed and supplemented with novel ideas on possible impact factors. Their effects on granule and tablet properties and the residence time distribution of granules within the granulator were then evaluated in these experiments.

3.2.2 Overview of applied scale-up strategies

As the aim for the scale-up was to keep disturbances by known impact factors, such as the barrel temperature, the L/S-ratio, and the screw configuration as minimal as possible, these process parameters were kept constant during the experiment with the exception of the L/S-ratio, where a few additional runs were performed to reference its effects.

The PFN (see Eq. (3)), which was introduced by Osorio et al. [113] as a surrogate for the fill level was also kept at similar levels for all the applied scale-up strategies, to facilitate ideal scale-up conditions based on previously conducted experiments [80], [113]

For strategy 1 (S1) the PFR was increased 4-fold to reach a similar PFN and thus a comparable barrel fill level on the large-scale granulator (screw diameter of 25 mm versus 16 mm on the small scale) without changing the SS. The concept for this strategy was to investigate the similarity of product properties for both tablets and granules and simultaneously study the RTDs of particles in the granulator when only the dimensions of the screw and granulator were scaled up and most other parameters, such as the fill level and the L/S-ratio were kept as similar as possible.

Strategy 2 (S2) aimed at achieving a similar outer CS of the screws (similar to the calculated tip speeds reported by Pohl [76]) on both scales, as the CS of screws at similar SSs increases proportionally with increasing screw diameters (see Eq.(6)). Thus, the PFR was scaled accordingly (~2.5-fold) to reach a similar CS and PFN as on the small scale.

$$\mathrm{CS} = d * \pi * n \qquad (6)$$

Where CS is the circumferential speed [m/s], d is the screw diameter [m] and n is the screw speed [s^{-1}].

Lastly, to achieve a realistic scale up from laboratory scale to a production scale and explore the performance of the VFBD at high capacity, the PFR was increased tenfold for strategy 3 (S3), while the SS was increased 2.5-fold to keep a similar PFN.

In addition to the three developed scale-up strategies an additional “reference” run (***R***) was performed on the large line for which all granulation parameters (SS, PFR, L/S-ratio and barrel temperature) were kept identical to the run on the small scale. As PFR and SS were kept similar on a significantly larger granulator, the drastically lower fill level caused a “starved” condition in contrast to the established scale-up strategies where a similar PFN was aimed for. As the low throughput led to a drastic underfill of the drier as well, and thus a grey color signal would be measured whenever the bottom plate of the drier was not fully occupied by powder, no reliable data for the RTDs could be gathered for this run.

3.2.3 Scale-up experiments

For these first scale-up experiments, the same formulation 1 and respective screw configuration (see Table 16 in 5.2.2.2) as in the previous chapter were used. An overview of different input and output parameters can be found in Table 6.

Table 6 Overview of parameters during scale-up

	SS [rpm]	PFR [kg/h]	L/S-Ratio	Vib. acc. [m/s²]	Air Flow [Nm³/h]	Air Temp. [°C]	PFN	tmax [s]	MRT [s]	Circ. speed [m/s]	LOD [%]	ρ_{bulk} [g/mL]	ρ_{tapped} [g/mL]	Hausner ratio
Q1	300	2	0.13	5	15	55	8.6E-03	6.9	13	0.25	1.43	0.49	0.60	1.24
	150	2	0.26	5	30	80	1.7E-02	18.3	40	0.13	2.18	0.52	0.62	1.20
	*300	2	0.26	5	30	80	8.6E-03	-	-	0.25	1.22	0.50	0.60	1.18
	225	1.5	0.195	5	22.5	55	8.6E-03	10.2	34	0.19	1.22	0.48	0.60	1.23
S1	300	8	0.13	5	100	60	8.8E-03	9.8	22	0.4	1.08	0.51	0.62	1.22
	150	8	0.26	5	275	60	1.8E-02	22.9	53	0.2	1.33	0.53	0.62	1.19
	*300	8	0.26	5	275	60	8.8E-03	12.9	54	0.4	1.41	0.51	0.61	1.18
	225	6	0.195	5	125	60	8.8E-03	14.1	47	0.3	1.37	0.51	0.61	1.20
S2	191	8	0.26	5	275	60	1.4E-02	18.7	53	0.25	1.35	0.53	0.62	1.17
	*191	5.08	0.26	5	175	60	8.8E-03	18.8	65	0.25	1.60	0.53	0.62	1.19
S3	750	20	0.13	5	120	85	8.8E-03	5.9	13	0.99	1.15	0.49	0.60	1.22
	375	20	0.26	5	333	85	1.8E-02	9.4	35	0.49	0.80	0.52	0.63	1.16
	*750	20	0.26	5	333	85	8.8E-03	6.6	28	0.99	1.15	0.53	0.62	1.20
	563	15	0.195	5	135	85	8.8E-03	11.8	33	0.74	1.39	0.52	0.61	1.18
R	*300	2	0.26	8	110	75	2.2E-03	-	-	0.4	0.91	0.52	0.61	1.20
	225	1.5	0.195	8	100	60	2.2E-03	-	-	0.3	0.89	0.52	0.63	1.18

Runs marked with a * were commonly used for comparisons in figures and discussions

Drying parameters were determined in preliminary trials to ensure a sufficiently low LOD was reached at the end of each run and product properties and processing of

scale-up would not be impacted by largely different LODs. The impact of process parameters of the VFBD on GSD has recently been investigated by Kiricenko and Kleinebudde [102]. They found contradictory results based on the used formulation as no significant impact on GSD was observed with their mannitol-based formulation but the d10, d50 and d90 percentiles of the formulation based on lactose and microcrystalline cellulose (MCC) were significantly impacted by drying temperature and airflow. However, they also recognized that this might be caused by the high remaining moisture content of lactose-MCC based granules (> 3 %) after some of the performed runs, indicating that granules could not be sufficiently dried and were therefore bound by higher cohesive forces.

Thus, drying parameters for runs in this work package were set with a target LOD of < 2 % in mind, which could be reached in all cases with the exception for one run performed on the QbCon© 1, where the warm-up time for the drier in between runs seems to have been too low and thus a slightly but not excessively higher LOD (2.18 %) was measured that was still deemed acceptable.

As can be seen in Figure 12a, there were substantial differences in the GSDs of granules based on the scale before milling, while after milling the impact of the selected scale-up strategy and even of the drastically underfilled reference run were very in comparison. Similar observations were made in previous scale-up experiments by Osorio et al. [113] and are most likely caused by the physical differences in gap size of the granulator, which limits the granule growth naturally by the available space and is also taken into account in recent population balance models for TSWG [140], [141]. In contrast to the observed effects of different L/S-ratios during the DoE in 3.1.3, these differences in GSD almost diminished after the milling process, indicating that while the critical size within the granulator differed, all granules produced at the same L/S-ratio were similarly strong affected by the milling process.

These observations were further quantified by the computed EMD (Table 7).

Before milling the calculated EMDs were larger than 500 µm for runs performed at similar L/S-ratios on different scales. After milling the EMDs were then drastically reduced to a level comparable to the prior reproducibility experiments (~20 µm for most runs). Analyzing the effect of different L/S-ratios on the large-scale granulator further

confirmed these observations as the differences in GSDs were persistent before and after milling (Figure 12b) and the respective EMDs were also all larger than 100 µm after milling. As the L/S-difference between the compared GSDs increased, the EMD also increased significantly for granules before and after milling.

Table 7 EMD overview Placebo formulation. Measurement runs were compared to the respective reference run. Q1 signals the run was performed on the small scale, Q25 means it was performed on the QbCon 25

		EMD [µm]		
Reference	Measurement Run	before milling	after milling	L/S-difference between runs
Q1	Q25 -S1	740	40	0
	Q25 - S2	570	23	0
	Q25 - S3	764	18	0
	Q25 - R	533	23	0
Q1 - L/S 0.13	Q1 - L/S 0.195	177	107	0.065
Q1 - L/S 0.195	Q1 - L/S 0.26	158	114	0.065
Q1 - L/S 0.13	Q1 - L/S 0.26	302	147	0.13
Q25 - L/S 0.13	Q25 - L/S 0.195	287	103	0.065
Q25 - L/S 0.195	Q25 - L/S 0.26	201	118	0.065
Q25 - L/S 0.13	Q25 - L/S 0.26	487	221	0.13

EMD Range for reproducibility runs: 2-24 µm

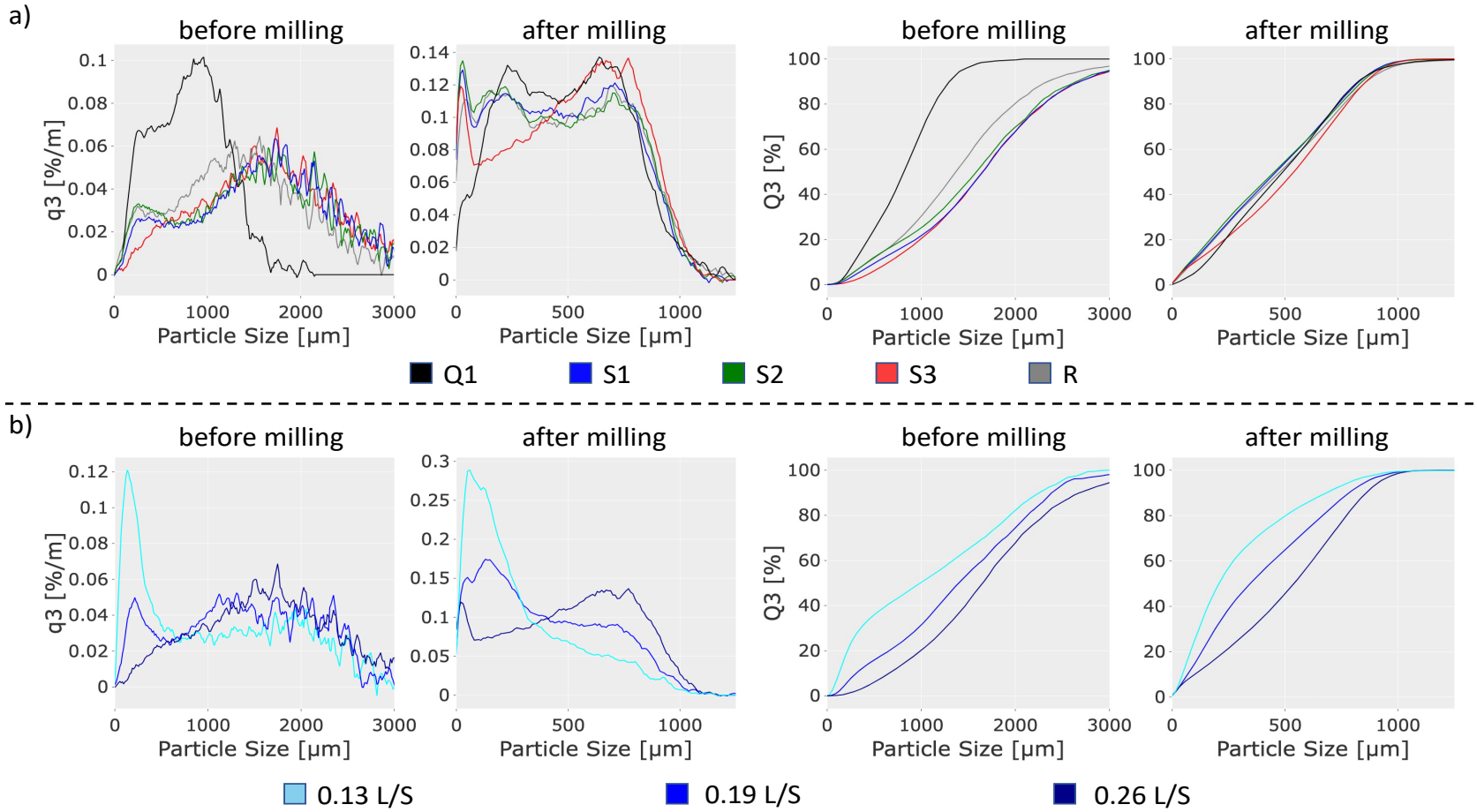

Figure 12 GSD of granules before and after milling. a) based on granulator scale and scale-up strategy (Q1 – QbCon© 1, S1 – strategy 1, S2 – strategy 2, S3 – strategy 3, R – reference run) and b) based on the L/S-ratio (0.13, 0.19, 0.26) during granulation on the QbCon© 25.

Regarding the flowability of the produced granules, only minor differences between any of the strategies could be observed (see Table 6). However, as can be seen in Figure 13, the mean Hausner ratio for granules performed on the large granulator was slightly lower (indicating slightly better flow properties) than the Hausner ratio for runs performed on the small granulator. On the small scale a slight trend towards lower Hausner ratios with increasing L/S-ratio was also observed, which also occurred for the granules produced on the QbCon© 25 but to such a small extent, that the impact is likely neither significant nor practically relevant. As measurements were only performed once, these results are subject to uncertainty as the data available is not sufficient for a definite statement.

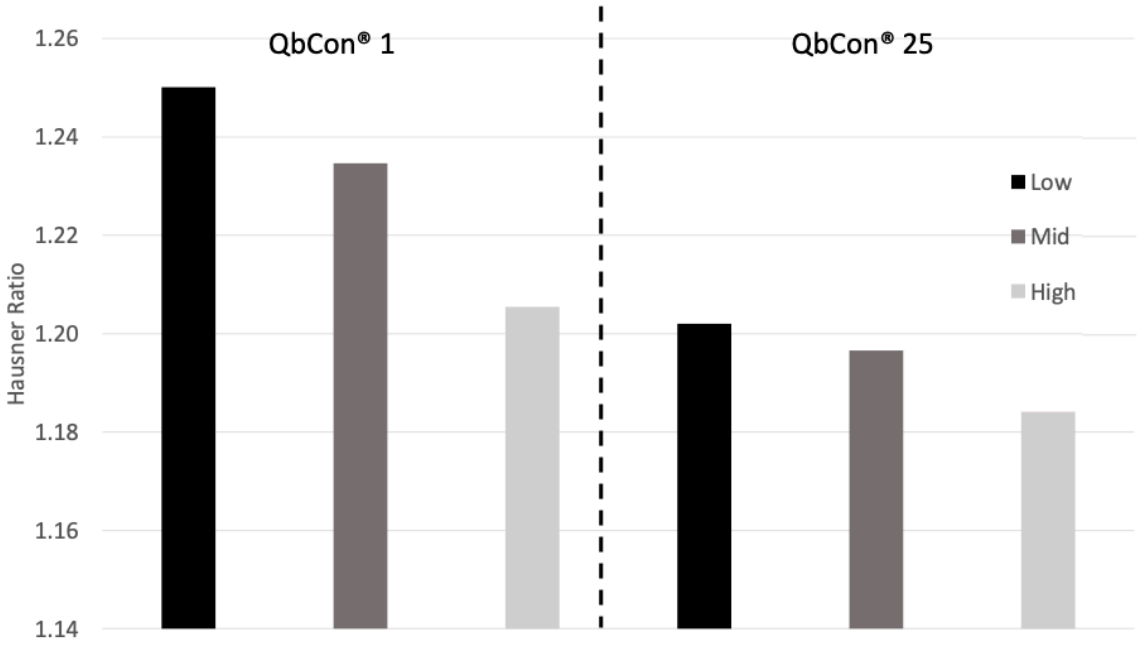

Figure 13 Mean Hausner Ratio of granules produced on both scales based on all runs included in Table 6 grouped by L/S-Ratios (Low – 0.13, Mid – 0.195, High – 0.26) first published in the International Journal of Pharmaceutics, [125] and used by courtesy of Elsevier

As the effect of SS on MRT and RTD was also reported by various other research groups , it came as no surprise that the RTDs for the granulator (Table 6) were strongly affected by the employed scale-up strategy as the SS and PFR varied greatly between those runs. In direct comparison of scale-up strategies with the respective run performed on the QbCon® 1, the MRT decreases significantly with increasing screw speed among all observations (e.g., sorted from lowest SS to highest for the runs highlighted with a * in Table 6: 65 s for S 2, 54 s for S1, 28 s for S3). The L/S-ratio also

affected the measured residence times strongly as can be seen in direct comparison of runs with otherwise identical process parameters (22 s versus 54 s MRT for S1 and 13 s versus 28 s for S3). As the measurements were carried out using an almost hydrophobic color dye with a very low solubility in water, no bleed-out of the color onto all granules occurred and thus the observed color gradient was most likely caused by dye particles being attached to the surface of the granules. At higher liquid rates the binding capacity of the added PVP increased and thus larger particles were created overall. These larger particles were more likely to be held back and be subject to further breakage inside the granulator and thus the overall material flow was slowed down while more back-mixing occurred. Similar observations were also made by Liu et al. with even higher L/S-ratios [89]. Despite substantial differences in t_{Max} and MRT between scale-up strategies and runs performed on the smaller scale (and thus differences in exposure time of the dry binder and powder blend to the liquid), there did not seem to be any direct effect on the resulting granule or tablet strength. This is indicative of a comparable liquid-solid distribution inside the granulator independent of the MRT.

Consistent with observations made in the previous DoE, tabletability also increased with increasing L/S-ratio (exemplary shown for S1 in Figure 14a) on the large-scale granulator. While this was in line with expectations, the high similarity in the tabletability of granules produced based on different scale-up strategies and especially their respective reference runs on both scales (Q1 and R) was not anticipated (Figure 14b).

Despite substantial differences in CS, MRT, PFN and overall throughput among the strategies and the reference run, the observed tensile strengths of the tablets were fairly similar (i.e., between 1.70 MPa and 1.97 MPa for different strategies and 1.76 MPa for tablets pressed at 150 MPa with the referenced parameters on the small scale) while significantly larger differences were observed for runs performed at different L/S-ratios (1.48 MPa at L/S 0.13 to 2.13 at L/S 0.26 MPa on the small scale and 1.45 to 2.08 MPa on the large TSWG line respectively).

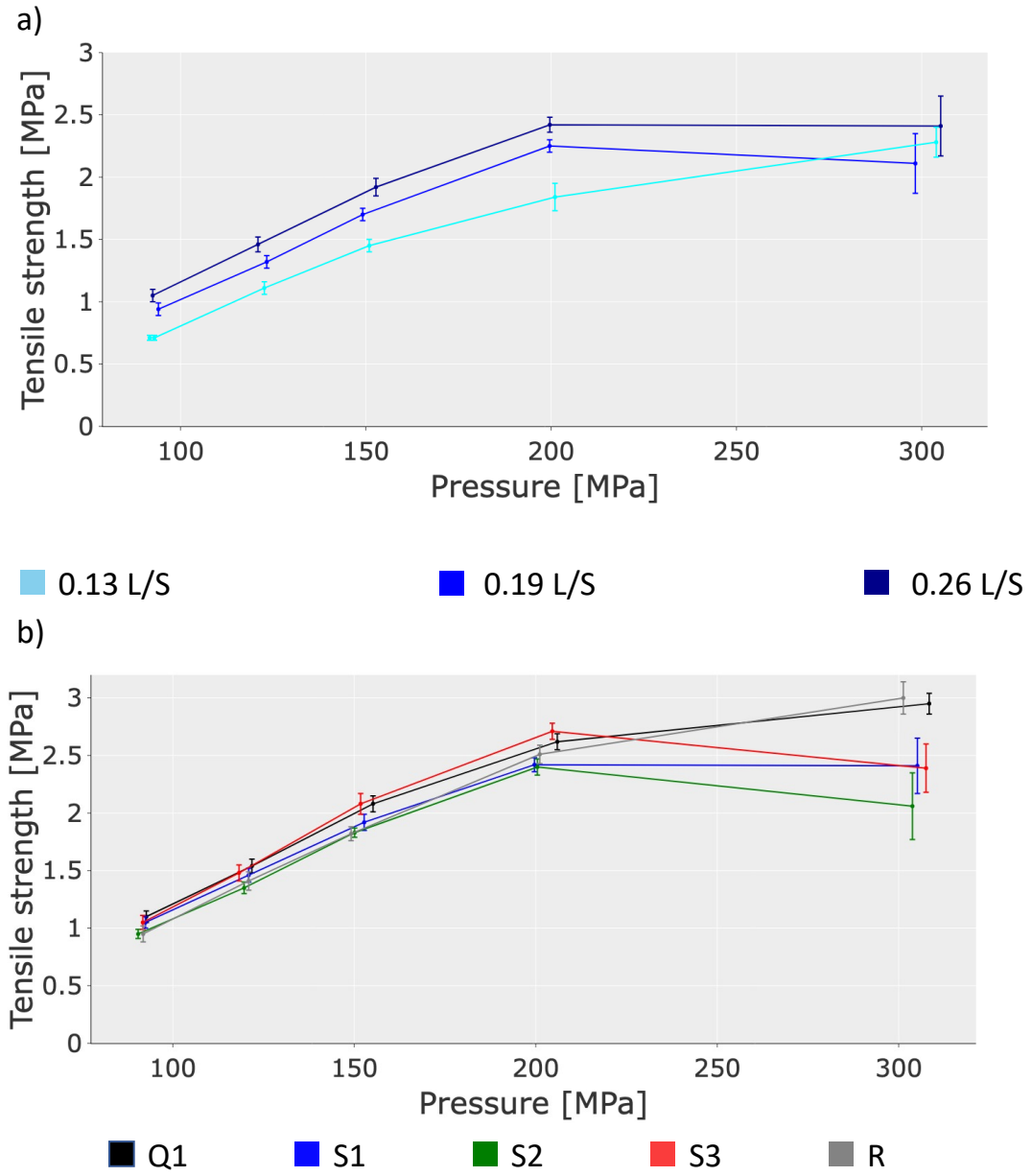

Figure 14 Tabletability from scale-up experiments. a) for S1 at different L/S-ratios but constant SS/PFR, b) based on different scales and strategies (see legend); mean ± standard deviation; n=20

Furthermore, as can be seen for S2 in Figure 14b, in some cases the tensile strength of compressed tablets decreased when the compaction pressure increased from 200 MPa to 300 MPa, while the standard deviation increased. Both, extensive mixing times with the lubricant, which are known to have a negative impact on tablet strength [150], [151], and possible segregation within the feed shoe of the tablet press could be rejected as potential causes for this effect in additional tableting experiments. Mazel and Tchoreloff [152] described high compaction speeds with insufficient precompression pressures as one possible cause for lamination of tablets at high

compaction pressures in their work. Thus, additional tablets using a different compaction cycle (see 5.2.2.7) were made from granules where this effect was observed and analyzed. This resulted in significantly higher tensile strengths at 300 MPa without any irregularities in the standard deviation. Therefore, in all further experiments the compaction cycle was adapted to prevent disturbances caused by the tableting process.

The requirements for tablet disintegration time defined by the European Pharmacopeia [4] (disintegration time < 15 minutes) were met.

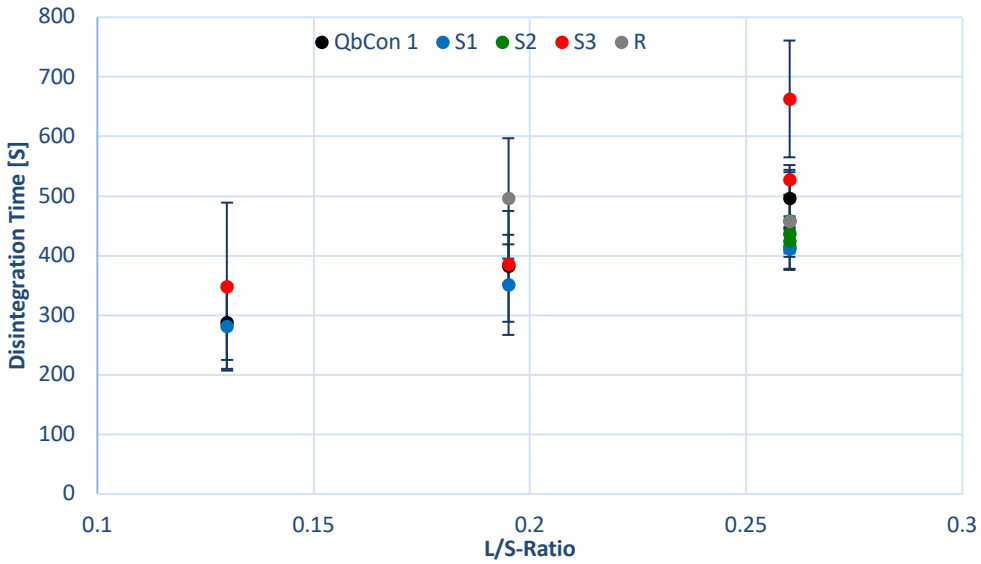

Figure 15 Disintegration time of tablets (compressed at 150 MPa) plotted against L/S-Ratios for all runs performed during scale-up; mean ± standard deviation; n=6, first published in the International Journal of Pharmaceutics, [125] and used by courtesy of Elsevier

However, in many cases internal requirements of pharmaceutical companies aim for lower disintegration times (e.g., below 10 minutes) to ensure the highest quality standards are met. With the exception of one run on the large-scale granulator (S3, 0.26 L/S, 300 SS), all tablets that were compressed at 150 MPa disintegrated within 10 minutes (Figure 15). However, as can be seen, the mean variance was relatively high, which might have been caused by the devices' automatic endpoint detection, which seemed to be delayed or not working in some cases. Similar to observations made during the DoE on the small scale, the friability of tablets at all compaction pressures was sufficient with high (0.26) L/S-ratios while tablets compressed from granules produced at L/S 0.13 (and partly with 0.195) did only meet the requirements

(friability < 1 %) at compaction pressures of 120 MPa or higher (Figure 16). At higher compaction pressures the observed differences were mitigated as the overall friability was reduced to values lower than 0.5 % in all cases.

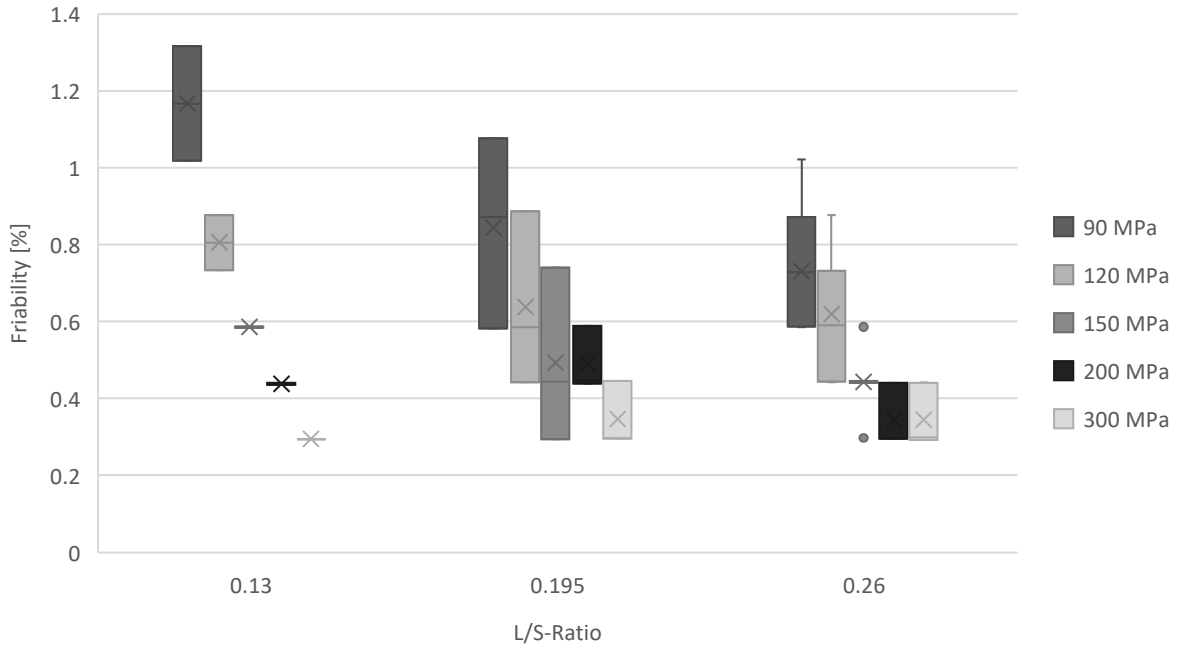

Figure 16 Friability of tablets produced from granules made at different L/S-ratios (0.13, 0.195, 0.26), compressed at 90 MPa, 120 MPa, 150 MPa, 200 MPa and 300 MPa respectively.

3.2.4 Summary

Scale-up experiments were performed based on three previously developed scale-up strategies where the PFN as dimensionless surrogate of the fill level was kept constant while other process variables, such as the RTD in the granulator, the CS of the screws or the PFR were changed. Concurrently, an additional reference run, where all granulation process parameters were used without any adaptations to either the PFR or the SS, was performed, thus imposing a high level of starvation in the large granulator due to the unusually low PFR. In addition to the selected strategies and the reference run further granulations were performed at varying L/S-ratios to compare its effects on both scales.

The highest impact of the granulator scale was observed for the GSD prior to milling, where the different sizes of the granulator substantially impacted the maximum granule size and thus large EMDs indicating a high dissimilarity were computed when the different scale-up strategies were compared to the respective run on the small-scale.

Other than differences in GSD caused by different L/S-ratios, which seem to persist after milling due to varying granule strengths, the differences in GSD became almost negligible after milling. Unsurprisingly, RTDs of granules were strongly impacted by the selected scale-up strategy as the SS was adjusted heavily.

Since all three developed scale-up strategies were based on keeping a similar PFN and thus barrel fill level while simultaneously constraining known disturbance factors, such as the L/S-ratio and the barrel temperature, the high similarity in tablet properties was not unexpected. More surprisingly though, the differences in tabletability were neglectable even at the substantially lower barrel fill level and thus a high level of starvation inside the granulator during the reference run ***R***.

This raised the question whether the TSWG was simply robust and offered an uncomplicated scale-up experience when L/S-ratio was kept constant and similar dimensions were used for granulator and screws, or if the used placebo formulation was simply not sensitive enough to changes in process parameters.

3.3 Impact of different formulations on scale-up behavior

Parts of this section have already been published in the International Journal of Pharmaceutics [125] and in Pharmaceutical Development and Technology [153].

Adaptions for this work include:

- Linguistic changes
- Extension of datasets
- Changes and additions in graphs, labels and legends

3.3.1 Introduction

Newly found drug substances used in the development stage of pharmaceutical companies are usually remarkably variable in their physicochemical properties and required dosage and can thus provide a multitude of challenges for drug product developers without offering any universal approach that can be used. While some APIs can be used in concentrations < 1 % and typically do not have a strong impact on the overall processing of the powder blend, other APIs might require a high drug load and heavily impact the granulation and tableting behavior.

Various studies in TSWG have been performed to investigate the effect of differing excipient grades, and blend and binder composition at low and high drug loads [84], [133], [142], [154], [155]. Except for the studies performed by Djuric et al., where the experimental setup for the process setup was not ideal due to differences in granulator and screw dimensions, as well as screw configuration and geometry of the used elements, no scale-up studies have been performed to investigate the effect of formulation parameters on the overall scale-up behavior. All other scale-up related studies known to the author [80], [113], [125] have used placebo formulations in their investigations and found similar results on measured outcomes, such as GSD and tensile strength despite differences in e.g., screw configuration.

Therefore, it was worth examining how scale-up results might be impacted by different formulations that are potentially more sensitive to changes in other process parameters. For this reason, similar scale-up experiments as in 3.2 were performed using different formulations.

Formulations 2a and 3 (see Table 15 in 5.2.2.1) were based on the previously used placebo formulation (formulation 1) where metformin and praziquantel were added as model substances for a highly soluble API (metformin) and a poorly soluble API (praziquantel) to study the effect of the solubility on the scale-up behavior. For the selection of the third formulation used in this study, preliminary trials were performed to find one that would ideally be more sensitive to changes in process parameters and differ sufficiently from the other formulations in its composition.

In those preliminary trials two formulations (4 and 5, see Table 15 5.2.2.1) were compared regarding their granulation behavior on the small scale. Formulation 4 was a controlled release formulation that was previously used by Vanhoorne et al. [98] and contained HPMC as a binder which was reported to be more sensitive to changes in screw speed and PFR in another study by Thompson and O'Donnell [156]. Contrary to observations made in previous studies here (see 3.1), they showed a decrease in d50 and an increase in fines at increasing PFRs. Formulation 5 was based on experiments performed by colleagues in drug formulation at Merck Healthcare KGaA and described as overall more sensitive to changes in process parameters during granulation.

3.3.2 Preliminary trials for formulation selection

For the preliminary trials, the PFR was set to 2 kg/h and the barrel temperature to 30°C. The L/S-ratio was experimentally set so that the granules produced at a SS of 400 rpm were considered feasible after visual inspection (Figure 17) and could still be sufficiently dried in the VBFD (< 2 % LOD).

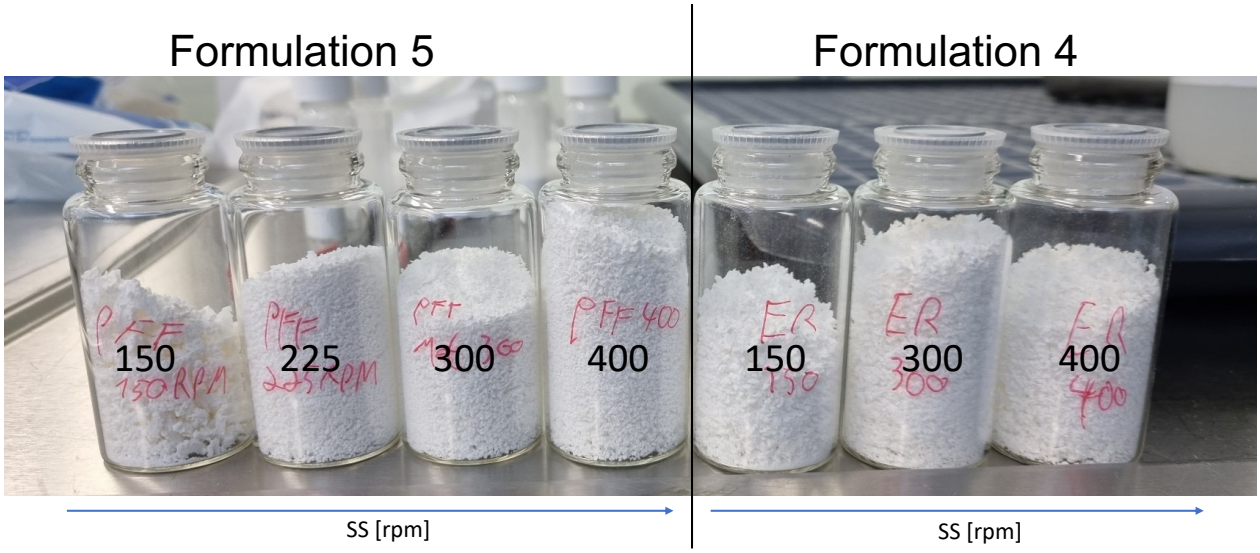

Figure 17 Granules produced at different SSs made from formulations 4 and 5. SS increasing from left to right

Thus, the L/S-ratio for formulation 4 was set to 0.15 and for formulation 5 to 0.18. A similar screw configuration as for previous scale-up experiments with formulation 1 was used during these preliminary trials. In the experimental setup, the SS was reduced after sample collection and thus samples for SSs of 400 rpm, 300 rpm and 150 rpm for formulation 4 and 400 rpm, 300 rpm, 225 rpm and 150 rpm for formulation 5 were collected. With decreasing SS, the occurrence of process disturbances caused by a blocked nozzle for the liquid feed increased significantly as the fill level of the granulator approached a flooded status and thus the likelihood increased that the nozzle was blocked by the sticky granulation mass (Figure 18). As a result, no further liquid could be pumped through the nozzle into the granulator and the running pump built up pressure behind the nozzle until the blockage was removed in one unconstrained splash that led to an immediate over-wetting of the dry blend and ultimately to the granulator and entry of the drier being blocked by a gummy-like substance that had to be manually removed before granulation could be continued.

a)

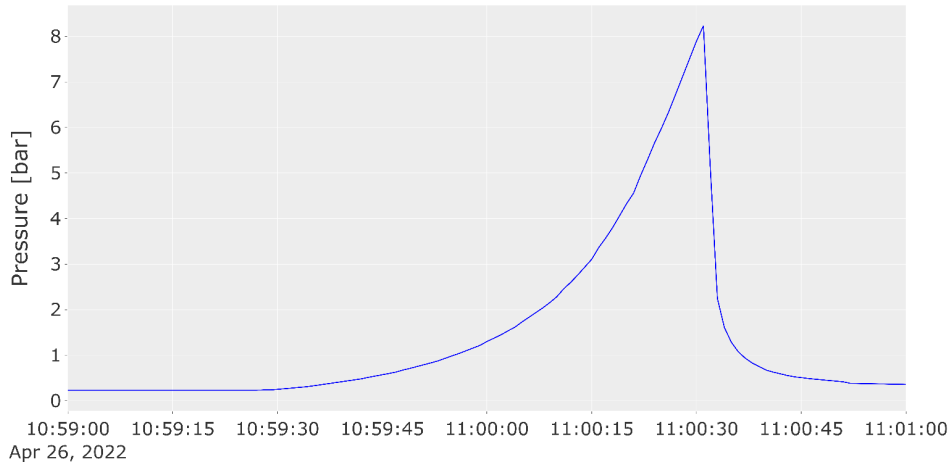

b)

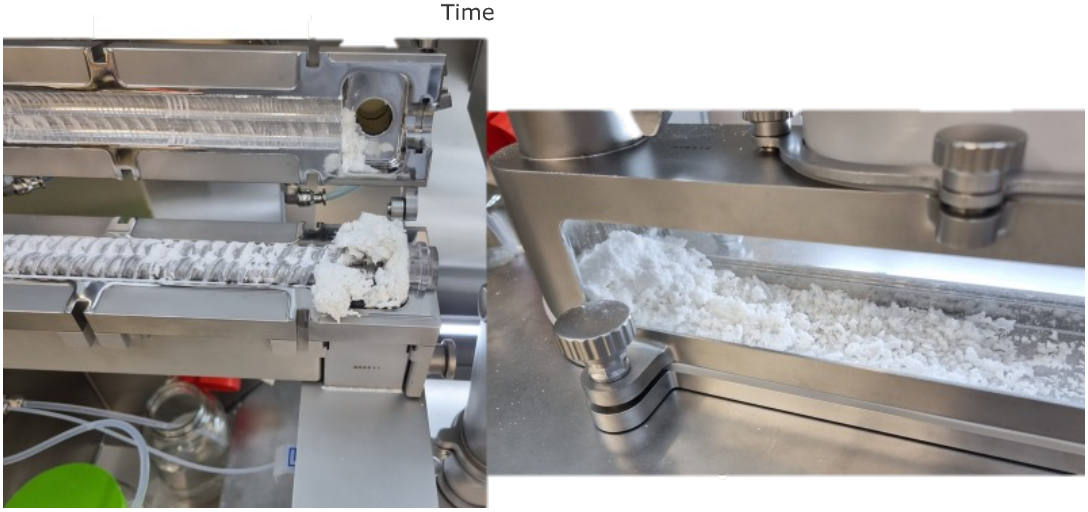

Figure 18 a) shows how pressure built up for the liquid pump during blockage of the nozzle until a high enough pressure was reached to remove the blockage b) is a visual representation of the occurrences inside the granulator and drier when the blockage is removed by an unrestrained splash, first published in Pharmaceutical Development and Technology [153] and used by courtesy of Taylor & Francis

As previously mentioned, the frequency of these disturbances increased with decreasing screw speed. It could, however, be slightly reduced by using a smaller nozzle with a diameter of 0.12 mm. Nevertheless, at the lowest SS setting of 150 rpm these blockages could not be prevented entirely for either of the formulations even after the nozzle size was reduced. For further evaluation and to select one of the formulations for further scale-up experiments the GSDs before and after milling and the effect of the SS (and thus indirectly the fill level) on the GSDs were examined (*Figure 19*).

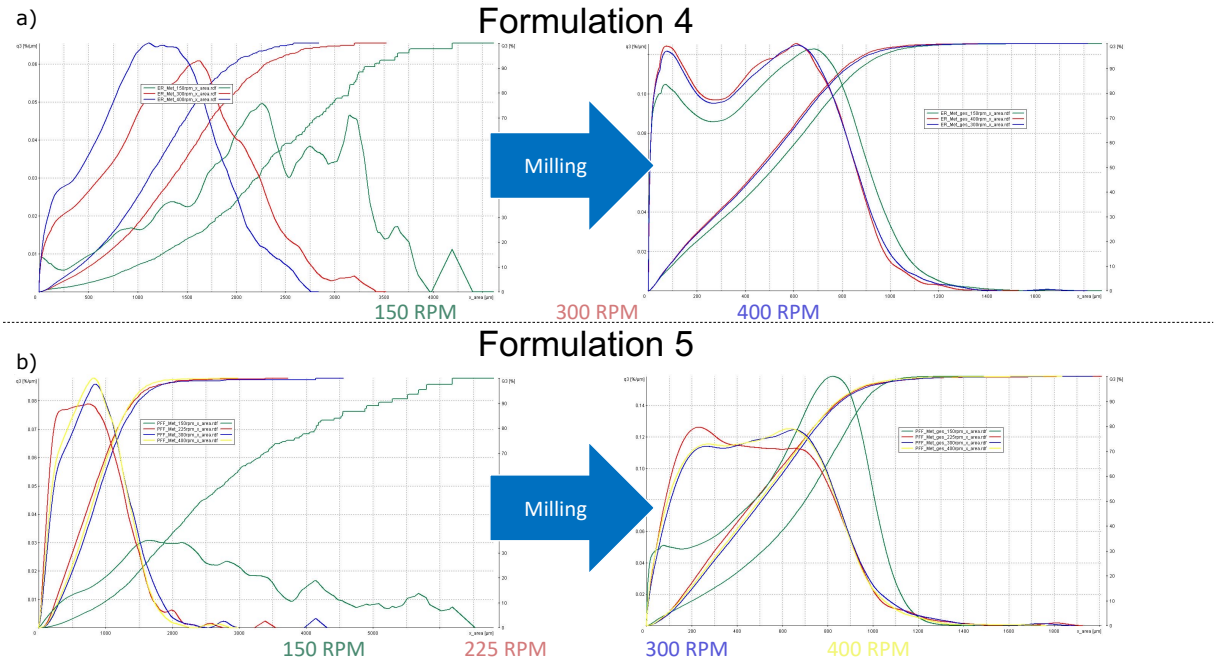

Figure 19 GSDs of granules produced at different screw speeds (between 150 and 400 rpm) during the preliminary trials. Y-axis shows q3 [%/mm, x-axis for the particle size [µm].

While for formulation 5 the size of particles increased substantially at 150 rpm and no further distinctions for the other settings could be made, the GSD of granules manufactured from formulation 4 before milling were more distinct for each of the three screw speed settings. After milling the GSDs for both formulations were rather similar at SSs higher than 150 rpm but still shifting towards larger granule sizes at 150 rpm where the effect was strongest for formulation 5.

The focus of this work was set to be the TSWG process and since formulation 4 allowed for a better distinction of granules produced at different screw speeds right after granulation and differed substantially in its composition (all excipients differed from formulations 2a and 3), it was selected to be used for further scale-up experiments while formulation 5 was discarded. As a formulation that was initially designed for controlled release tablets, it also offered the opportunity to investigate the impact of the different scale-up strategies on the dissolution of tablets as an additional output parameter.

3.3.3 Impact of different formulations on the scale-up experience

The process parameters for all scales and strategies can be found in Table 8. Displayed process parameters were determined during additional preliminary trials beforehand to ensure a sufficient drying of granules (LOD < ~1.5 %) and reduce the occurrence of the observed pump blockage on the small scale (thus minimum SS is set to 175 rpm for formulation 4). Additionally, the smallest nozzle (0.12 mm) was selected for runs with formulation 4 and the first conveying zone was prolonged by an additional CE taken from conveying zone 2 (see Table 16 and Figure 36 in 5.2.2.2) to prevent powder build-up in front of the liquid addition and thus reduce the occurrence of blockage of the nozzle and enable a stable process even at lower SSs. Interestingly, this blockage did not occur on the large-scale granulator even when the kneading zone was not moved further away from the nozzle, which is most likely caused by the higher liquid pressure (higher than 1 bar on the large scale versus 0.3 bar on the small scale at similar fill levels when using the same nozzle (0.12 mm) at overall higher liquid feed rates). A similarly low liquid pressure was only observed during the reference runs ***R*** where the large-scale granulator was at a substantially lower PFN and thus in a starved condition where blockage of the nozzle was less likely to occur.

Granulation runs performed on the larger scale, where a pre-blend of the powder was transported from a large container into the feeding and blending unit (FBU) posed an unforeseen challenge for formulation 3 as the process on the large scale was regularly interrupted when the feeder of the granulator could not be automatically refilled. The feeding and blending unit consisted not only of the continuous feeder or the continuous blender, where particles were actively transported, and the process could thus adapt even to poorly flowing powders, but also of different pipes where the powder was transported by gravitational force only. As a reason for the interrupted flow to the feeder, powder bridging was observed in some of these pipes (see Figure 40 in the appendix) most likely due to the poor flowability of the blend (ffc 3.7 and thus classified as ‘cohesive’ according to Jenike [157] versus 5.3 for formulation 4 and 9.1 for formulation 2a, which is both classified as “easy flowing”). The poor flowability could potentially be corrected by adding e.g., silica nanoparticles as glidants [158].

Table 8 Overview of process parameters and LOD for granulator and drier during scale-up experiments for different formulations. SS – screw speed, PFR – powder feed rate, PFN – powder feed number, CS – circumferential speed, DT – drying temperature and LOD – loss on drying

	Strategy	SS [min^{-1}]	PFR [kg/h]	L/S-Ratio [%]	PFN	CS [m/s]	Vib. Acc. [m/s]	Airflow [Nm^3/h]	DT [°C]	LOD [%]
Formulation 2a	Q1	150	2	0.195	1.50E-02	0.13	5.0	30	75	1.34
		300	2	0.195	7.60E-03	0.25	5.0	30	75	1.11
	S1	150	8	0.195	1.60E-02	0.20	5.0	300	70	1.12
		300	8	0.195	7.80E-03	0.40	5.0	300	70	1.22
	S2	95	5.1	0.195	1.50E-02	0.13	5.0	175	65	1.13
		190	5.1	0.195	7.70E-03	0.25	5.0	175	65	1.15
	S3	375	20	0.195	1.60E-02	0.49	5.0	320	90	1.29
		750	20	0.195	7.80E-03	0.99	5.0	320	90	1.06
	R	150	2	0.195	3.90E-03	0.20	5.0	125	70	1.52
		300	2	0.195	1.90E-03	0.40	5.0	110	65	1.34
Formulation 3	Q1	150	2	0.26	1.70E-02	0.13	5.0	30	80	1.15
		300	2	0.26	8.30E-03	0.25	5.0	30	80	1.11
	S1	150	8	0.26	1.60E-02	0.20	5.0	300	60	1.43
		300	8	0.26	7.80E-03	0.40	5.0	300	60	1.35
	S2	95	5.1	0.26	1.50E-02	0.13	5.0	200	50	1.07
		190	5.1	0.26	7.70E-03	0.25	5.0	200	50	1.15
	S3	375	20	0.26	1.60E-02	0.49	5.0	330	90	1.41
		750	20	0.26	7.80E-03	0.99	5.0	330	90	1.39
	R	150	2	0.26	3.90E-03	0.20	8.0	130	70	1.33
		300	2	0.26	1.90E-03		8.0	130	70	1.48
Formulation 4	Q1	175	2	0.13	1.50E-02	0.15	5.0	30	90	1.24
		300	2	0.13	7.80E-03	0.25	5.0	30	90	1.08
	S1	175	8	0.13	1.30E-02	0.23	4.5	200	80	1.2
		300	8	0.13	7.80E-03	0.40	4.5	200	80	1.24
	S2	111	5.1	0.13	1.30E-02	0.15	4.5	150	80	1.23
		190	5.1	0.13	7.70E-03	0.25	4.5	150	80	1.35
	S3	438	20	0.13	1.30E-02	0.58	4.5	300	85	1.02
		750	20	0.13	7.80E-03	0.99	4.5	300	85	0.91
	R	175	2	0.13	3.30E-03	0.23	8.0	130	70	1.44
		300	2	0.13	1.90E-03	0.40	8.0	130	70	1.38

Similar to prior observations with formulation 1 and in line with the findings made by Osorio et al. [114, the GSD of granules (Figure 20a) prior to milling and their respectivecumulative distributions (Figure 20b) were significantly impacted by the granulator scale for formulations 2a and 3, which were both based on mannitol, MCC and PVP.

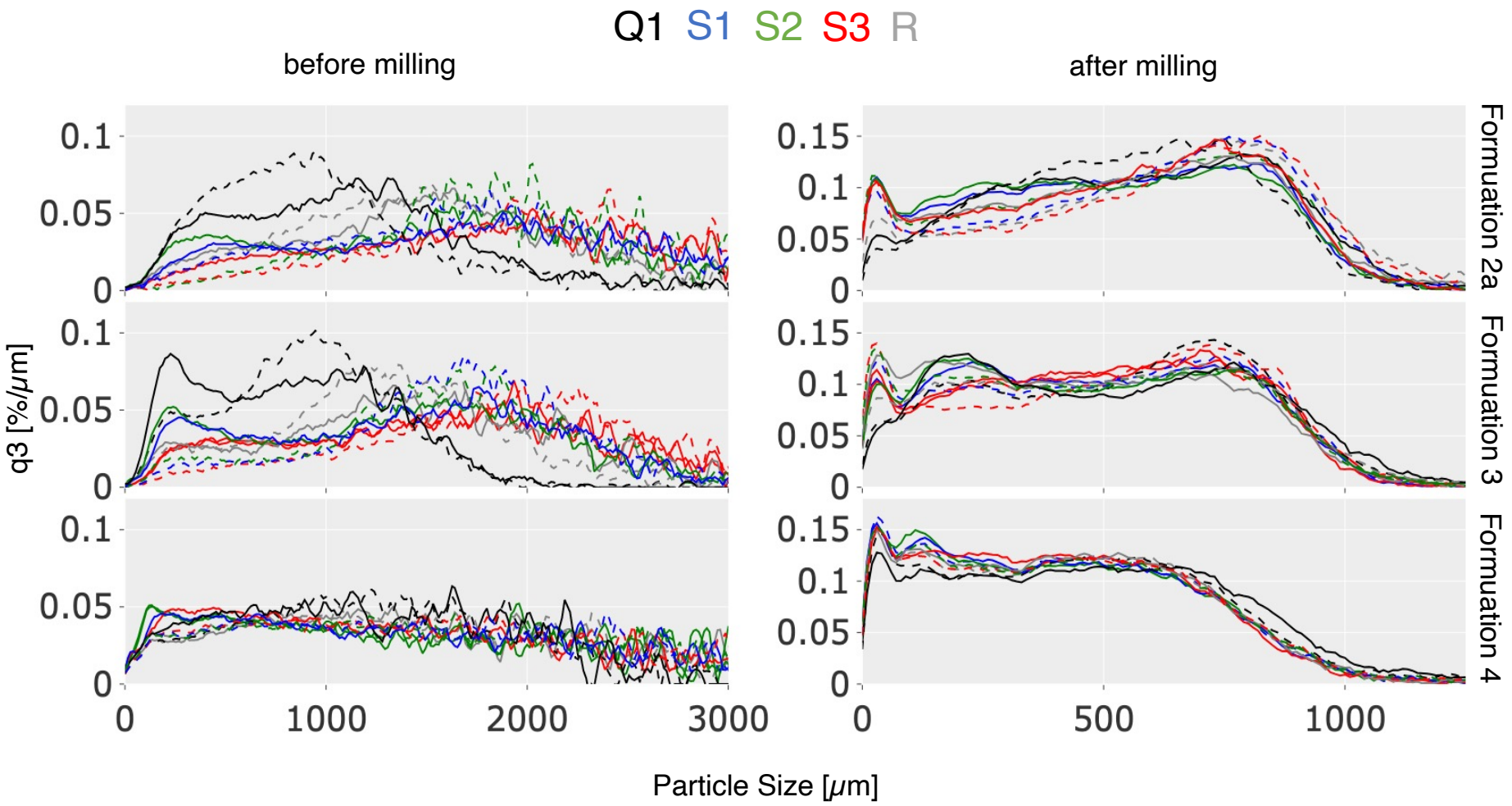

Figure 20a GSD of granules for each formulation, Strategies and scales depicted in different colors (S1 – blue, S2 – green, S3 – red, R – grey) with black lines as reference for the small-scale. Dashed lines for high SS settings

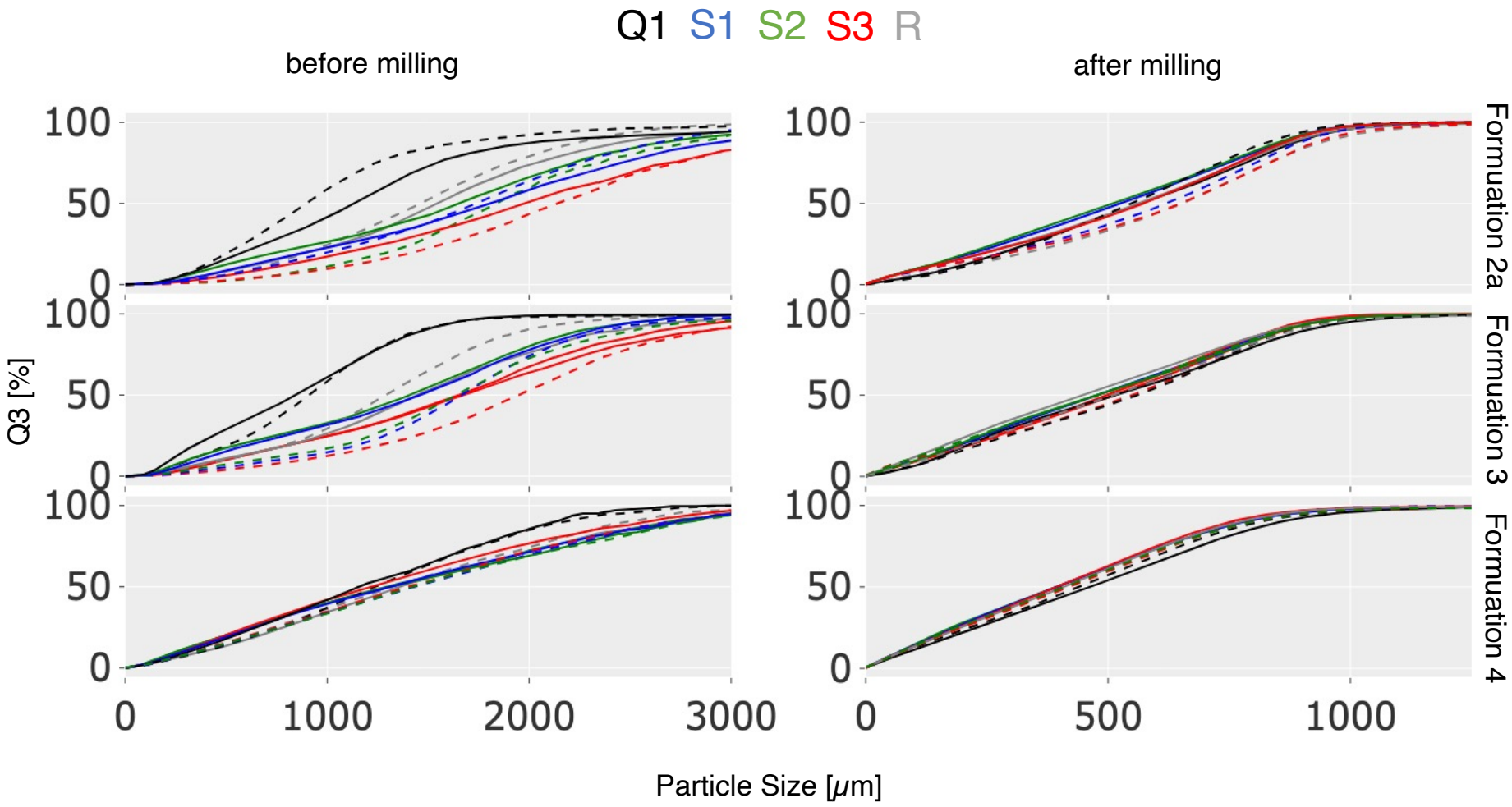

Figure 20b respective sum distributions of GSDs shown in Figure 20a, Strategies and scales depicted in different colors (S1 – blue, S2 – green, S3 – red, R – grey) with black lines as reference for the small-scale. Dashed lines for high SS settings

Remarkably, for formulation 4, the GSDs of granules were much more similar compared to the other formulations even before additional milling occurred and granules that were much larger than what appeared to be the critical granule size for the other formulations on the smaller scale could be produced. For additional comparisons the EMDs were computed to evaluate the differences in GSD between the different applied strategies and the respective runs on the smaller granulator (Table 9). While EMDs of granules prior to milling ranged from 370 to 1100 µm for formulation 2a and from 380 to 1005 µm for formulation 3, the range for formulation 4 was much narrower and the overall values were substantially smaller (140 – 260 µm), further confirming this observation.

Another noteworthy aspect is the relatively similar GSD of granules produced from formulation 2a and 3 despite the differences in L/S-ratio. Granules produced at the lower L/S-ratio (formulation 2a) even appear to have fewer fines than those produced at a L/S-ratio of 0.26 with formulation 3. Similar findings related to the hydrophobicity of the used drug substance (here metformin versus praziquantel as model substance) have been reported by other research groups [95], [159], [160]. With decreasing solubility in water, the particle size of granules at similar L/S-ratios decreased and the blend becomes less sensitive to binder spreading as the API itself interacts less with the liquid.

Expectedly and analogous to the observations made previously with the placebo formulation, differences in GSD between scales were drastically reduced after an additional milling step (see also Figure 41 in the appendix). In some cases, slightly higher EMDs than in previous work packages were observed (e.g., 86 µm and 88 µm for S3 and ***R*** at high SS settings for formulation 2a), but no correlation was found to either the EMD prior to milling or any process parameters. A trend towards higher EMDs at the high SS setting for the scale-up strategies (but not for ***R***) could be observed prior to milling, which did not persist after milling, however.

Table 9 Earth Mover's Distance for comparison of scale-up strategies with small scalel at different SS levels

Formulation	Reference	Strategy	Low SS		High SS	
			Before milling	After milling	Before milling	After milling
2a	Q1	S1	560 µm	45 µm	710 µm	59 µm
		S2	420 µm	54 µm	870 µm	34 µm
		S3	700 µm	20 µm	1100 µm	86 µm
		R	370 µm	21 µm	480 µm	88 µm
3	Q1	S1	540 µm	26 µm	720 µm	26 µm
		S2	500 µm	42 µm	702 µm	59 µm
		S3	740 µm	32 µm	1005 µm	20 µm
		R	620 µm	16 µm	380 µm	25 µm
4	Q1	S1	221 µm	60 µm	240 µm	23 µm
		S2	227 µm	62 µm	250 µm	37 µm
		S3	146 µm	66 µm	210 µm	41 µm
		R	260 µm	56 µm	140 µm	23 µm

Remarkably, despite vast differences in the applied L/S-ratio between formulations 2a (L/S 0.195), 3 (L/S 0.26) and 4 (L/S 0.13), and thus the total amount of water that was added during granulation at similar PFRs, the process parameters that were set for the continuous drier to reach a similar residual moisture of granules, were relatively similar amongst runs with otherwise identical granulation parameters.

The success of the continuous drying process is determined by the amount of water that needs to be removed, the drying time (and thus the RTD in the VFBD [102]) and the drying rate, which is dependent on air conditions (i.e., temperature, humidity and flow rate) as well as particle size and layer thickness inside the drier [103], [161], [162]. As the amount of water varied substantially, while air conditions were similar among all runs, it seems plausible, that either the RTD for the drying process was shorter for the drier granules as transportation through the drier might be faster for lighter particles or the drying rates differed significantly due to e.g., a higher layer thickness inside the drier.

Conforming to its purpose, the granulation increased the flowability measured by the ffc of all powder blends substantially (Table 10). All milled granules could be classified either as freely flowing (ffc >10) or as easy flowing (ffc between 4 and 10). Overall, the ffc appears to be slightly higher for granules produced on the smaller scale, however, as measurements were only performed once in most cases due to limitations in the

remaining sample size, the available data was not sufficient to identify trends with any significance.

Table 10 Overview of product properties of milled granules (runs are depicted similarly to Table 8: first row for each strategy used for low SS settings, second row for high SS settings) used by courtesy of the International Journal of Pharmaceutics, Elsevier

	Strategy	ρ_{bulk} [g/mL]	ρ_{tapped} [g/mL]	ffc	Tensile Strength (at 150 Mpa) [MPa]	Friability (at 150 MPa) [%]
Formulation 2a	Q1	0.55	0.65	24.3	2.36	0.27
		~~0.51*~~	~~0.59*~~	21.3	2.49	0.24
	S1	0.58	0.69	19.1	2.19	0.29
		0.58	0.68	11.6	1.84	0.21
	S2	0.58	0.68	15.9	2.18	0.34
		0.58	0.68	18.2	2.17	0.26
	S3	0.57	0.69	15.6	1.98	0.26
		0.59	0.71	14.1	1.99	0.34
	R	0.58	0.69	12.3	2.02	0.22
		0.58	0.68	15.0	2.11	0.12
Formulation 3	Q1	0.51	0.60	13.1	3.00	0.24
		0.50	0.59	11.4	3.41	0.22
	S1	0.53	0.63	11.5	2.95	0.29
		0.53	0.63	9.7	3.26	0.26
	S2	0.52	0.62	11.0	3.00	0.34
		0.52	0.63	12.1	3.43	0.27
	S3	0.53	0.62	12.0	2.96	0.37
		0.54	0.65	11.0	3.20	0.28
	R	0.51	0.62	11.3	3.28	0.22
		0.53	0.63	10.8	3.14	0.15
Formulation 4	Q1	0.47	0.57	9.1	1.30	0.57
		0.48	0.60	11.8	1.31	0.63
	S1	0.50	0.62	10.2	1.27	0.59
		0.49	0.60	9.9	1.65	-
	S2	0.50	0.62	-	1.45	0.52
		0.50	0.61	8.8	1.51	0.43
	S3	0.50	0.62	8.9	1.43	0.40
		0.49	0.60	8.9	1.35	0.41
	R	0.48	0.60	8.9	1.39	0.52
		0.48	0.61	9.5	1.61	0.32

*as measurements were only performed with n=1 this measurement could be a potential outlier caused by an inaccurate measurement

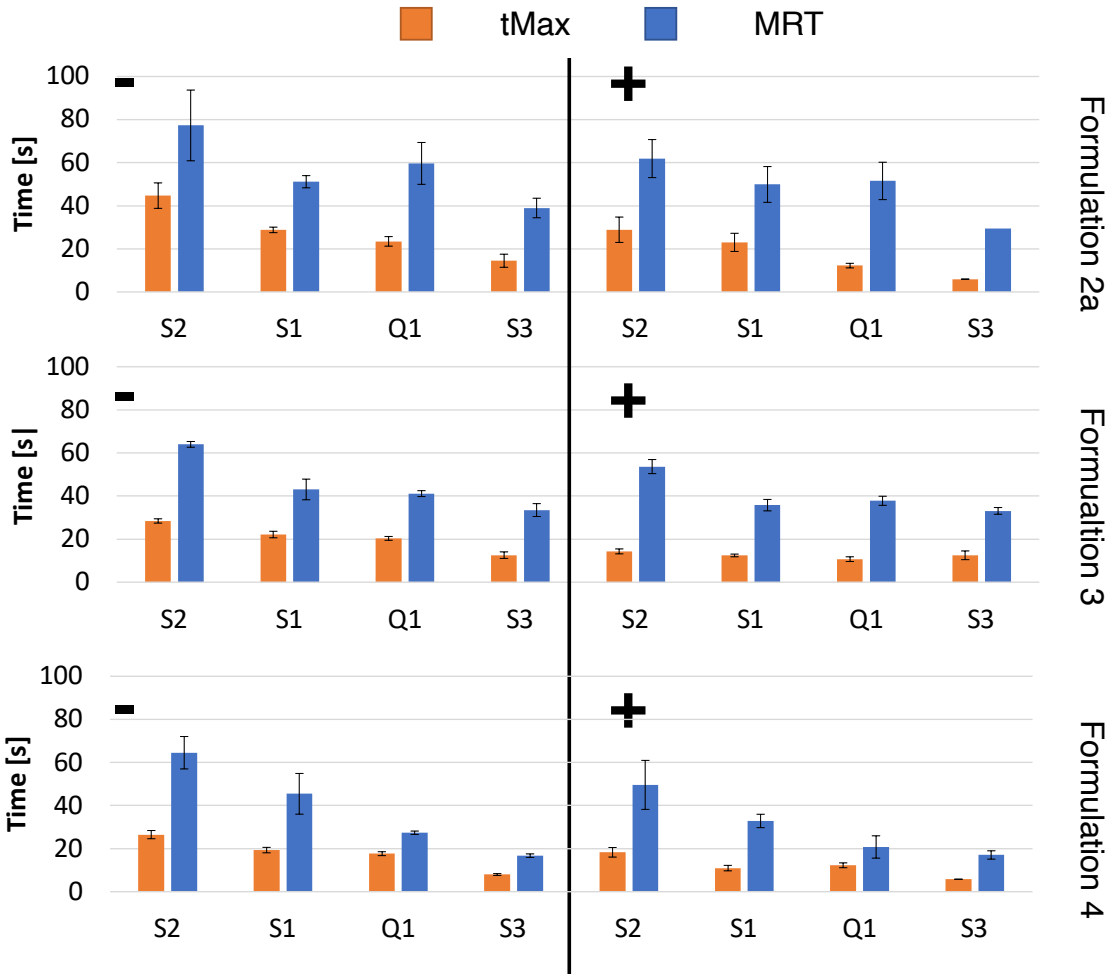

Figure 21 Overview of t_{Max} and MRT for all runs. + for respective high SS setting of each strategy, - for low SS setting. Runs are ordered from lowest to highest SS on each side (-/+), respectively; mean ± standard deviation; n=3. first published in Pharmaceutical Development and Technology [153] and used by courtesy of Taylor & Francis

In accordance with prior experiments and observations in literature, RTDs of granules inside of the granulator were strongly affected by the SS during granulation. Consequently, highest t_{Max} and MRT were observed for S2, while the shortest t_{Max} and MRT occurred for S3 where the SS was set highest (Figure 21). In agreement with the desired goal for S1 (achieving similar residence times on both scales), both t_{Max} and MRT for S1 and Q1 were bearing the greatest resemblance especially for formulations 2a and 3 where the computed values were in some cases within measurement uncertainties. This reveals a comparable powder flow throughout two differently sized granulators when PFN, SS, barrel temperature and L/S-ratio are kept similar, and the screw and barrel geometry are comparable despite the much higher surface area inside the larger granulator and thus the increased potential for friction around the inner

walls. Another interesting observation that could be made was that differences in RTDs between different strategies were more pronounced for formulations 2a and 4, while RTDs for Formulation 3 were more similar, especially at high SSs where a higher overlap occurs in the measured color signal curves (see Figure 44 in the appendix).

Regarding the tabletability, a few notable observations can be made from Figure 22 as well as Figure 42 and Figure 43 in the appendix. Firstly, between the three formulation groups, there were significant differences in tensile strength of tablets among all performed runs (Figure 42). As expected, the formulations varied greatly and the L/S-ratio, one of the most significant impact factors in TSWG, was also substantially different for each formulation [92], [132], [133], [163]. Secondly, a relatively big spread among the tensile strengths of both, tablets from different scale-up strategies, and the runs performed on the small-scale granulator could be observed (i.e., 1.84 MPa – 2.49 MPa for formulation 2a, 2.95 MPa – 3.43 MPa for formulation 3 and 1.27 MPa – 1.65 MPa for formulation 4 at a compaction pressure of 150 MPa, Table 10). Even though sufficiently hard tablets could be produced for all three formulations, these differences indicate that the different process parameters for the scale-up strategies did have an impact on the tablet properties as the reproducibility of runs has proven to be decently high when the process parameters were kept constant (see 3.1.4).

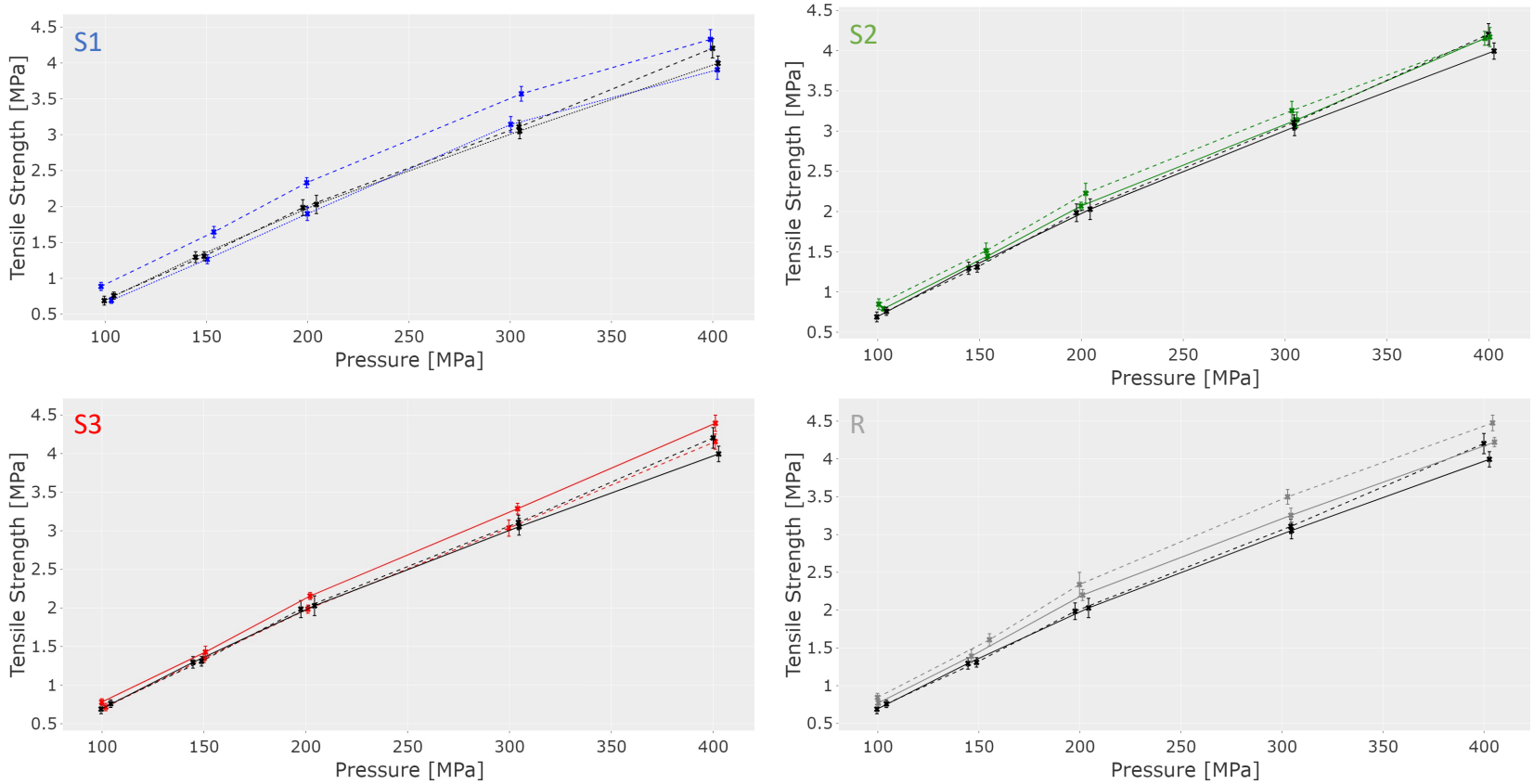

Figure 22 Exemplary showcase of tabletability based on scale-up strategy for formulation 4. Dashed lines correspond to high SS settings. Strategies depicted in different colors (S1 – blue, S2 – green, S3 – red, R – grey) with black lines as reference for the small scale (mean±SD, n=20), first published in Pharmaceutical Development and Technology [153] and used by courtesy of Taylor & Francis

To provide a more comparative analysis: at a compaction pressure of 150 MPa, tabletability ranged from 1.7 MPa to 1.97 MPa for experiments with the previous formulation (3.2.2) at similar L/S-ratios and between 1.45 MPa and 2.08 MPa at different L/S-ratios. However, the extragranular excipients that were added in the previous study accounted for 15 % of the total blend and thus likely reduced the differences in the blends to a higher degree than the 1 % lubricant added in the present context. Therefore, it seems reasonable that the tablet properties are affected by the changes in process scale and parameters, however it is questionable if these changes can be described by any universal model as the TSWG process is a highly complex interplay of different process parameters and formulation properties. In the context of this investigation, no clear trends based on the selected scale-up strategy, the SS, CS, PFR, PFN or the scale could be identified. Even though all tablets produced on the small scale for formulation 2a had a higher tensile strength than tablets produced on the larger scale, it is unclear if this is caused by a higher sensitivity specific to this formulation towards the process scale-up or if this was just an inconsequential phenomenon.

Irrespective of the reasons for this observation, it seems reasonable to assume that akin to the observations with formulation 1, the L/S-ratio would have a significantly stronger impact on the tensile strength of tablets than the process parameters that were adjusted for the different strategies and could therefore be used to offset differences in tensile strength during scale-up if necessary. Coincidentally, in this study, the formulations are sorted in similar order for both, increasing L/S-ratio and increasing tensile strength. However, due to the high complexity introduced by having different excipients between formulations 2a/3 and 4 and different APIs for formulations 2a and 3 the matter cannot simply be reduced to an impact of only the L/S-ratio.

Friability of tablets compressed at 150 MPa was sufficiently low (<1 %) for all performed runs independent of the selected formulation or scale-ups strategy (Table 10).

No significant differences in dissolution behavior between scale-up strategies or granulator scale could be observed for formulation 4 in this work (Figure 23). This is in line with the observations made by Vanhoorne et al., where the drug release was attributed to HPMC as a matrix former and neither the barrel temperature, SS, PFR nor the filler composition seemed to impact the drug release profiles in any way.

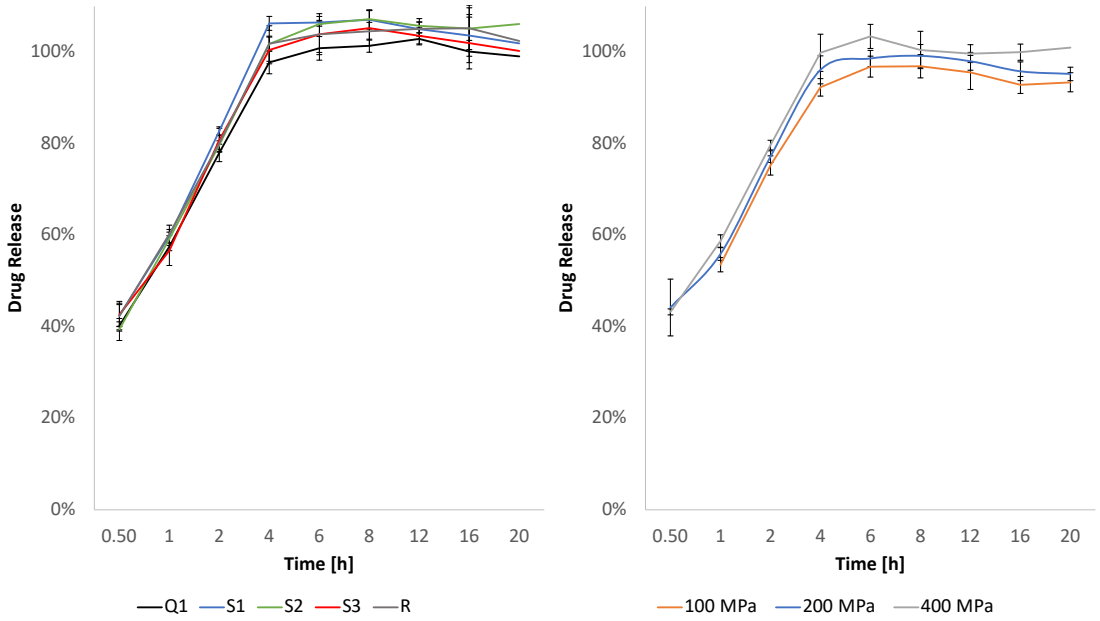

Figure 23 Drug release for formulation 4. Left: Exemplary data for each strategy (low SS), right: dissolution at three different compaction pressures for S1 (high SS) (mean±SD, n=3) first published in Pharmaceutical Development and Technology [153] and used by courtesy of Taylor & Francis

In another study, Lakio et al. [164] have shown that drug release for HPMC formulations was not impacted by the applied compaction pressure and thus the porosity of the tablets did not seem to impact the dissolution behavior. These results are in line with the observations shown in Figure 23. Overall, 50 % of drug release was already reached after between 0.5 and 1 hours and after 4 hours all of the metformin was released, which is substantially faster than the observed 16-20 h reported by Vanhoorne et al [98]. However, this is most likely caused by differences in diffusivity of the selected API (metformin versus metoprolol tartrate) and more importantly by the tablet diameter (13 mm versus 11.28 mm in this study) and their overall aspect ratio and surface area, which are known to impact release rates in extended release formulations based on HPMC [165].

3.3.4 Summary

The overall scale-up behavior of three different formulations in TSWG was explored based on scale-up strategies developed in previous experiments (see 3.2.2). Two of the used formulations were adapted from the placebo formulation of the previous study by adding an API that was either highly soluble in water (metformin) or almost insoluble in water (praziquantel) to examine the effect of hydrophobicity on overall granulation and scale-up behavior. The third formulation was selected in preliminary trials as its overall composition differed substantially from the other two blends in this study and it appeared to be potentially more sensitive to changes in process parameters. Furthermore, contrary to observations made with formulation 1, this formulation showed a decrease in GSDs with increasing PFRs during preliminary trials.

The selected formulations revealed additional challenges, such as powder bridging in the feeding and blending unit that was used to automatically refill the feeder of the granulator on the larger scale, or nozzle blockages caused by low liquid pressure in combination with a stickier binder at the water addition port on the smaller scale where the liquid pressure was lower.

Despite differences in the applied L/S-ratio, the GSD of formulations 2a and 3 where only the added API and its solubility changed was remarkably similar, especially after milling. For the controlled release formulation (4) the amount of oversized granules was significantly higher at the small scale, where typically very few particles > 2000 µm were observed in case of the other formulations. EMD as a measure of GSD similarity was significantly lower for these granules before milling versus granules produced from other blends so far. Nonetheless, EMDs for all granules irrespective of formulation or scale-up strategy decreased substantially (< 100 µm) after milling even at starved conditions during the reference runs, where all granulation parameters were kept similar for runs performed on the significantly larger granulator.

Plausibly influenced by the reduction in the amount of extragranular excipients to only 1 % (w/w) of lubricant added versus a total of 15 % (w/w) in 3.2.3, the differences in tensile strengths of tablets based on granulator scale and scale-up strategy were higher but nonetheless smaller than those observed with the placebo formulation at different L/S-ratios in 3.1 and 3.2. For formulation 2a, tablets produced on the smaller scale showed a minor trend towards higher tensile strengths that was not present in any other formulation so far and should be considered subject to uncertainty due to the

limited amount of data and the possibility of external impact factors, e.g., batch-to-batch variations in the pre-granulation blend. In addition to that, no universal trends based on SS, CS, PFR, PFN or RTDs could be identified.

As anticipated, the similarity in RTDs between runs performed based on S1 versus runs performed on the small scale where both PFN and SS were similar was notable and unsurprisingly shorter RTDs were observed with increasing SS.

Conclusively, the significance of the overall granulator fill referenced by the PFN seems to be smaller than expected provided that the process is not run in a flooded state, where the fill level is close to maximum capacity and a shift in GSD towards larger granules could be observed in preliminary trials. Furthermore, the importance of a downstream milling process to mitigate scale- or process-based differences in GSD and reduce the amount of oversized granules irrespective of the applied strategy was confirmed. In direct comparison, the usage of a highly soluble API at lower L/S-ratios led to relatively similar GSDs compared to a poorly soluble drug substance where more water had to be added during granulation. Remarkably setpoints for process parameters of the VFBD were relatively close among different formulations at similar throughputs despite substantial differences in the applied L/S-ratio.

3.4 From powder to tablet: Comparing fully continuous production of tablets to manual downstream processing of TSWG granules

3.4.1 Introduction

So far, all scale-up or process transfer studies for TSWG known to the author were performed on devices, where the granulation and occasionally the drying process were performed fully continuously. However, to the best of the author's knowledge, no holistic studies have researched the effect of other unit operations prior or after TSWG for a continuous production from powder to tablet in this context. In previous studies in this work (3.2.3, 3.3) and in current literature [80], [113] the effect of granulator scale on GSDs and especially the amount of oversized granules, which increased significantly at larger granulator scales, was shown. As these oversized granules could reach particle sizes of 1 mm or more on larger scales, the necessity of a milling process to obtain similar granule and tablet properties at different granulator scales without drastically reducing yield or negatively impacting further downstream processes became clear.

However, currently it is still uncertain whether similar results would be obtained on a fully continuous line, where the milling process is more dynamic and subject to additional processing conditions, such as an applied vacuum to transport milled granules to the feeding and blending unit where the extragranular excipients are then added fully continuously before tableting. This becomes especially relevant when on the small-scale a standalone TSWG device for research and development is used and GMP production is then performed on fully continuous lines from powder to tablet.

Consequently, the objective of this study was to investigate how fully continuous downstream processing after TSWG and drying impacts the GSDs of milled granules and relevant tablet properties, such as tensile strength, disintegration time and content uniformity, which could potentially be affected by differences in the milling or blending process.

3.4.2 Experimental setup & process parameters

As the fully continuous TSWG-line to cover the demand for clinical trial supply was still under development at Merck Healthcare KGaA in Darmstadt (Figure 45 in the appendix), it was not yet available for scale-up experiments in this thesis.

Therefore, all experiments were performed on the production scale line at L.B. Bohle in Ennigerloh based on two operational methodologies for further evaluation (see Figure 24):

1. Continuous granulation and drying and subsequently manual processing (MP) of the collected samples (milling, blending, and tableting) analogous to prior experiments performed during scale-up (blue product path).
2. Fully continuous (FC) granulation, milling, vacuum transportation, blending, and tableting (Blue + orange product path).

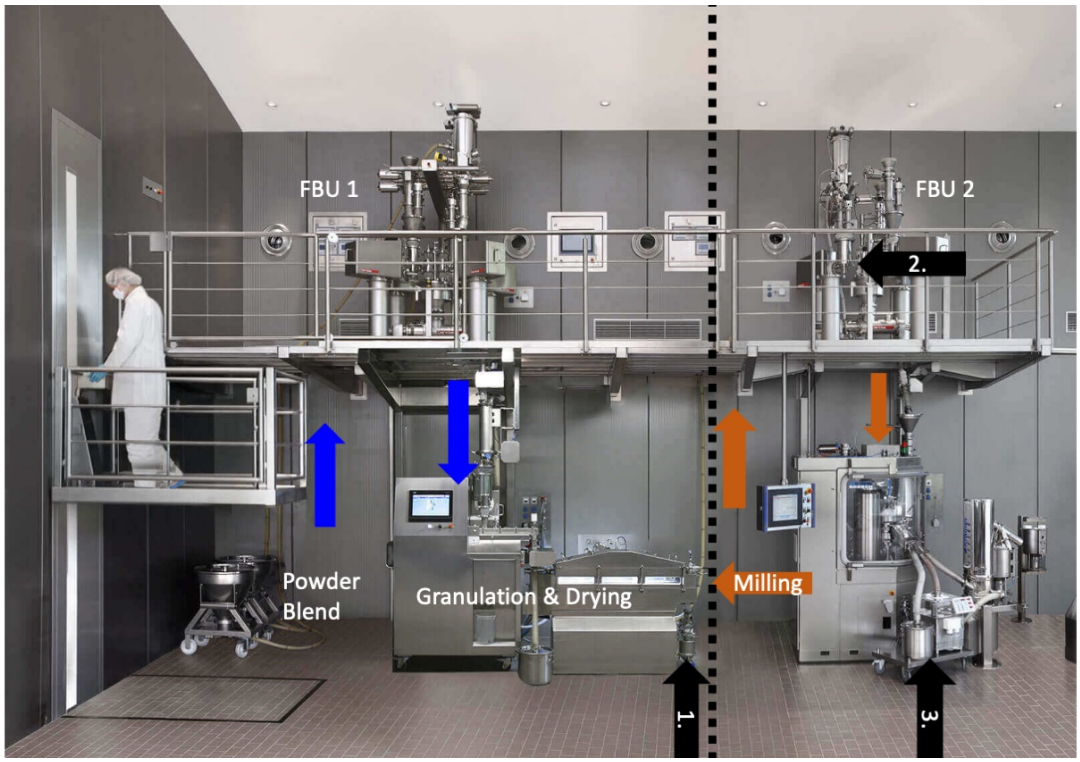

Figure 24 Overview of the fully continuous line in Ennigerloh. Left of the dotted line: Product flow follows the arrows from left to right. Blue arrows demonstrate the product path for continuous granulation & drying in this process, where granules were further processed manually afterwards (see 3.2, 3.3. and partly 3.4). Orange arrows showcase the remaining steps and product flow to complete the fully continuous line from powder to tablet as used for experiments in 3.4 (right of the dotted line). Black arrows point to where samples of granules (1. & 2.) and tablets (3.) for characterization and further processing were taken from during experiments. FBU: Feeding & blending unit. - with courtesy of L.B. Bohle Maschinen + Verfahren

Process parameters were kept identical wherever possible to remove any potential impact factor outside of the modus operandi of the line. To gain additional insights into the reproducibility of granules prior to milling on the large scale and reduce time and resources spent on preliminary trials to determine feasible process settings, these experiments were conducted with a similar powder blend for granulation as formulation 2a used in 3.2.3, where only an additional disintegrant was added as an extragranular excipient to enable a direct comparison of disintegration times of tablets (see formulation 2b in Table 15). Consequently, samples of granules before and after milling were taken (1. and 2. black arrow in Figure 24), as well as samples of tablets as final product after the rotary press. A comparative process overview that also includes the small-scale line can also be found in Figure 46)

Granulation settings were based on the previously applied scale-up strategies not including the reference run ***R***, as the throughput would have been too low to ensure a sufficiently stable feed rate for the addition of the extragranular excipients during fully continuous blending and the speed of the tableting press would have been unrealistically low at 2 kg/h. Instead, an additional run for each operational mode (MP/FC) was performed at a higher capacity of 25 kg/h to examine whether this would prove to be more challenging for the VFBD or any of the follow-up operations on the continuous line (Table 11).

Table 11 Overview of granulation and drying parameters for runs performed in this work package

Granulator			**VFBD**		
PFR [kg/h]	SS [rpm]	L/S-Ratio	Air Flow [Nm^3/h]	Air Temp. [°C]	Vibration Acceleration [m/s^2]
5.1	191	0.195	120	90	5
8	300	0.195	155	70	5
20	750	0.195	280	90	5
25	750	0.195	305	90	5

Process parameters for all downstream processing steps (milling, blending, tableting) in FC mode were tested in preliminary trials to ensure that no bottlenecks or powder bridges in e.g., the continuous milling or blending process would impact the stability of the process and to find suitable parameters for tableting at four different compaction pressures for each run. This led to a change from a 1 mm hole sieve as was originally used in previous experiments (3.3) where the milling process was not performed fully

continuously to a 1 mm grated sieve to increase milling capacity [166], as otherwise not all of the granules were sufficiently milled and congestion within the sieve occurred. Ideally, short residence times for particles during milling should be ensured on all scales to prevent a potential bottleneck for the throughput on a fully continuous line.

3.4.3 Comparison of GSDs to prior studies

While the focus of this work package lies on the comparison of granule and tablet properties based on the operational mode (MP versus FC), the high similarity to previous runs performed in 3.3 with formulation 2a allows for additional comparisons of both work packages.

Firstly, a direct comparison could be made in Figure 25 to further confirm the high reproducibility of granules on the larger granulator and an additional validation that runs performed in both work packages were produced from a similar powder blend at similar process settings.

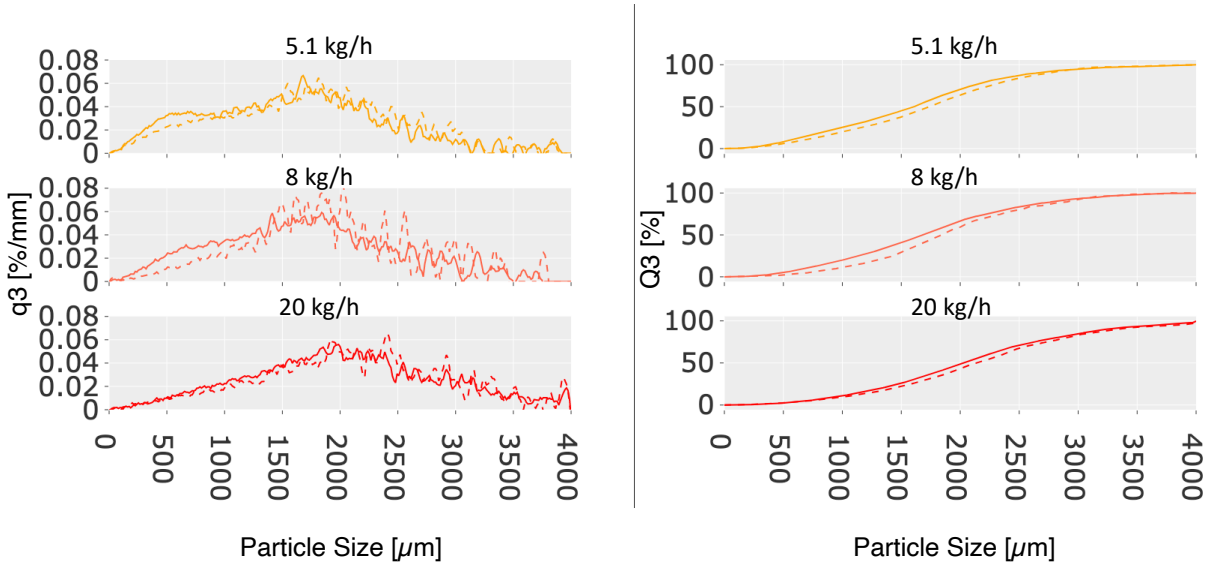

Figure 25 GSD of granules produced from a similar powder blend at identical granulation parameters in 3.3 (dashed lines) versus GSD of granules produced for experiments in this chapter (solid line) prior to milling..

Secondly, as the GSD of the unmilled granules was confirmed to be similar and the manually executed milling process was performed at the same process parameters but with a 1 mm rasping sieve instead of a 1 mm round hole sieve (as used in 3.3), the impact of this change could be further evaluated (see Figure 26).

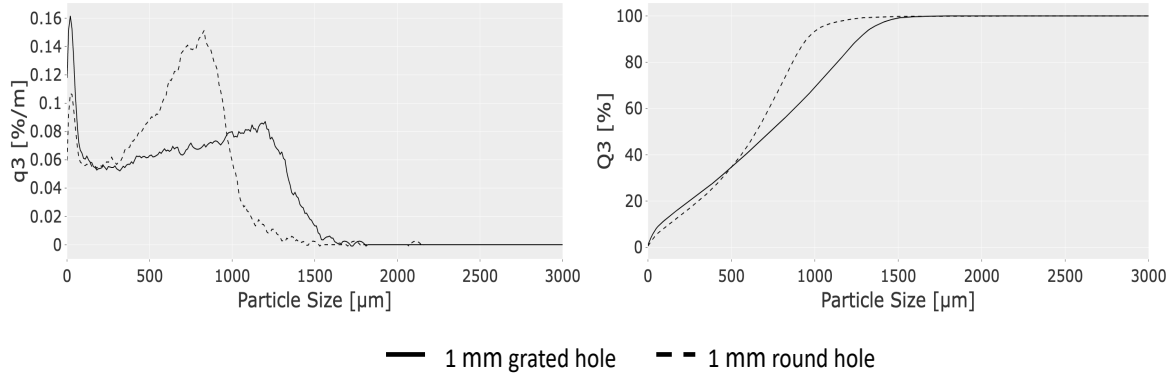

Figure 26 GSDs after milling based on the selected sieve (1 mm round versus 1 mm rasping screens). Exemplarily shown for granules produced at a throughput of 20 kg/h

In accordance with results reported by Verheezen et al. [167], a higher size reduction could be observed during milling with a round screen due to the increased residence time. Furthermore, contrary to Schenck and Plank [168] and in line with results reported by Kotamarthy et al. [169], a slightly higher amount of fines for the milling performed with the rasping sieve could be observed, indicating additional occurrence of granule breakage caused by the rough surface of the grated screen.

3.4.4 Impact of downstream processing mode after granulation

During manual milling of the granules collected from granulation at a throughput of 8 kg/h, a blockage of the 1 mm rasping sieve occurred which led to a much larger residence time for the particles remaining in the sieve as no particles could flow through the screens while the impeller was still rotating and further grinding particles against the rasps. This resulted in granules with a very high percentage of fines compared to any of the other runs and thus even though these granules were still further processed and analyzed as all other samples, the results are not indicative of a realistic scenario and should be taken in with caution (see Figure 27).

One observation that all runs have in common is that after manual milling, no particles larger than ~1500 µm were present during GSD measurements, while particle sizes up to ~2000 µm (and a few even larger ones) could be found in all granules that were milled fully continuously while a negative pressure was applied simultaneously to transport granules further along the line. A probable factor contributing to this is a shorter residence time within the sieve caused by the suction of the applied vacuum, which directs and aligns the particles more towards the holes of the screen and pulls them through. During manual milling no vacuum was applied and particles had to be broken up until they were small enough to fit through the screen without any additional dragging force.

Remarkably, while the GSDs were almost identical for all MP milled granules shown in Figure 28, particle sizes of samples from FC milling could essentially be grouped in lower throughput (5.1 kg/h and 8 kg/h) with a lower amount of finer particles (i.e., < 200 µm) versus higher throughput (20 kg/h and 25 kg/h) with a significantly higher amount of finer particles. The data collected did not provide a clear answer if this is related to e.g., a potential segregation within the feeder of the FBU 2 where the samples to determine the GSDs were taken, which would potentially manifest earlier at higher feed rates, or other more process-specific reasons.

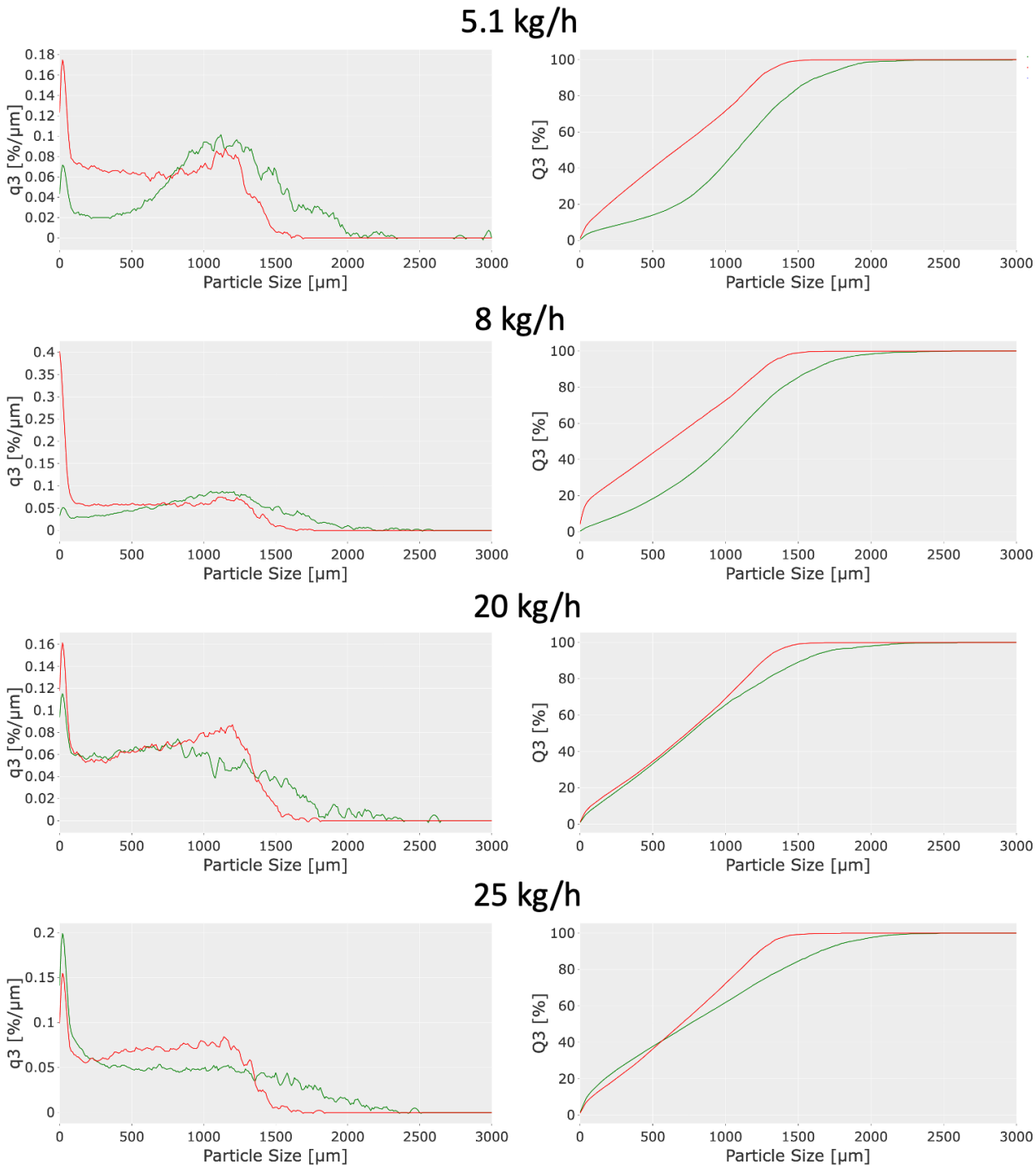

Figure 27 Overview of GSDs of milled granules at different throughputs. Red lines are for granules where the milling process was performed manually, green lines represent granules that were milled fully continuously and simultaneously transported to the FBU2 via vacuum

A significant impact of the impeller speed on GSDs for conical sieving is well documented in literature [170], however, during this experiment it was kept constant at 700 rpm for all milling operations performed and could therefore not cause any differences in GSD. Another potential explanation that could be excluded based on the

process setting was the batch load and thus the fill level of the conical sieve, which would expectedly differ at various throughputs of the line due to the nature of the process. Granules that were discarded at the outlet of the drier were accumulating for a set time interval during which the mill was idle. Afterwards these granules were transported through the mill to the following FBU 2 during a pre-defined duration of milling. For the runs performed at 8 kg/h, 20 kg/h and 25 kg/h these intervals were set to 45 s wait period followed by a 15 s milling period, while for the run at 5.1 kg/h the wait period was increased so that a comparable granule holdup to the runs at 20 kg/h would occur after the drier (165 s wait followed by 15 s of milling). Therefore, if the GSD was strongly affected by the batch load during the continuous milling, this effect would be expected to occur most strongly between the runs performed at 5.1 kg/h and 8 kg/h as the difference in fill level would be most drastic there.

Overall, more specific experiments are required to investigate what might have caused these differences in GSD for the granules that were milled fully continuously.

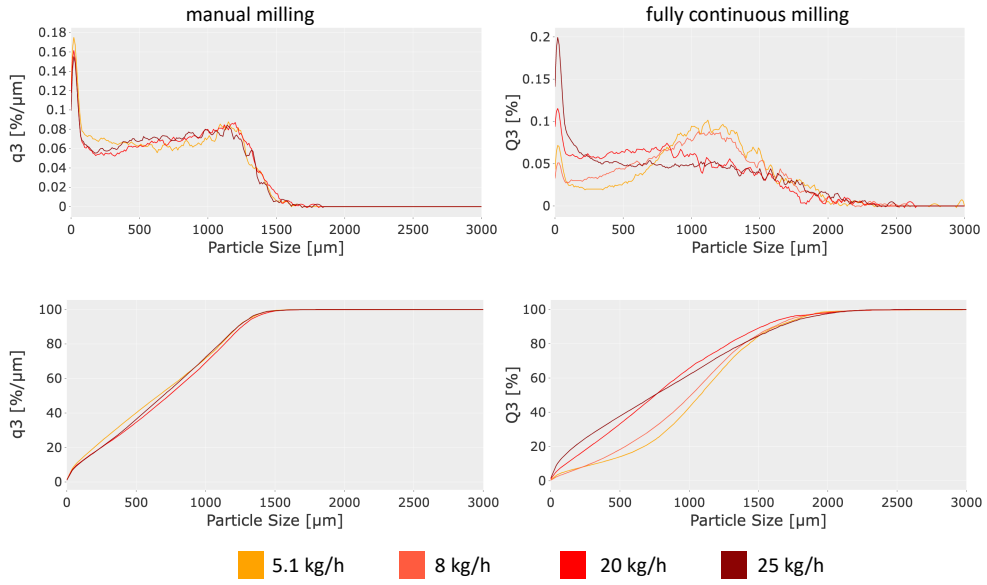

Figure 28 GSD after manual milling versus fully continuous milling for granules produced at different throughputs (5.1 kg/h, 8 kg/h, 20 kg/h and 25 kg/h). 8 kg/h manual milling was excluded in this figure to prevent distortion of the y-axis from the unrealistically high amount of fines (see Fig. 21)

Based on the data shown in Figure 29, several noteworthy observations regarding the tabletability can be made.

First and most surprisingly was that tablets produced from MP granules (granules produced at a throughput of 8 kg/h excluded for previously described reasons) showed a significantly lower tensile strength than tablets that were produced fully continuously despite using otherwise identical processes and process parameters.

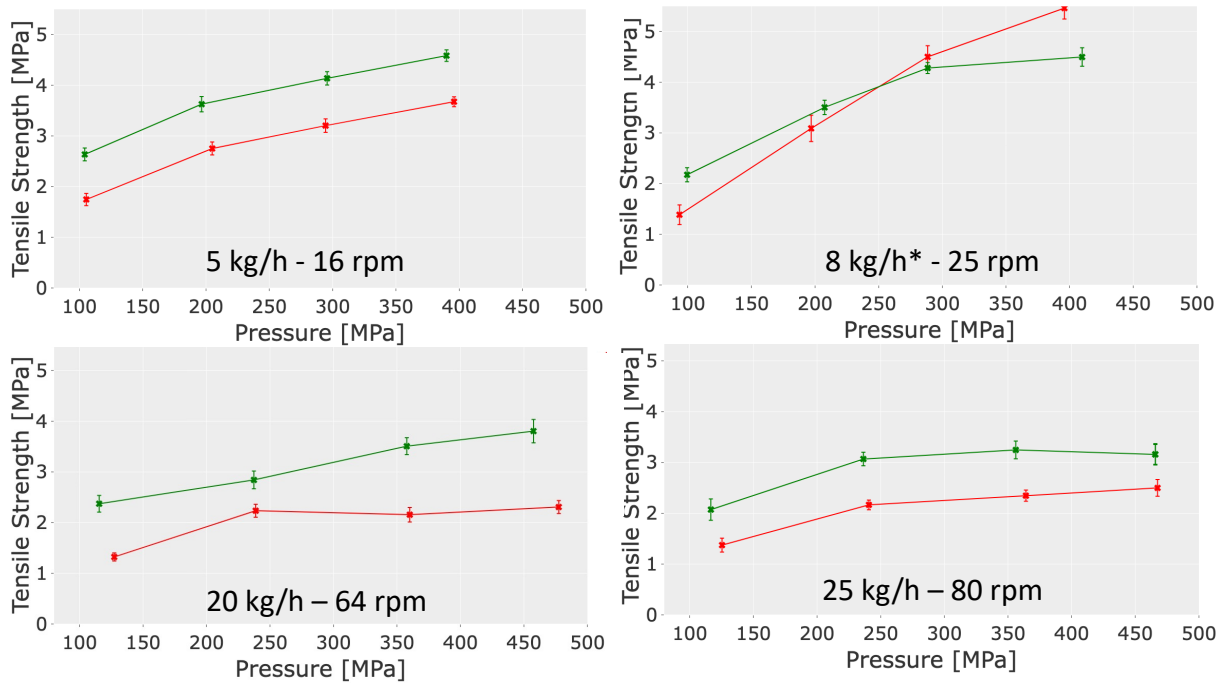

*Figure 29 Tabletability of granules produced at different PFRs either by manual processing (red lines) or fully continuously (green lines) on the line. Powder throughput (in kg/h) and rotor speed of the rotary press (in rpm) added to each diagram for reference (mean±SD, n=20). *as described earlier, manually milled granules produced at 8 kg/h had a much higher amount of fines due to a blockage during the milling process.*

Secondly, despite already slightly increased compaction pressures compared to runs at lower throughputs and rotor speeds (120, 240, 360 and 480 MPa versus 100, 200, 300 and 400 kN respectively), tensile strength of tablets produced at higher throughputs (and therefore with more rpm on the tablet press) were significantly lower.

Lastly and not unexpectedly, the tabletability profile of the granules with a much higher number of fines caused by the blockage of the mill deviated substantially from all others and showed a significantly higher tensile strength at higher compaction pressures compared to other MP runs. These results are in line with other research that has been carried out regarding the influence of particle size on mechanical strength of tablets, where an increase in breaking force/tensile strength with decreasing particle sizes was

shown and attributed to a higher packing efficiency achieved by the smaller particles [171]–[174].

Regarding the first two observations, further experiments on the StylOne Evolution compaction simulator (Medelpharm, France, see 5.2.2.7) and a thorough analysis of the available data were performed for further investigations.

A negative correlation between the compaction speed of tablets and the resulting tensile strength at similar compaction pressures is also well documented in literature [175]–[177]. It is linked to the deformation behavior of material, especially for material that tends towards more plastic and viscoelastic deformation, while more brittle material seems to be less affected as fragmentation occurs more extensively.

This sensitivity to the compaction speed of the used tableting blend (formulation 2b) could be confirmed during additional tableting experiments performed at four different compaction speeds (see Figure 30). Increasing the compaction speed from 20 % to 80 % (equivalent to the 4-fold increase from 16 rpm to 64 rpm between runs that were carried out at a throughput of 5 kg/h and 20 kg/h respectively) drastically reduced the resulting tensile strength of produced tablets.

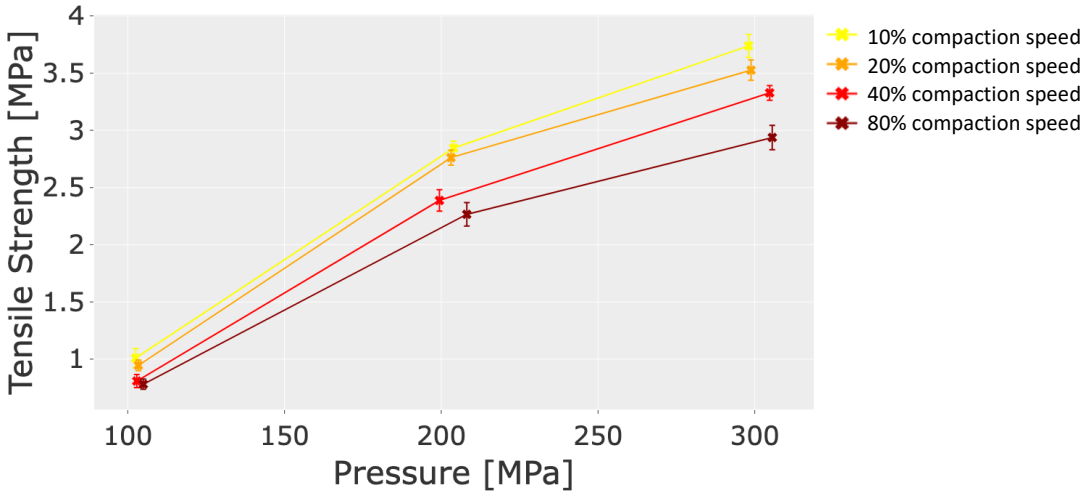

Figure 30 Exemplary showcase of the influence of tableting speed on tensile strength for granule samples taken after continuous milling at a throughput of 25 kg/h (mean±SD, n=10)

For the last remaining observation of the substantially higher tensile strength of tablets that were produced continuously instead of being manually processed, a few aspects were investigated that were presumed to demonstrate a potential correlation. First of all, the tableting parameters on the rotary press and tablet weights for all performed runs were analyzed (see Table 12) to see if there might be a straightforward explanation based on e.g., differences in the edge thickness, the tablet weight or its variability, the applied compaction pressure or other factors. However, except for slight deviations in the pre-compression thickness, a small misconfiguration of the rotor speed at a throughput of 8 kg/h for MP granules (25 rpm instead of 26 rpm as in the FC runs) and some differences in the filling height of tablets especially for granules produced at lower throughputs, indicating a potentially better flowability for MP granule, no significant differences could be found that would explain this remarkable discrepancy in the tensile strength of tablets.

The observed differences in the GSD of granules were another alternative explanation that was examined in further experiments. Even though the increase in the amount of fines was less pronounced for the FC granules than for the improperly milled granules, where a drastically higher amount of very fine material was observed, further compaction studies were performed in Darmstadt. For that, milled granule samples were taken either after manual milling or collected after the continuous milling process in-line from the 5 kg/h and 25 kg/h runs and then compressed at five different compaction pressures similar to the procedure in previous studies to confirm and potentially further investigate differences in the deformation behavior during compaction through e.g., Heckel analysis.

As disintegration tests were already performed with the tablets produced on the rotary press, only the lubricant was added during those additional tableting experiments to reduce the ejection force during tableting and thus the overall tableting blend and process was similar to the one in previous experiments in chapter 3.3. Thus, in addition to the investigations regarding the differences in the tabletability profiles of tablets produced in MP and FC runs, a direct comparison could be made for the tabletability of granules milled with a 1 mm round sieve in 3.3.

Table 12 Overview of tableting parameters on the rotary press.

Throughput [kg/h]	Mode	Compaction Pressure [MPa]	Rotor Speed	Filling Height [mm]	Edge Thickness		Tablet Weight [mg]
					Pre-compression [mm]	Main compression [mm]	
5.1	MP	105	16	5.40	1.90	1.90	201 ± 1.6
		205			2.00	1.55	205 ± 1.8
		294			1.80	1.40	203 ± 1.4
		396			1.70	1.27	204 ± 1.4
	FC	104		5.90	2.30	1.85	202 ± 2.0
		197			1.80	1.63	202 ± 2.3
		296			1.80	1.45	202 ± 1.5
		390			1.80	1.31	201 ± 1.1
8	MP	94	25	5.80	2.00	2.00	200 ± 2.7
		197		6.10	2.00	1.65	199 ± 2.6
		288		6.05	1.80	1.47	200 ± 2.5
		396		5.80	1.80	1.35	199 ± 2.1
	FC	99	26	6.35	2.20	1.75	203 ± 2.1
		207			1.85	1.62	201 ± 2.3
		288			1.85	1.45	199 ± 1.6
		410			1.80	1.28	198 ± 2.5
20	MP	127	64	5.40	2.10	1.90	203 ± 1.2
		239			2.00	1.55	201 ± 1.6
		360			1.80	1.40	203 ± 1.1
		477			1.80	1.27	202 ± 1.2
	FC	115		5.35	2.00	1.92	202 ± 1.8
		237			2.00	1.60	201 ± 1.9
		358			2.00	1.42	202 ± 1.7
		458			2.00	1.28	203 ± 3.4
25	MP	119	80	5.40	2.20	1.85	200 ± 1.7
		241			1.90	1.58	201 ± 1.8
		364			1.80	1.37	200 ± 1.1
		468			1.80	1.24	200 ± 2.7
	FC	117		5.50	2.00	1.90	204 ± 1.8
		236			2.00	1.60	200 ± 1.9
		356			1.80	1.39	200 ± 2.4
		466			1.80	1.29	202 ± 2.4

In that regard, there are two notable aspects depicted in Figure 31:

Firstly, the previously observed substantial increase in tensile strength of tablets that were produced fully continuously versus those that were processed and compressed manually was no longer present and even mildly inversed as tablets from MP granules showed a slightly (but much less pronounced) higher tensile strength at similar compaction pressures. Thus, it seems unlikely that the previously shown differences in tensile strength (Figure 29) are interconnected and this hypothesis was discarded.

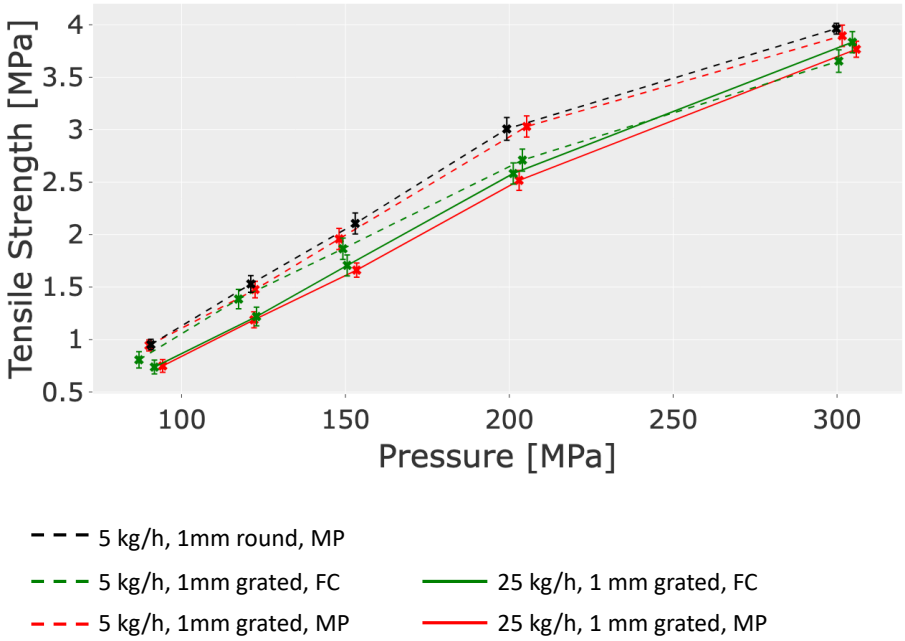

Figure 31 Tabletability of milled granules produced during current experiments (formulation 2, green & red), where granules were either milled fully continuously in line (FC) or manually with similar milling parameters (MP). Black line shows tabletability of granules produced from previous runs in 3.3, which was milled with a round holed screen instead of a grated screen (mean±SD, n=20).

Secondly, the tabletability profile of tablets produced in previous experiments (see 3.3) was almost congruent with the tabletability profile of the MP run performed at similar granulation parameters in this work package, despite large differences in the respective maximum particle size and the amount of particles larger than 1000 µm (Figure 26). It appears that the GSDs of both tableting blends were still similar enough to not impact the packing efficiency to an extent where the mechanical strength of the tablets is affected. This might be due to the relatively similar number of fines compared

to the granules produced during mill blockage, where this effect was observable, as the smaller particles would be expected to have the most significant effect on particle arrangement inside the die.

As the observed differences in GSD based on the operational mode could be excluded as the main driver for the significant variation in tensile strength that was previously found, more focus was put on potential differences of the tableting process on the continuous line. Thus, the limited data that was collected during preliminary trials was also further evaluated and provided some additional insights that helped narrow down relevant factors that might have influenced the tablets tensile strength. As can be seen in Figure 32, during preliminary trials the tabletability profile of tablets produced from milled FC granules was much more similar to the tabletability profile of the tablets produced from milled MP granules during later experiments than to the tabletability profile that was observed for the FC runs then.

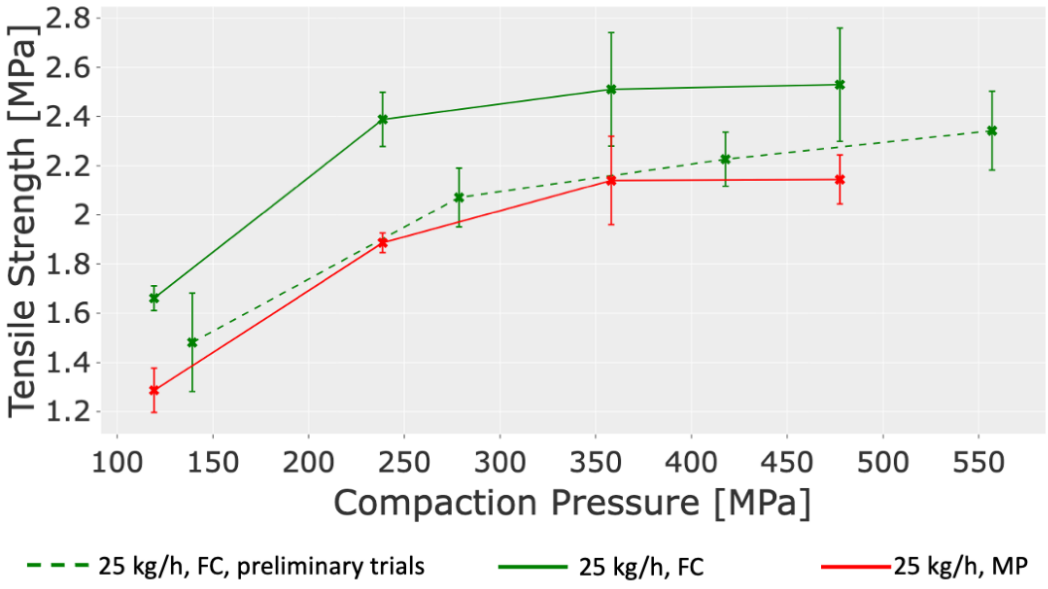

Figure 32 Tabletability of milled granules produced at a throughput of 25 kg/h during preliminary trials (dashed line) and during the experiment (continuous lines). (mean±SD, n=5)

It is important to note that the discrepancy in tensile strength between similar runs shown in Figure 29 and Figure 32 can be attributed to the time span between tablet compression and the measurement of the breaking force. All tensile strengths shown in Figure 29 are based on measurements that were performed about two weeks after the tablets were compressed, which potentially led to an additional hardening of tablets

through particle rearrangement of the solid material and potential recrystallization of dissolved material in the tablet, which is well described in literature [178], [179]. Furthermore, during the preliminary trials, the applied compaction forces were slightly higher (7, 14, 21 and 28 kN versus 6, 12, 18 and 24 kN). As only limited data for the preliminary trials was recorded, no other runs could be shown for comparison. The main difference between tablets produced in preliminary trials and those that were produced during later experiments for the FC runs was a timeout of the process after continuous milling during preliminary trials. Granules were produced and milled fully continuously and then stored in sealed bags over the weekend before they were put into the FBU 2 again to be mixed and compressed fully continuously. During the later experiments, tablets were directly compressed after continuous milling and mixing without any delay in between. Thus, it seems that the additional storage of the granules at room temperature, which would occur naturally for the MP granules as the manual processing steps required more time and thus the MP granules were usually tableted a day after their production, led to a decrease in tensile strength of the produced tablets in MP mode but not in an uninterrupted FC mode.

Potential explanations for this effect may include a difference in residual moisture of the FC milled granules, as even though the LOD was measured and controlled for the unmilled granules at line, no measurements were performed directly after the continuous milling process. Thus, it cannot be ruled out that a higher amount of residual moisture caused by water inclusion in larger particles was present shortly after milling but potentially evaporated during storage of the milled granules. The effect of residual moisture of granules on their tabletability has been well described in literature [180]–[182] and might be linked to an increase in tensile strength in this case. The moisture content of granules prior to the additional tabletability studies performed for Figure 31 was measured and found to be in the range of 1.3 % - 1.5 % for all granules that were compacted.

Another speculative explanation could be the re-agglomeration of particles and thus a decrease in fines during storage after milling, as pure metformin is known to agglomerate heavily [183]. However, this effect would likely be mitigated by the relatively low percentage of metformin inside the powder blend and seems unlikely to occur to an extent where the tensile strength could be affected this strongly within a day. Nevertheless, more experiments are required to determine if this observed effect was just a formulation-specific edge case or if this might be a common occurrence

when comparing a fully continuous TSWG & tableting route where granules are compacted almost immediately after granulation & milling.

More surprisingly, as can be seen in Figure 33, despite the measured differences in tensile strength of tablets, overall, there were no substantial differences in the disintegration times. The MP run at 8 kg/h with the drastically higher number of fines showed a general, but minor decrease in the disintegration times observed versus its FC equivalent, while FC tablets from the 20 kg/h run showed a minor increase in disintegration times versus their MP equivalent. Overall, disintegration times for all tablets met the requirements of the European Pharmacopeia (Section 2.9.1, disintegration times < 15 minutes) and the differences observed are mostly not significant and could be attributed to measurement uncertainties as the automatic endpoint detection of the device did not seem to properly trigger sometimes.

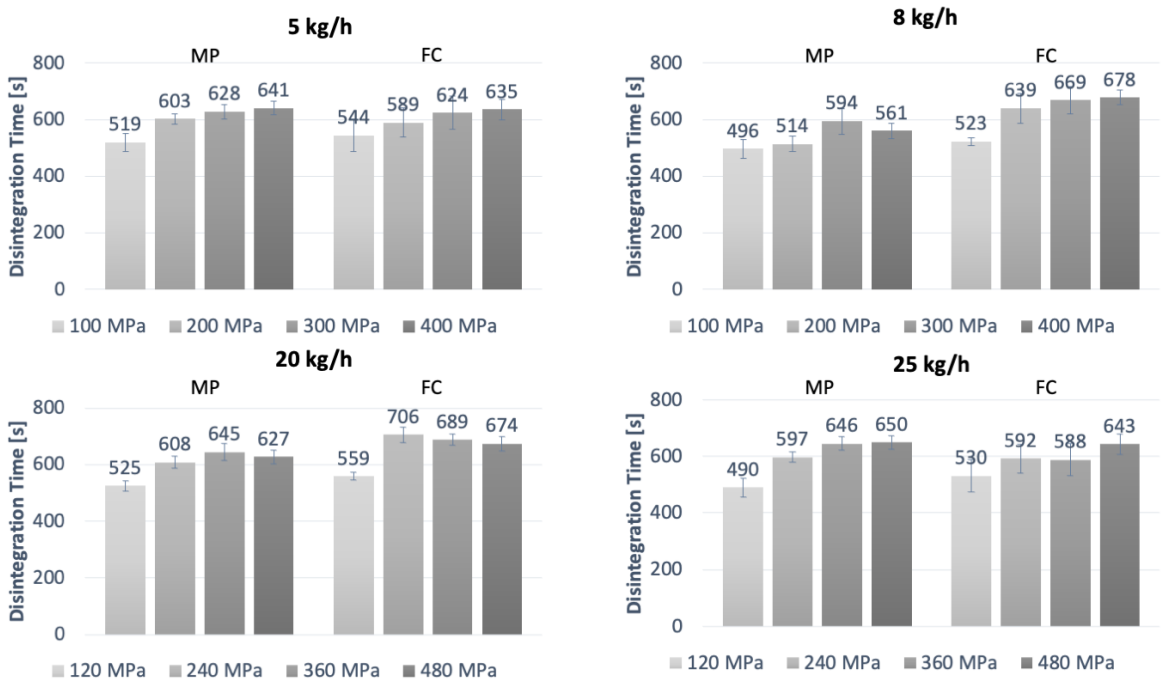

Figure 33 Disintegration times of tablets produced from MP versus FC granules at four different throughputs (mean±SD, n=6).

As can be seen in Table 13, all but one run passed the criteria for sufficient content uniformity defined by section 2.9.5 of the Ph. Eur. [4] for an acceptance value (AV) < L1 (which was 15 % for a sample size of n = 10). Due to the lower determined mean content (96.7 % MP vs 95.9 % FC) and the higher overall variation (standard deviation: 4.5 % MP vs 6.0 % FC), the FC run at 20 kg/h did not meet the requirements. However, as at throughputs of 5 kg/h and 25 kg/h similar or better results were achieved for the FC runs, it seems more likely that the one failed content uniformity check was caused by a random effect and relatively high measurement uncertainties than by the operating mode of the line as other publications have shown no indication of insufficient blend uniformity for continuous feeders [184], [185].

Table 13 Content Uniformity of tablets produced at different throughputs for MP and FC runs.

Throughput	Operating Mode	Mean Content [%]	Standard Deviation [%]	AV [%]
5 kg/h	MP	96.8	3.3	9.5
	FC	97.7	3.7	9.3
20 kg/h	MP	96.7	4.5	12.6
	FC	95.9	6.0	16.4
25 kg/h	MP	95.9	5.0	14.2
	FC	101.1	4.6	10.0

Friability of all compressed tablets was < 0.2 % and thus also met the requirements imposed in section 2.9.7 of the Ph. Eur. [4] (friability < 1 %).

.

3.4.5 Summary

In contrast to previous studies and work packages in this work, where the scale of the TSWG process was the focus and processing steps further down the line from powder to tablet were kept as similar as possible, the effect of the operational mode of downstream unit operations after the granulation and drying process were investigated in this study.

A noticeable impact on the GSD was found and attributed to the suction effect of the vacuum applied for further transportation during the milling process on the fully continuous line. Concurrently, it could be shown that the tablet tensile strength was not directly affected by the differences in GSD even at larger differences that occurred when comparing granules milled with a 1 mm rasping sieve in this study versus a 1 mm round hole sieve in a previous work package.

However, the tabletability of the produced granules varied significantly based on the mode of operation and was substantially higher for tablets produced fully continuously from powder to tablet. As this observation did not occur when the fully continuously milled granules were compressed a few days after the granulation process, it seems that somehow the resulting tabletability decreased significantly during storage within a short period of time (hours to a few days) after granulation. Whether this was caused by e.g., differences in the residual moisture of milled granules, particle agglomeration or other potential interactions within the blend could not be determined and should be investigated in further studies. At the same time, if a general increase in tensile strength on fully continuous lines should be observed and confirmed in further studies, it could even be viewed as a positive outcome as no impact on the disintegration times of tablets was observed for tablets with higher tensile strength.

No differences in content uniformity of the compressed tablets could be observed for the different blending processes (MP/FC) either at 5 kg/h or 20 kg/h, confirming a sufficiently high mixing quality of the feeding and blending unit at different feeding speeds and fill levels of the continuous blender.

4 Summary & Outlook

Over the last two decades, TSWG has been established as a viable route for wet granulation in pharmaceutical manufacturing of granules and tablets. While many process parameters are well researched and understood, the process itself and the various challenges imposed by different formulations are too complex to apply a “one fits all approach” which often led to conflicting observations based on e.g., the selected screw configuration or the wetting behavior of the granulation blend.

Therefore, even though the focus of this thesis was to enable a successful scale-up from the laboratory scale line to a production line, the first experiments aimed at establishing a sufficient process understanding for one specific combination of screw configuration, process settings and formulation. The L/S-ratio and to a smaller extent the PFR were identified as the most significant impact factors on the resulting product properties after granulation and tableting on the small scale. Furthermore, the reproducibility of output parameters (GSD, tablet tensile strength) was investigated in center points of a DoE and in an additional reproducibility study over multiple days, and found to be quite high. Lastly, an attempt on the experimental determination of the fill level was made with dental silicone as there is still no way to accurately confirm theoretical estimations of the fill level as the granulators are usually made of metal and thus opaque to visual and spectroscopic analysis. However, this idea was not further pursued, as the benefit of determining an exact fill level for the scale-up was found to be questionable and assuring that the whole granulator volume was filled with the dental silicone to get an exact mold of the remaining free volume after granulation proved to be more challenging than initially anticipated.

Different scale-up strategies based on (1) similar SS settings to aim for a comparable RTD, (2) a similar CS of the screws or (3) a tenfold increase of the PFR to reach a realistic production capacity at similar estimated fill levels were performed on the large scale. Additionally, a reference run with identical process parameters and thus a drastic underfill of the granulator on the larger scale was performed to investigate how large differences in the fill level would affect the outcome. Consequently, the product properties of granules and tablets produced in this work package were compared to those that were made on the small scale. Differences in the GSDs of the different samples were assessed by the EMD, and it was shown that there were substantial differences in GSD observed prior to milling based on the device scale, which were

then drastically mitigated by the additional milling process for granules produced at a similar L/S-ratio on both scales. It was further shown that even though there were small differences in the output parameters (e.g., GSD, tabletability or disintegration times of tablets) based on device scale, the impact of the applied L/S-ratio was much stronger and similar results could be achieved at similar L/S-ratios, despite drastic differences in various other input parameters (RTD, CS, PFR, SS and even the PFN).

Overall, these first scale-up experiments were considered successful and the granules and tablets insensitive to differences in most process parameters, so that further scale-up experiments with different formulations were planned and performed next. The aim of these additional experiments was to investigate if similar observations could be made when the scale-up strategies were applied to other potentially more sensitive formulations and to find out how the solubility of an added API would impact the scale-up behavior. Thus, the same scale-up strategies were applied on three different formulations: Two of them were of a similar composition as the previous placebo formulation but with either metformin as highly soluble or praziquantel as poorly soluble API added. The third formulation was picked in preliminary trials based on a potentially greater sensitivity to changes in granulation parameters and a higher dissimilarity of the overall blend composition. The solubility had an impact on both, the feasible and the necessary L/S-ratio for granulation, meaning that with the highly soluble metformin larger particles were observed at lower L/S-ratios already while a much higher L/S-ratio had to be applied to reach visually comparable granules with the poorly soluble praziquantel formulation. Furthermore, it was shown that based on the granulator scale and the addition of automated processing steps on a continuous line, different challenges might arise, such as an interrupted powder flow in pipes used for transportation with a poorly flowing powder blend (ffc <4) or a blocked nozzle at the water inlet due to the lower water pressure at total liquid feed rates on the small scale. Regarding the output parameters it was once again shown that the GSDs of granules produced and milled on the large scale were fairly similar to granules produced on the small scale, while prior to milling larger differences occurred. However, it was also demonstrated that the extent of how large these differences are can be formulation-dependent as the extended-release formulation used in this work package showed a much larger maximum particle size for the small-scale granulator with an almost

identical screw configuration (-0.25 D CE on the large scale). As the extragranular excipients were reduced to the bare minimum and only 1 % of magnesium stearate was added, the overall differences in tabletability were higher than in previous studies and no disintegration testing could be performed due to the lack of disintegrant. However, sufficiently high tensile strengths could be achieved for tablets with all formulations and scale-up strategies and the previously shown effect of L/S-ratio on the tabletability was higher than the observed differences between strategies, even with only 1 % of extragranular excipients added so it seems reasonable to assume that some differences in tensile strength could potentially be compensated by an adaption of the L/S-ratio if necessary. Furthermore, no clear trend could be identified for either the scale-up strategy or the device scale itself in terms of the measured tensile strength, except for the formulation based on the previously used placebo blend with the added metformin, where tablets on the small scale showed a slightly increased tensile strength. It was also shown that, unsurprisingly, the residence times were decreasing with increasing SS and that the residence times were most similar between the small scale and the large scale, when both the SS and the PFN were kept similar. In line with the results of other research groups, the dissolution of tablets compressed of the controlled release formulation were insensitive to changes in granulation parameters and applied compaction pressures.

Up to this point only granulation and drying were performed fully continuously on both scales and while the scale-up worked unexpectedly well with various formulations, first indications of additional challenges in a fully continuous mode arose (e.g., the pipe blockage in the FBU responsible for a continuous refill of the granulator with a poorly flowing powder blend) and the necessity of the downstream milling process to mitigate the strong differences in GSD based on the scale became clear. Thus, the question was raised how applicable the previous results would be to a fully continuous line where the operational mode of some processes that were previously performed “manually” and thus batch-wise would then be performed fully continuously from powder blend to tablet. For the continuous milling process it was found that RTDs had to be reduced to ensure a constant flow without granule build-up in the conical sieve by switching to a grated screen. GSDs were highly reproducible for manual processing of the milling step but showed a shift towards larger maximum particle sizes in continuous mode where the residence time was further decreased by the suction effect of the vacuum applied for transportation. Tablets produced fully continuously directly

after granulation showed a significantly higher tensile strength with similar disintegration times and a sufficient content uniformity and friability compared to tablets produced from MP granules where the tableting occurred with a time difference of a day due to the manual processing steps involved in between. Even if all process steps were performed fully continuously but a delay of at least a day was introduced between granulation and milling of granules, and mixing and tableting afterwards, these differences in tabletability vanished. Thus, there seems to be a time-dependent physical or chemical property (i.e., reagglomeration of particles, evaporation of adsorbed water, etc..) involved that had a strong impact on the consecutive tableting process and thus the resulting tensile strength of tablets. Surprisingly, differences in GSD of milled granules that were either caused by the screen type (grated versus round hole screens) or the operational mode (MP versus FC) did not show any strong impact on the resulting tablet properties except for one run where granules resided substantially longer in the mill due to a blockage of the screen and thus a drastically higher percentage of fines was produced. Another important point to keep in mind during scale-up of a fully continuous line is that in FC mode all unit operations are interlinked and thus process parameters, such as the rotor speed of a rotary press needs to be adjusted to the overall throughput of the line. This has a direct impact on dwell times during tableting and can lead to differences in the resulting tensile strength of compressed tablets at similar compaction pressures.

Overall, it became clear that TSWG-based CM lines from powder to tablet require a more holistic approach to process-transfer and scale-up as all process steps are connected and product properties (e.g., GSD of granules or tensile strength of tablets) can be affected by factors and effects that might not occur or be less relevant during traditional batch manufacturing. A good balance needs to be found between understanding each unit operation and its impact on CQAs on its own and the big picture that results from the connection of all unit operations. Thus, ideally a fully continuous line should already be available for experiments in the development stage to further improve process understanding of the connecting steps and downstream unit operations for a successful and resource-saving process transfer. By implementing various process analytical technology methods along the line e.g., to determine residual moisture [43], [51], [101] and GSD [49], [50], [186], [187] before and after

milling, measure the residence time [88], [90], [135], [188], [189] or analyze blend uniformity [185], [190], [191], a thorough process understanding of the individual steps could be gained simultaneously to their potential effects further down the line to develop suitable control strategies and push the implementation of QbD principles as early as possible. Furthermore, a well implemented fully continuous line with various PAT-probes could generate a significant amount of data, which could potentially be used as input to create more accurate and sophisticated machine learning models to predict specific output parameters based on e.g., deep learning models that are emerging across many industries [192]–[194]. However, there is still a lot of work to be done and questions to be answered from a technical, operational and regulatory standpoint to implement feasible control strategies and hopefully achieve real time release as a standard for newly implemented CM lines [39], [41], [195], [196].

5 Experimental part

5.1 Material

5.1.1 Active pharmaceutical ingredients

Two active pharmaceutical ingredients were used as model substances during scale-up experiments.

1. Metformin hydrochloride (Batch no: C22429, Merck, France) as a model substance for a highly soluble API
2. Praziquantel (Praziquantel USP, Batch no: MBF121045A, Solara Active Pharma Sciences Ltd., India) as a model substance for a poorly soluble API

5.1.2 Excipients

A list of all the solid excipients that were used with various functions in different powder blends is given in Table 13.

Table 14 Overview of used excipients

Excipient	Trade Name	Batch No.	Manufacturer	Function
Croscarmellose Sodium	Ac-Di-Sol	K48453094_G2	FMC BioPolymer, Germany	Disintegrant
Lactose Monohydrate	GranuLac 200	L101853020A533	Meggle, Germany	Filler
Magnesium stearate	Ligamed MF-2-2V	K49308091G1, K50398991G2 K50548291G1, K50584291	Peter Greven, Netherlands	Lubricant
Mannitol	Parteck M 200	MP17032519	Merck KGaA, Germany	Filler
	Pearlitol 160C	K50959031, E218P, E297D, E297N	Roquette, France	Filler
Methyl-cellulose	HPMC E5	K43195635	Dow Chemical, USA	Binder
	Methocel K100M	D180J72002, K48315376	DDP Specialty Electronic Materials, USA	Binder
Microcrystalline Cellulose	Vivapur 101	66101212319, 66101194831, 66101200806,	JRS Pharma, Germany	Filler/Binder

Povidone	Kollidon 25	85464788Q0, K47603443,	BASF, Germany	Binder

Demineralized water was used as a granulation liquid.

5.2 Methods

5.2.1 General methods

5.2.1.1 Sample preparation

For granule characterization, samples were representatively divided using a riffle splitter (Retsch, Germany) until an appropriately sized sample for the specific method was collected. Sample sizes are described in the corresponding methods.

5.2.1.2 Residence time measurements

To determine the residence time distribution of particles inside the TSWG-line, ExtruVis®3 (MeltPrep, Austria) was used with a corresponding camera (USB-CAM-052H, Phytec, Germany). Sudan Black B (Alfa Aesar, Germany), a hydrophobic color dye, was added to the running granulation process at the powder inlet of the barrel as a one-time pulse. The amount of tracer that was added was dependent on the throughput of the run and corresponded to ~4 % of the amount of powder that was fed to the granulator every second. Residence time measurements for the granulator were performed with the camera focusing on the entrance area of the drier to reduce noise and thus get more accurate measurements than focusing on the exit of the granulator screws. To reduce disturbances due to reflections or different lighting conditions, the camera and its surrounding area were covered with a black apron or a white lab-coat (Figure 34). Furthermore, the automatic filter cleaning inside the drier was disabled during RTD measurements as the influx of particles generated by the blow-out of the filter would disturb the measurement and lead to small spikes in the measured signal.

A minimum of three measurements was performed in-line at each process setting.

During the first 10 seconds of each measurement a baseline intensity value was recorded and afterwards the software measured and returned the intensity of different color signals for later evaluation.

The blue color signal was used for the evaluation and analyzed through an in-house Python (v3.7.1) script at Merck and the different process steps are depicted in Figure 35.

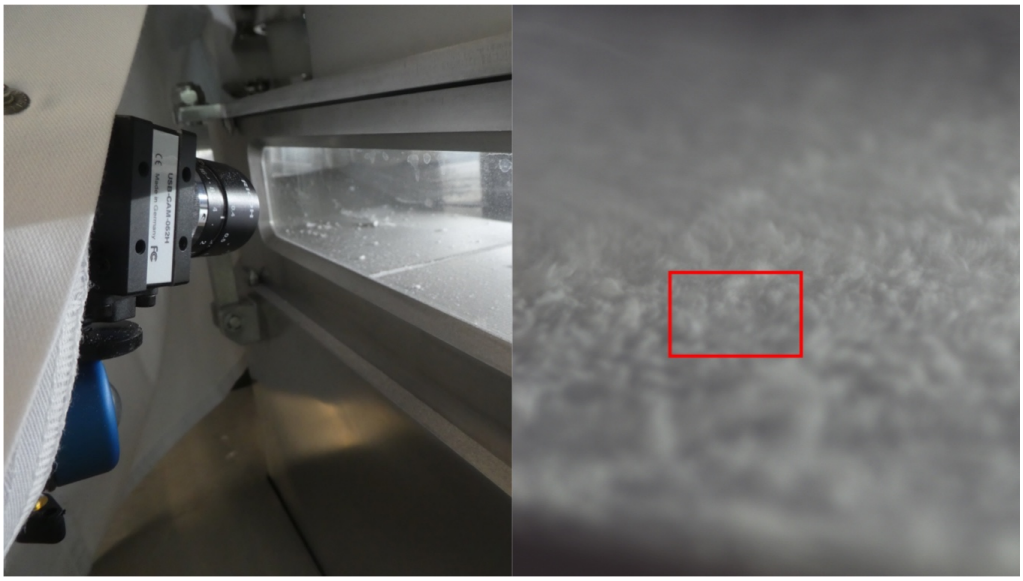

Figure 34 Experimental setup for RTD measurements – camera setup before the start of granulation to the left, right picture shows exemplary overview of measurement area and the selected frame at the entrance of the drier during granulation

Firstly, to reduce noise, the signal was smoothed by applying a Savitzky-Golay filter with polynomial order 3. Next, to offset the baseline shift that would happen occasionally, a rubber-band correction was applied. Lastly, the two-compartment model, which was originally used by Reitz et al. [197] (Eq.(7)), was fitted using the method of least squares, and the MRT was determined as the ratio of the first and the zeroth moment of the residence time density function according to Eq. (8). Additional libraries used for the different processing steps were scipy (v1.7.3), numpy (v.1.21.2) and pandas (v1. 3.5).

$$\mathrm{c(t)} = c_0 * 0.5 * e^{0.5*k^2*\sigma^2-k*(t-t_{dead})} * erfc\left(\frac{k*\sigma^2-(t-t_{dead})}{\sqrt{2}*\sigma}\right) = \frac{c_0}{k}E(t) \qquad (7)$$

Where E(t) is the residence time density function estimated by multiple parameters for the PLS: The dead time (t_{dead}), which originates from the residence time of plug flow through a pipe, a rate constant (k) as a representation of the dilution rate within a continuously stirred tank, the standard deviation (σ) to characterize the backmixing that occurs in the granulator, a scaling factor (c_0) and the time (t).

$$\mathrm{MRT} = \frac{\int_0^\infty t * E(t)dt}{\int_0^\infty E(t)dt} \qquad (8)$$

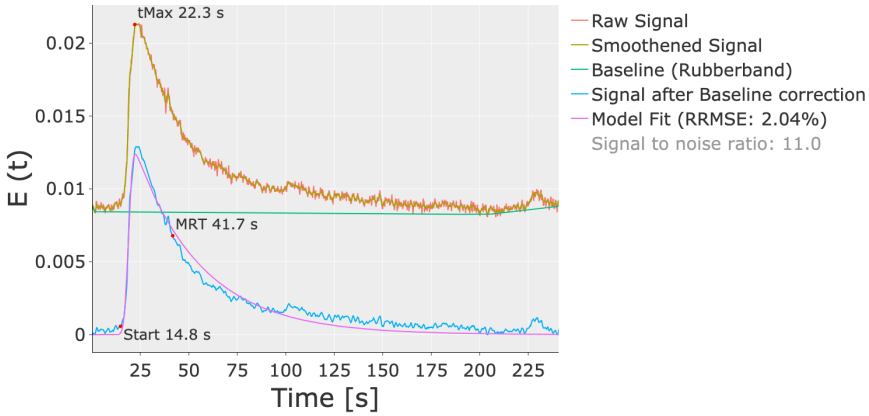

Figure 35 Evaluation of RTD-Data from ExtruVis system. Processing steps include: 1. Smoothing the data. 2. Baseline adjustments through rubber-band algorithms. 3. Fitting the two-compartment model through partial-least squares regression, first published in the International Journal of Pharmaceutics, [125] and used by courtesy of Elsevier

5.2.2 Manufacturing methods

5.2.2.1 Preparation of powder mixtures

A powder blend was created for the granulation process. Therefore, all intragranular components (Table 15) were first weighed in a large container (120 L at the site in Darmstadt versus 300 L at the site in Ennigerloh) and then milled through a 1 mm conical hole sieve using either a BTS100 in Darmstadt or a BTS200 in Ennigerloh (L.B. Bohle, Germany) with 600-700 rpm. Afterwards in Darmstadt the blend was mixed for 15 minutes at 12 rpm in a freefall blender (Servolift GmbH, Germany) or for 10 minutes at 6 rpm in a 300 L container by a bin blender (PM 600, L.B. Bohle GmbH, Germany) in Ennigerloh. The composition of the different powder mixtures is provided in Table 15.

Table 15 Overview of the different blends used during experiments

		Formulation					
		1	2a	2b	3	4	5
intragranular	Metformin	-	17.47 %	16.77 %	-	19.8 %	17.47 %
	Praziquantel	-	-		17.47 %	-	-
	Pearlitol© 160c	66 %	59.4 %	57 %	59.4%	-	-
	MCC 101	15 %	17.47 %	16.77 %	17.47 %	-	17.47 %
	PVP 25	4 %	4.65 %	4.46 %	4.65 %	-	-
	GranuLac 200	-	-	-	-	59.4 %	59.4 %
	HPMC K100M	-	-	-	-	19.8 %	-
	HPMC E5	-	-	-	-	-	4.65 %
extragranular	Parteck M200©	11 %	-	-	-	-	-
	Ac-Di-Sol©	3 %	-	4 %	-	-	-
	Mg-stearate	1 %	1 %	1 %	1 %	1 %	1 %

5.2.2.2 Twin-screw granulation

In most work packages, granulation was performed on two different scales of twin-screw granulators. The screw configuration for formulation 2a, 2b, 3 and 5 on the QbCon© 25 can be found in Figure 36, while an overview for all screw configurations used in this work are shown in Table 16.

Table 16 Overview of screw configurations used during scale-up experiments with respective formulations. Zones where slight variations occurred are highlighted in bold. Configuration for QbCon© 25 was slightly different (-0.25D for the first conveying zone) after small design changes to the mounting of the screw were added that reduced the total length to 19.75D and increased the stabilization (Formulations 2-4).

Device	Formulations	Screw Configuration
QbCon© 1	1, 2a, 2b, 3	**6D CE**, 1D KE (60° thick discs), **6D CE**, 1D KE (60°, thin discs), 2.5D CE, 1D DME, 2.5D CE
	4	**7D CE,** 1D KE (60° thick discs), **5D CE**, 1D KE (60°, thin discs), 2.5D CE, 1D DME, 2.5D CE
QbCon© 25	1	**6D CE**, 1D KE (60° thick discs), **6D CE**, 1D KE (60°, thin discs), 2.5D CE, 1D DME, 2.5D CE
	2a, 2b, 3	**5.75D CE**, 1D KE (60° thick discs), **5D CE**, 1D KE (60°, thin discs), 2.5D CE, 1D DME, 2.5D CE (Figure 36)
	4	**6.75D CE**, 1D KE (60° thick discs), **5D CE**, 1D KE (60°, thin discs), 2.5D CE, 1D DME, 2.5D CE

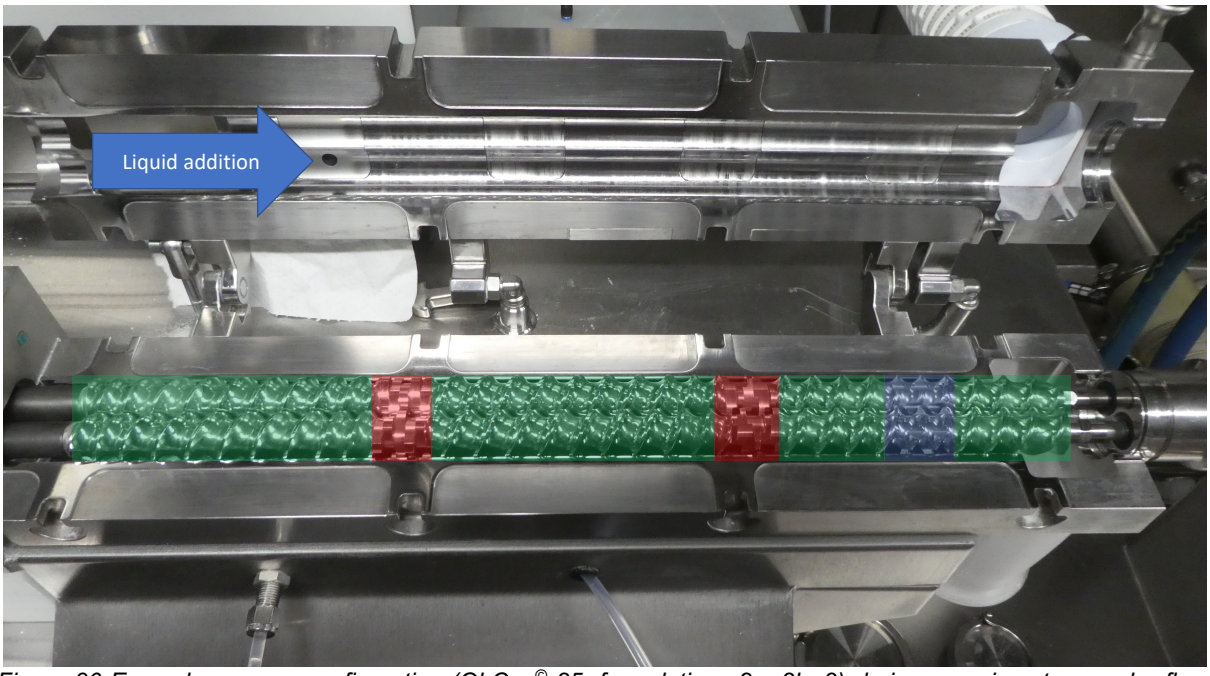

Figure 36 Exemplary screw configuration (QbCon© 25, formulations 2a, 2b, 3) during experiments, powder flow from left to right; green zones consist of medium pitched CEs only, red zones are for kneading elements (first with normal discs, second with thinned disks), blue zone consists of a DME. Length of first two conveying zones varied based on the used formulation.

At Merck in Darmstadt, the QbCon© 1, consisting of a gravimetric powder feeder (GZD 150.12, Gericke AG, Switzerland), a twin-screw granulator with 16 mm of screw diameter and a continuous fluid bed dryer was used for experiments on the smaller scale. Manual refills of the powder feeder were performed, whenever the fill level reached about 20 %. During every refill, the feeder was turned into “volumetric mode” to avoid disturbances in the process.

The QbCon© 25 line contains a feeding & blending unit (FBU) consisting of a continuous feeder (GZD 200.12, Gericke AG, Switzerland) and a continuous blender (GCM450, Gericke AG, Switzerland) with the weir set to position 0 for the lowest residence time as the powder blend was already mixed in advance. This first FBU was then connected to another gravimetric feeder (GZD200.22, Gericke AG, Switzerland) followed by the twin-screw granulator with 25 mm screw diameter and a larger continuous fluid-bed dryer to compensate for the higher throughput. The product flow of the whole line can be seen in Figure 24, including further downstream operations that are described in consecutive sections (Milling, Preparation of the tableting mix and Tableting).

Both twin-screw granulators had a L/D-ratio of 20:1 and similar geometries for screw elements (such as pitch, flight, number of kneading discs for each kneading block). Liquid was pumped into the barrel through a nozzle (0.12 mm inner diameter on the small scale and 0.12 or 0.25 mm on the large scale) by an incorporated micro annular gear pump (MZR 7255, HNP Mikrosysteme, Germany).

Temperature was kept constant at 30°C as the barrel jacket was cooled through an external cooling system (CH-6-6-L, Single Temperiertechnik, Germany).

5.2.2.3 Continuous fluid bed drying

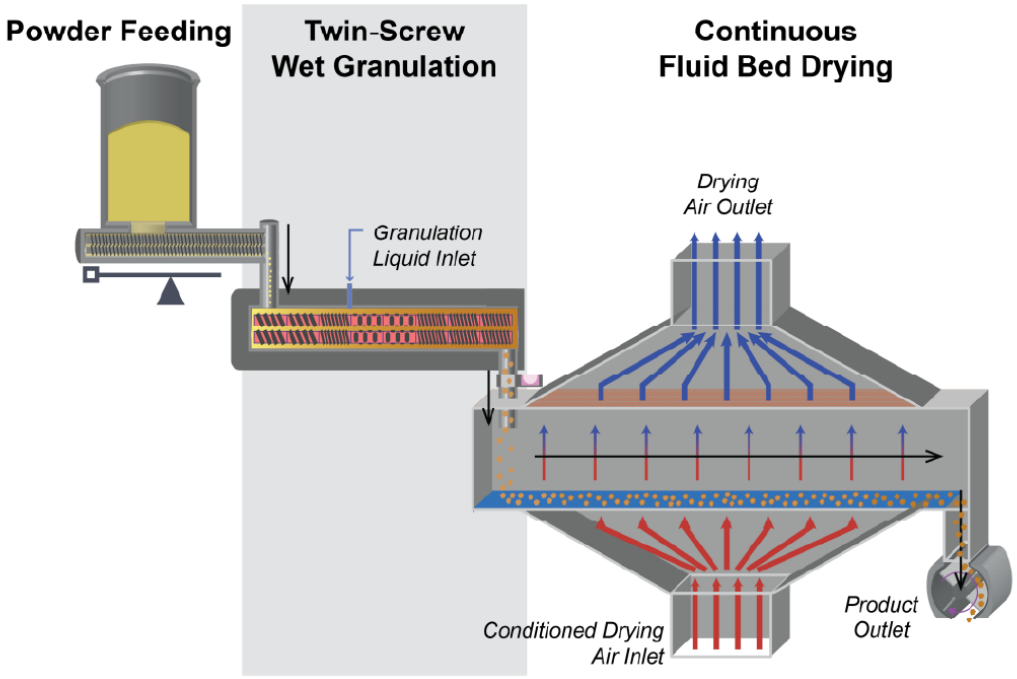

Figure 37 QbCon concept for TSWG & VFBD kindly provided by L.B.Bohle

As described in 1.4.3 granules were transported directly from the exit of the granulator into the inlet of the VFBD (Figure 37). To ensure that the airstream is directed towards the product filter and outlet of the dryer and does not interfere with the prior granulation and feeding processes, a negative pressure (-0.8 mbar) was applied constantly.

Both, the airflow and the heating were already activated 30 minutes prior to any granulation run to ensure that the whole drying unit was already reaching the desired temperature for the granulation process and thus reduce time until a steady state is reached in the drier.

The drying parameters (air flow, air temperature and vibration acceleration) were selected in preliminary trials based on previous experience and the applied granulation parameters (especially throughput and L/S-ratio). A first estimation for suitable air temperature, air flow and vibration acceleration was used and the powder flow through the drier was observed:

If large lumps remained at the entrance of the drier either the airflow or the vibration acceleration could be increased to enhance the transportation. If a high number of particles was dispersed in the air and directed towards the filters, this could be attributed to the airflow being too high and corrected by decreasing it to achieve a more stable and controlled transportation through the granulator. After exiting the drier,

granules were held up on top of a rotary valve to measure product temperature and potentially enable additional PAT-measurements before they are discharged. The LOD was then measured at least three times over a period of 10-15 minutes according to 5.2.3.1 and if it was found to be in a range between approximately 0.8 % and 1.5 % the drying parameters were considered suitable for the applied granulation parameters. If the LOD was too low, the drying capacity was decreased by reducing the air temperature or air flow and the LOD was measured again after the process was stable and sufficient time had passed to ensure new material was presented. Similarly, if the LOD was too high the drying capacity was increased by inversing the procedure.

As the dimensions for the drier of the QbCon© 25 were scaled to increase the drying capacity by approximately 10-fold and thus the drier was substantially underfilled during the reference runs performed at 2 kg/h, the vibration acceleration had to be drastically increased to the maximum of 8 m/s^2 to ensure that the granules were not overdried.

An overview of the granulation and drying parameters for each work package can be found in the respective chapters.

5.2.2.4 Granule sample collection

As both the granulation and drying process were continuous processes, process parameters for each specific run could be adjusted right after the previous run. However, it is well described in literature that a certain stabilization period is necessary for TSWG to ensure that all the parameters have reached a steady state condition [198]. Therefore, a waiting period of about 15 minutes between a parameter change and the collection of the next samples was introduced to ensure the process was stable and no granules from the previous run were still left in the continuous granulator and drier.

The LOD of the granules at the drier outlet was measured at the beginning and at the end of the sample collection for each run, which started after the initial waiting period and lasted until approximately 500 g of granules on the small scale and 1 kg of samples on the large scale were collected for further processing and analysis.

For experiments conducted in 3.4, the sample size was increased to 5 kg as more granules were required for the tableting process on the rotary press versus the compaction simulator.

5.2.2.5 Milling

For further characterization and processing, granules produced on the twin-screw granulator were milled on a BTS-100 in Darmstadt or on a BTS-200 (both conical mills by L.B. Bohle, Germany) for experiments that were done in Ennigerloh. During milling about two thirds of the manufactured granules (300-700 g) were added to a 1 mm conical hole sieve which was then powered at 600-700 rpm until all particles were milled. The sieve was dry-cleaned by hand with a vacuum cleaner and a brush in between batches of the same formulation and fully cleaned whenever a different formulation went through the sieve.

For the comparison of MP versus FC in 3.4, a 1 mm conical rasping sieve (L.B. Bohle, Ennigerloh) was used instead of the hole sieve to ensure a sufficient milling performance without the piling up of residual granules. Additionally, for the FC line, an interval and a duration could be set for the milling process and the simultaneously applied vacuum to transport granules up to the FBU (settings provided in the discussion of 3.4.4 directly).

5.2.2.6 Preparation of the tableting mix

Before tableting, the extragranular components (Table 15) except for the lubricant were added to 200-300 g of the milled granules and mixed on a lab-scale blender (Turbula®, WAB, Germany) at 20 rpm for 10 minutes. Afterwards, the magnesium stearate was added as a lubricant and the blend was mixed for additional five minutes unless specified otherwise.

For experiments performed in 3.4, a blend of both extragranular components (disintegrant and lubricant, see Table 15) was prepared in a 20 L container with a laboratory scale blender (LM 40, L.B. Bohle, Ennigerloh, 5 minutes at 20 rpm). This extragranular blend was then either added manually to the milled granules and blended for another 5 minutes at 20 rpm (manual processing) or fed to the fully continuous blender in the second FBU (GCM450, Gericke AG, Switzerland, weir position 5 at 100 rpm) by a feeder (GZD 200.12, Gericke AG, Switzerland) at 5 % of the total throughput (fully continuous line).

5.2.2.7 Tableting

50 tablets with an individual weight of 400 mg were compressed at five different compaction pressures (90 MPa, 120 MPa, 150 MPa, 200 MPa and 300 MPa for formulations 1-3; 100 MPa, 150 MPa, 200 MPa, 300 MPa for formulation 4) on a single punch tablet press (STYL'One Evolution, Medelpharm, France). A flat faced Euro B punch of 11.28 mm diameter was used. A simulation of the Korsch XL 100 tablet press (3.1 & 3.2) was set as a compression cycle with a set pre-compaction pressure of 8-9 MPa and 50 rpm. The standard compaction cycle of the STYL'One Evolution was used for additional investigations in chapter 3.2 and subsequently for all compactions in chapter 3.3 at 20 % speed to avoid the lamination of tablets that was observed at high compaction pressures in chapter 3.2. For the cycle simulation of a Korsch XL 100, the maximum punch velocity was about 60 mm/s and for the standard compaction cycle around 30 mm/s.

Tablets for 3.4 were compressed at four different compaction pressures (see Table 12) on a rotary press (X3, Korsch AG, Germany), at L.B. Bohle in Ennigerloh, Germany using 8 mm biconvex punches and an average weight of 200 mg. The tablet press was either refilled manually (manual processing) or fully continuously by the second FBU. The compaction speed of the tablet press was adapted based on the total throughput of the continuous line. Furthermore, additional tablets (400 mg weight, 11.28 mm diameter) were compressed in Darmstadt with the standard compaction cycle five different compaction pressures (on the STYL'One Evolution to further investigate potential differences in tabletability resulting from the operational mode of the experiments in 3.4 (MP versus FC) and additionally at four different compaction speeds (10 %, 20 %, 40 % and 80 %) and three different compaction pressures (100 MPa, 200 MPa, 300 MPa) to determine the impact of the compression speed on the tensile strength of tablets.

5.2.3 Characterization Methods

5.2.3.1 Loss on drying

For the determination of LOD values, samples of approximately 3 g were collected directly at the exit of the continuous fluid bed dryer and measured by an off-line moisture analyzer (HE53/HR-73, Mettler-Toledo, Germany). For mannitol-based

formulations, granules were dried at 105°C until mass constancy was reached ($\Delta m < 1$ mg in 140 s) and lactose-based formulations were dried at 95 °C for 10 minutes to reduce impact on the measurement by crystal water. For each batch at least one measurement was done at the beginning of sample collection and one at the end. Furthermore, after milling, granule samples were randomly collected and measured (n=1) to confirm the previously obtained values and ensure no differences due to potential water inclusions in larger particles might affect downstream processes, such as blending and tableting.

LOD was automatically calculated by the device according to Eq. (9)

$$LOD = \frac{m_{start} - m_{dry}}{m_{start}} \cdot 100\,\% \tag{9}$$

5.2.3.2 Granule size distribution

To determine the GSD, 20-30 g of granules were prepared as described in 5.2.1.1 for both milled and unmilled granules respectively. Afterwards the GSD was assessed through dynamic image analysis (Camsizer X2, Retsch, Germany) of a dispersed particle stream. To separate loosely bound agglomerates, a dispersion pressure of 25 kPa was applied for each measurement.

For most batches, measurements were performed only once as a high reproducibility of the sample preparation through the riffle splitter and of the measurement results in general could be confirmed. Furthermore, random checks with n=3 were performed sporadically to further validate these observations. The given volume distributions were based on the x_area method, which provides the equivalent spherical diameter of the projected particle based on Eq. (10):

$$d = \sqrt{\frac{4A}{\pi}} \tag{10}$$

Where d is the equivalent spherical diameter and A is the area of the projected particle. Additionally, in some cases d_{10}, d_{30}, d_{50}, d_{70} and d_{90} were given as the respective 10 %/30 %/50 %/70 %/90 %-percentiles for the granule size distribution.

5.2.3.3 Comparing size distributions via Earth Mover's Distance

For further comparison of particle sizes and GSDs beyond percentiles of the volume distribution, the EMD, also described as Wasserstein distance, was applied. It is used to further quantify differences in GSDs between granules produced on the QbCon© 1 to those produced on the QbCon© 25. Unlike summary statistics, such as the different percentiles or peak values in the GSD, the EMD is used to compare the whole distribution profile and is thus better suited to compare different granules in this study as many GSDs show a bimodal distribution typical for TSWG.

In simple terms, the EMD is the solution to an underlying transportation problem: distributions that are compared to each other are conceptually represented as two piles of earth and the EMD represents the minimum amount of work necessary to transform one pile into another. The 'work' can be regarded as the distance a unit of earth is moved. The EMD has been previously used for different use cases, such as digital image retrieval [199], [200] and visual tracking [201] but has also been described in literature as a metric for the comparison of particle size distributions [76], [202].

For the computation of the EMD a linear programming problem is solved where: $\mathrm{P} = \{(\mathrm{w}_{p_1}, p_1), (\mathrm{w}_{p_2}, p_2), \dots, (\mathrm{w}_{p_m}, p_m)\}$ as a representation of the histogram for the first distribution profile (or metaphorically the first pile of earth) and $\mathrm{Q} = \{(\mathrm{w}_{q_1}, q_1), (\mathrm{w}_{q_2}, q_2), \dots, (\mathrm{w}_{q_n}, q_n)\}$ to reflect the histogram of the second distribution profile where p_i and q_i represent the respective location for the columns of the histogram and w_{p_i} and w_{q_i} indicate the weight for each column (or the height of the pile of earth at its respective location). To determine the ground distance between p_i and q_i a ground distance matrix $\mathrm{D} = [\mathrm{d_{ij}}]$ is defined and afterwards the ideal flow between p_i and q_i, $F = [f_{ij}]$, can be determined based on Eq. (11) to minimize the overall cost [202], [203].

$$WORK\,(F, P, Q) = \sum_{i=1}^{m}\sum_{j=1}^{n} f_{ij} d_{ij} \qquad (11)$$

where the following requirements must be met:

I. $f_{ij} \geq 0,\ 1 \leq i \leq m,\ 1 \leq j \leq n$

II. $\sum_{j=1}^{n} f_{ij} \leq w_{p_i},\ 1 \leq i \leq m$

III. $\sum_{i=1}^{n} f_{ij} \leq w_{q_j},\ 1 \leq i \leq n$

IV. $\sum_{i=1}^{m}\sum_{j=1}^{n} f_{ij} = min\left(\sum_{i=1}^{m} w_{p_i}, \sum_{i=1}^{n} w_{q_j}\right)$

The first constraint ensures that f_{ij} can't be negative and thus the flow is unidirectional from P to Q. The second boundary ensures that only as much weight can be moved from P to Q as is available in P, while the third boundary ensures that the moved weight does not exceed the maximum amount for Q. Lastly, the fourth constraint dictates, that all of the available weights have to be moved.

When this underlying transportation is solved and the optimal flow F is found, the EMD can be defined as the work normalized by the total flow according to Eq. (12) [202], [203]:

$$EMD\ (P,Q) = \frac{\sum_{i=1}^{m}\sum_{j=1}^{n} f_{ij} d_{ij}}{\sum_{i=1}^{m}\sum_{j=1}^{n} f_{ij}} \qquad (12)$$

Thus, the more the calculated EMD approaches zero, the more similar can the size distributions be considered, while higher EMDs indicate dissimilarity. As the resulting EMD value depends significantly on the scale (i.e., linear or logarithmic), the spacing of the input data provided and the definition of test and reference samples, EMD values can only be used as a comparative measure where similar input data was provided.

For this work, the q3 distributions of granules were compared using a python (v3.7.1) script and applying the stats.wasserstein_distance function, which was used as part of the scipy (v.1.7.3.) library. Measurements from 5.2.3.2 were exported covering a particle size range of 0-3000 µm for milled granules and 0-4000 µm for unmilled granules with the maximum amount of linear spacing (300 values).

5.2.3.4 Bulk and tapped density

For the determination of bulk and tapped density, ~15-20 g of milled granules were analyzed on a GranuPack (GranuTools, Belgium). The sample is placed in a metallic tube with defined dimensions and a hollow cylinder is added on top of the powder bed to keep the surface flat. For the measurement the cell is then tapped with a frequency of 1 Hz for 1000 taps (for the initial placebo experiments in the first two work packages

only 500 taps were applied). An inductive sensor determines the powder bed height after each tap to calculate volume and density of the sample in real-time [204].

To further determine flowability of the granules, the Hausner-ratio was calculated according to Ph. Eur. 2.9.36 [4] by Eq. (13):

$$Hausner\ ratio = \frac{V_0}{V_f} = \frac{\rho_{tapped}}{\rho_{bulk}} \quad (13)$$

where V_0 is the initial apparent volume, V_f is the final volume after all taps, ρ_{tapped} is the tapped density and ρ_{bulk} is the bulk density.

5.2.3.5 Ring shear cell tester

To determine flowability, the flow function coefficient (ffc) of both the pre-granulation powder blend and the granules of formulations 2-4 were determined by a ring shear tester RST-XS (Dietmar Schulze, Schüttgutmesstechnik, Germany). For the measurements a normal pre-shear stress of 9000 Pa and three different consolidation stresses of 1800, 4500 and 7200 Pa were applied.

Afterwards the ffc was calculated and evaluated according to Jenike [157] based on a ratio of major principal stress and unconfined yield strength Eq. (14).

$$ffc = \frac{major\ principle\ stress}{unconfined\ yield\ stress} \quad (14)$$

For the pre-granulation blends, measurements were done with n=3, while investigations on granules were mostly done with n=1 due to limitations in available granule. Materials were then classified based on their ffc value [157] (Table 17)

Table 17 Classification of powder flow based on ffc-values

ffc-value	**flow behavior**
ffc <1	not flowing
1 < ffc < 2	very cohesive
2 < ffc < 4	cohesive
4 < ffc < 10	easy flowing
10 < ffc	free flowing

5.2.3.6 Gas pycnometry

Pycnometric density (ρ_p) of the powders and granules was evaluated via gas displacement technique through nitrogen using an Ultrapyc 1200e (Quantachrome Instruments, USA). A test cell with a volume of 40 cm^3 was filled to about 80 % with the sample powder, and sample mass was determined.

Each sample was measured until the relative standard deviation of three consecutive runs dropped below 0.05 % and afterwards the mean of those three consecutive runs was given. Additionally, three measurements were performed for each material.

5.2.3.7 Microscopic imaging

Microscopic images of particles were taken using a Keyence digital microscope VHX7000 (Keyence Deutschland GmbH, Germany) at magnification ranges between 50x – 500x. For a better reference a scale was added to all images (Figure 41 in the appendix).

5.2.3.8 Granule strength and failure load

Both, granule strength and failure load of granules produced in 3.1 were measured based on an uniaxial confined compression analysis [205] on a STYL'One Evolution compaction simulator (Medelpharm, France). A die of 100 mm^2 base area and 10 mm height was filled manually, and the granules were compressed uniaxially at an upper punch speed of 3.5 mm/min until a final height of 5 mm was reached.

To reduce the influence of different GSDs during the comparison of batches, 40 – 80 g of milled granules were divided in four size classes: from 0 – 125 µm, from 125 – 355 µm, from 355 – 500 µm and from 500 – 800 µm. Granules larger than 800 µm were discarded as they made up less than 5 % of the blend and not enough material could be collected for this method. Five replicate measurements were conducted with each granule batch.

Analysis was then conducted as described in Arndt et al. [206] and is based on Eq. (15) [205]:

$$ln\,P = ln\left[\frac{\tau}{\alpha}\right] + \alpha\epsilon + ln\,(1 - e^{-\alpha\epsilon}) \quad (15)$$

where P is the applied compaction pressure, τ is the cohesive strength, α is the friction coefficient and ϵ is the natural strain. P was calculated from the force applied on the granules and the cross-sectional surface area of the punch. Plotting ϵ versus ln P and finding the linear portion of the graph allowed for the determination of α through the slope and $ln\left[\frac{\tau}{\alpha}\right]$ through the y-axis intercept.

To determine the failure load, Eq. (16) was applied [205].

$$F_{calc} = \frac{\pi d_a^2}{4} * \tau \quad (16)$$

Where d_a is the average agglomerate diameter of the selected fraction.

After determining both, the granule failure load and the cohesive strength for each fraction, a weighted average was computed based on the fractions (see Eq. (17)).

$$\bar{m} = \sum_{i=1}^{N} c_i m_i \quad (17)$$

Where c is the percentage weight of the fraction, m is the mean value of this fraction and N the number of fractions.

5.2.3.9 Tablet dimensions, weight and tensile strength

Tablet dimensions (height and diameter), weight and breaking force were determined automatically using either a MultiCheck VI (Erweka GmbH, Langen, Germany) for the first two work packages or a ST50 (Sotax AG, Switzerland) for work packages 3 and 4. On both devices a constant tablet breaking speed of 2.3 mm/s was used. Based on the measured breaking force of the tablets, tensile strength of 11.28 mm round tablets was calculated via Eq. (18) according to Fell and Newton [207]:

$$TS = \frac{2 * F}{t * d * \pi} \quad (18)$$

where TS is the tensile strength (in MPa), F is the force at which the tablet shattered (in N), t is the tablet height and d is the tablet diameter.

For biconvex tablets produced during experiments in 3.4, tensile strength was calculated via Eq. (19) according to Pitt et al. [208].

$$TS = \frac{10F}{\pi D^2 (2.84\frac{t}{D} - 0.126\frac{t}{W} + 3.15\frac{W}{D} + 0.01)} \quad (19)$$

Where similar to Eq. (18) TS and F are tensile strength and compaction force respectively, t is the tablet height, W is the wall height and D is the tablet diameter.

5.2.3.10 Tablet friability

Measurement of tablet friability was done according to Ph. Eur. 2.9.36 [4] using a sample of >6.5 g of tablets on a friabilator (TAR, Erweka, Germany) for 4 minutes at 25 rpm. The percentage weight loss was expressed as friability.

5.2.3.11 Disintegration of tablets

To measure disintegration times of tablets, for each run, 6 tablets were tested in demineralized water tempered at 37°C ± 2°C using a DT50 apparatus (Sotax AG, Switzerland) with automatic end-point detection.

5.2.3.12 Content uniformity of tablets

Content uniformity of metformin based tablets was determined through UV/Vis absorption at 232 nm. Tablets were weighed into a 100.0 mL volumetric flask and dissolved in an ultrasonic bath over 2 h in 100 mL of purified water. Afterwards 1.0 mL of this solution was added to a 50.0 mL volumetric flask and filled with purified water. This solution was then analyzed using a Cary 3500 (Agilent Technologies Inc., USA) UV/vis spectrometer at 232 nm wavelength.

A calibration curve (see Figure 38) was made by weighing metformin to reach final concentrations between 3 and 10 µg/mL and thus cover an absorption range between approximately 0.2 to 0.8, adding the same excipients that were used in the tablet matrix and treating the reference samples similarly as the measurement samples (2 dilution steps, 2 h preparation in an ultrasonic bath) to ensure applicability to the measurements.

The AV was then calculated based on the requirements of section 2.9.5 of the Ph. Eur.[4] (Eq. (20)):

$$AV = |M - \bar{X}| + ks \qquad (20)$$

Where M is the reference value [%], $\bar{X}$ is the mean of individual contents in reference to the label claim [%], k is the acceptability constant (2.4 for a sample size of n = 10 and 2.0 for a sample size of n = 30) and s is the sample standard deviation.

M = 98.5 %, when $\bar{X}$ < 98.5 %, M = 100% when 98.5 % < $\bar{X}$ < 101.5 % and M = 101.5% when $\bar{X}$ > 101.5%.

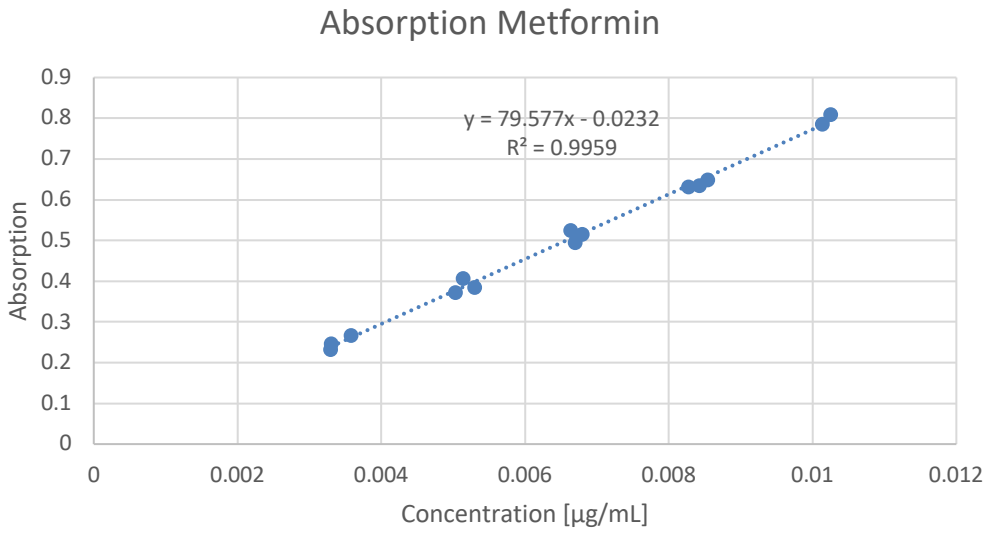

Figure 38 Calibration curve for metformin at 232 nm

5.2.3.13 Release profile of tablets

Tablets based on the extended-release formulation were tested for their dissolution profile using a AT7 Smart Semiautomatic Dissolution Tester (Sotax AG, Switzerland) with automatic sampling. Measurements were performed in triplicate in 900 mL of phosphate buffer with pH 6.8 using rotating baskets. Sample of 5 mL were taken automatically after 0.5, 1, 2, 4, 6, 8, 12, 16 and 20 hours respectively, filtered through a 25 mm glass microfiber filter (Whatman® 1822-025, GE Healthcare GmbH, Germany) and then analyzed by UV/Vis absorption at 232 nm with a Tecan Spark multimode plate reader (Tecan Trading AG, Switzerland).

6 Appendix

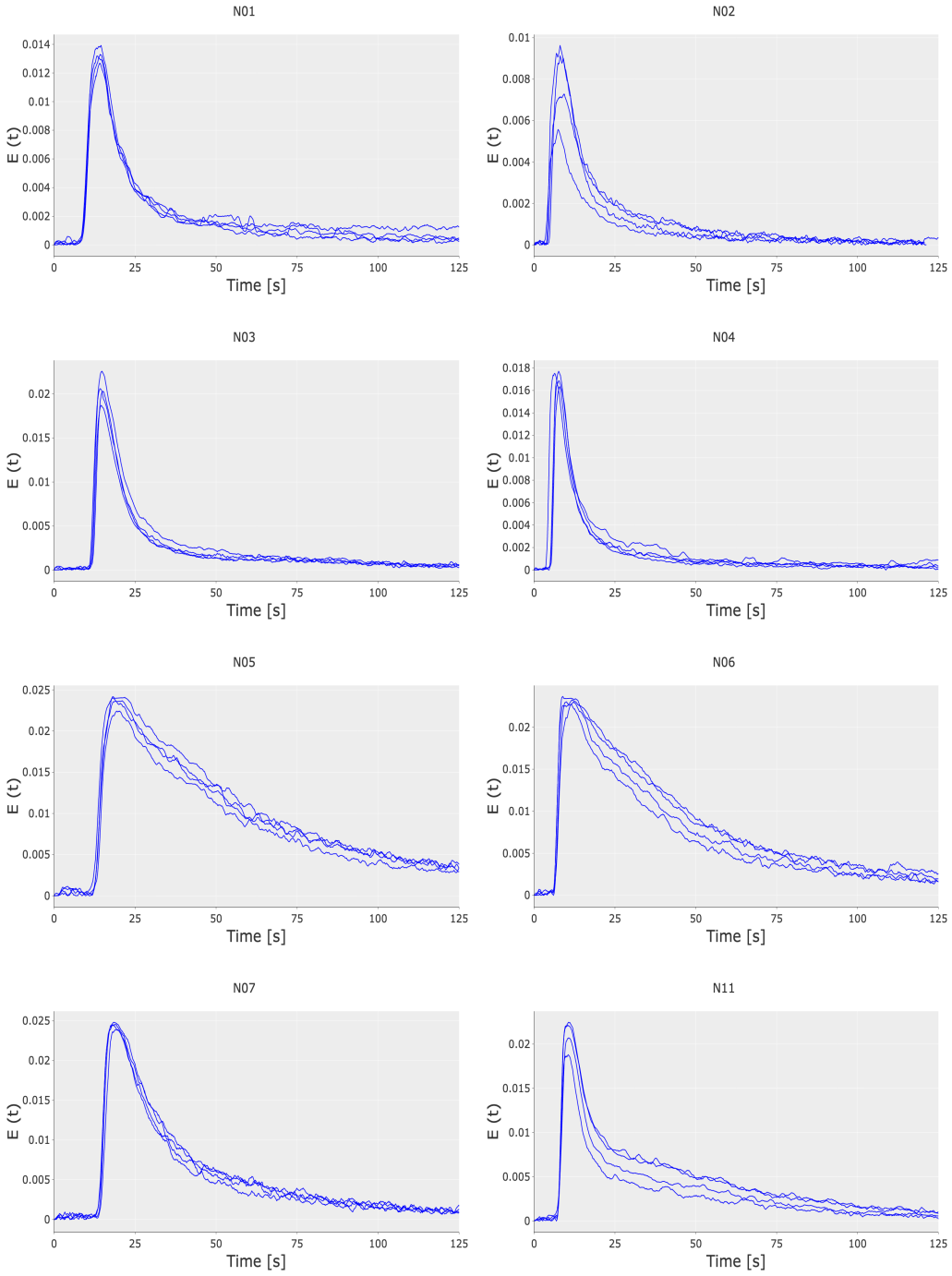

	N1	N2	N3	N4	N5	N6	N7	N11
tmax [s]	14	8	14	7	18	10	18	10
MRT [s]	23	17	22	13	70	49	40	34

Figure 39 Overview of RTD measurements during DoE performed in 3.1.3

Table 18 Measured values used for model creation in Table 2

			before milling			**after milling**							
Exp Name	Run Order	LOD [%]	d_{10} [µm]	d_{50} [µm]	d_{90} [µm]	d_{10} [µm]	d_{50} [µm]	d_{90} [µm]	Cohesive Strength [MPa]	Tensile Strength (150 MPa) [MPa]	Disintegration Time [s]	t_{Max} [s]	MRT [s]
N01	5	0.83	84	350	1247	51	171	548	0.82	1.48	183	14	23
N02	1	0.81	80	317	1159	50	172	603	0.88	1.46	199	8	17
N03	6	1.53	80	404	1098	52	193	662	0.93	1.76	288	14	22
N04	9	1.43	88	369	1228	54	182	595	0.90	1.74	375	7	13
N05	3	1.07	235	749	1290	131	439	802	1.64	1.81	497	18	70
N06	7	1.02	212	681	1225	127	420	798	1.61	1.92	399	10	49
N07	11	2.18	295	1006	1825	133	494	862	2.13	2.13	496	18	40
N08	10	1.22	307	853	1336	161	501	834	2.11	2.08	475		
N09	8	1.12	148	615	1320	89	276	728	1.29	1.71		10	32
N10	4	1.22	146	612	1300	87	289	749	1.37	1.76	382	10	40
N11	2	1.06	149	639	1315	83	269	729	1.42	1.81	372	10	39

Figure 40 Showcase of possible locations where powder bridging occurred during transportation of a poorly flowing pre-blend with an ffc < 4 (formulation 4) - with courtesy of L.B. Bohle Maschinen + Verfahren, first published in Pharmaceutical Development and Technology [153]*and used by courtesy of Taylor & Francis*

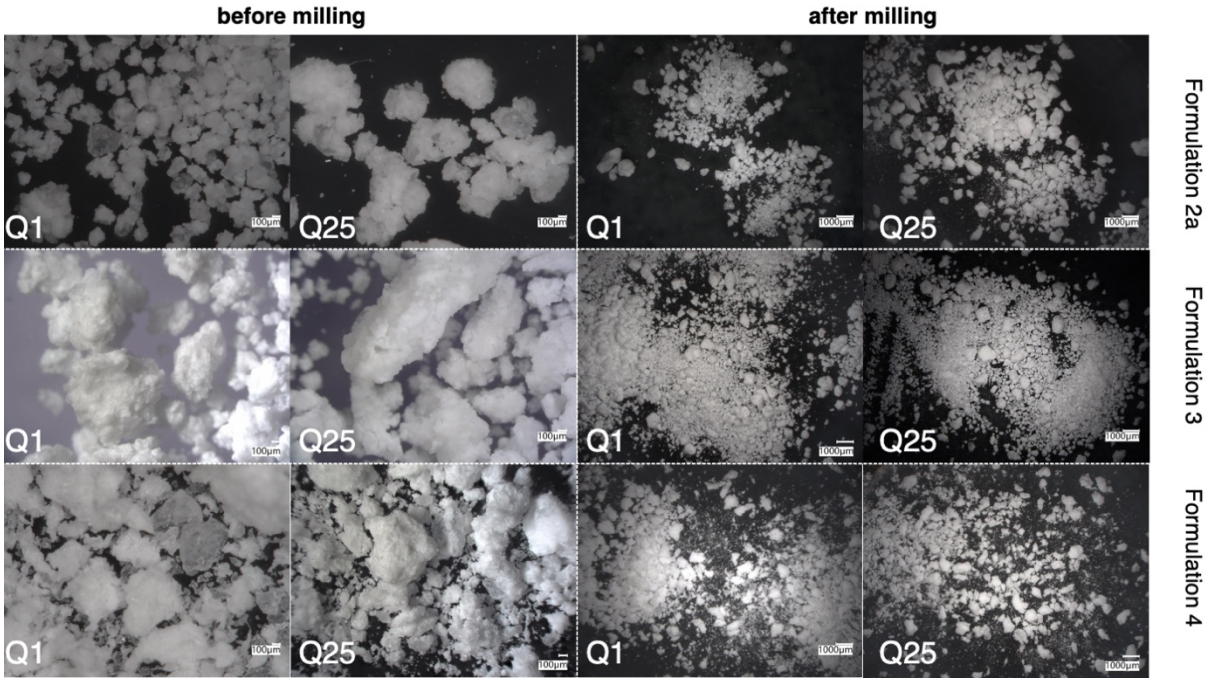

Figure 41 Microscopic images of granules before and after milling for both scales, first published in Pharmaceutical Development and Technology [153] and used by courtesy of Taylor & Francis

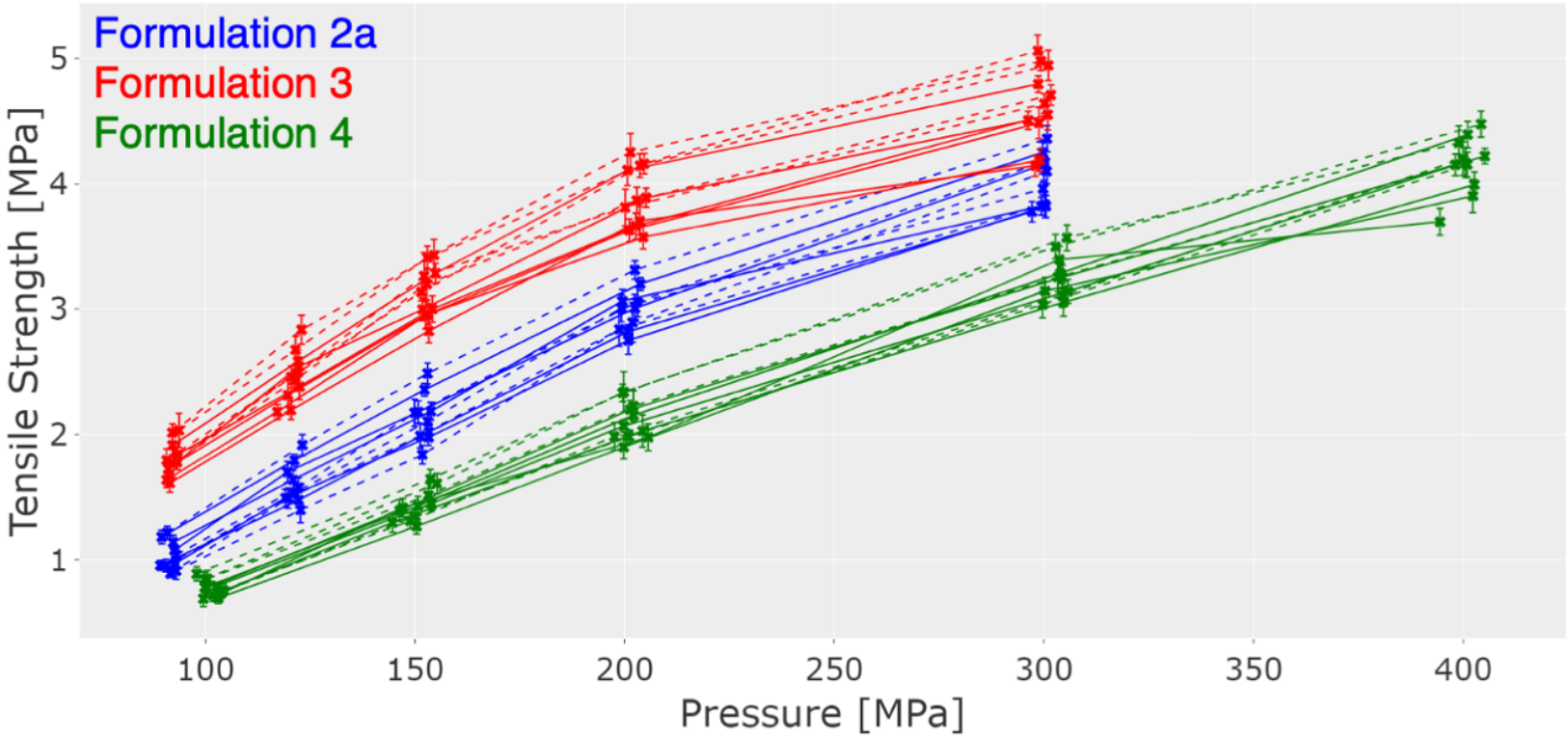

Figure 42 Formulation overview of tablet tabletability. Dashed lines correspond to high SS settings (mean±SD, n=20), first published in Pharmaceutical Development and Technology [153] and used by courtesy of Taylor & Francis

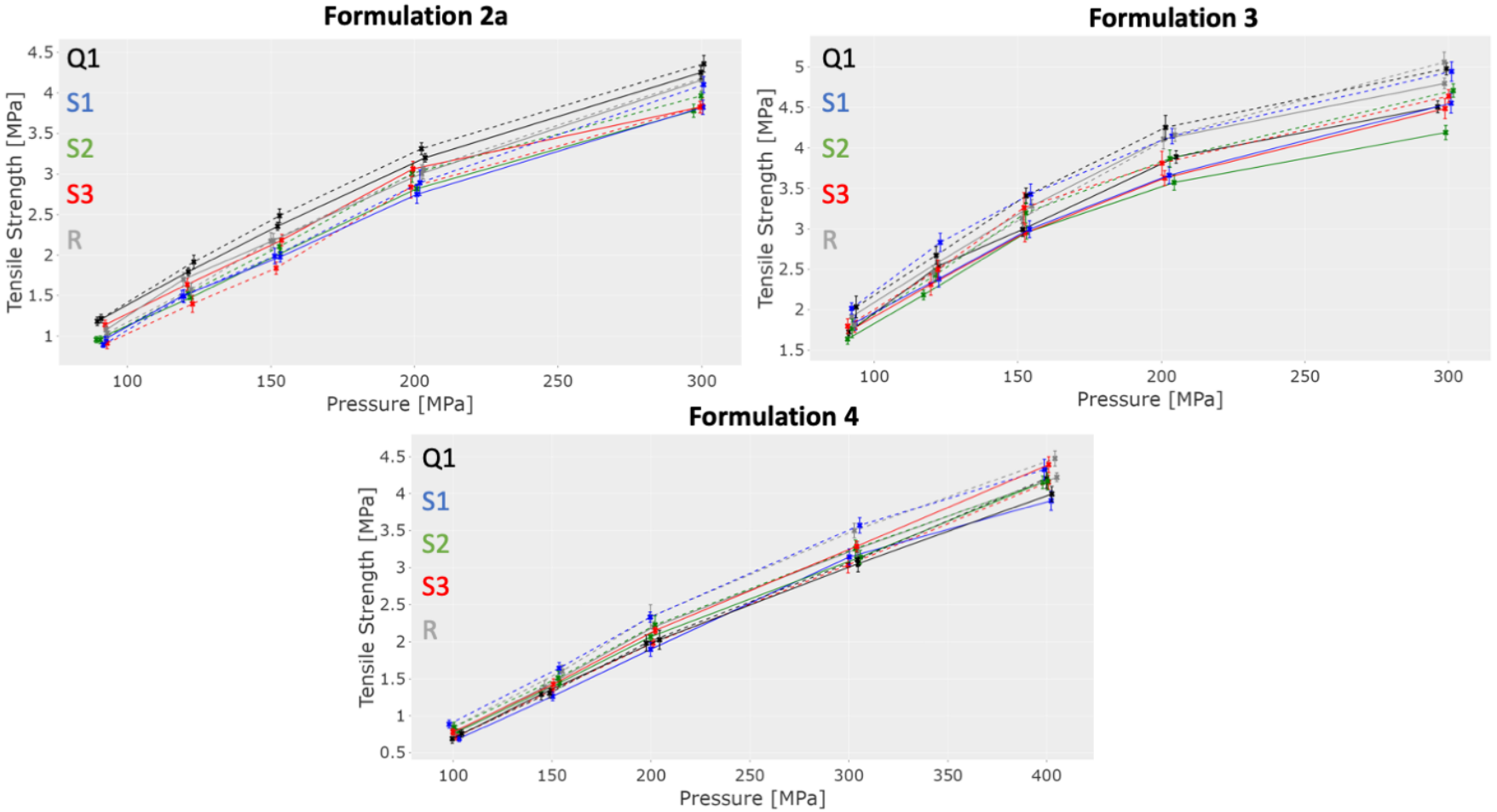

Figure 43 Overview of tabletability based on strategy for each formulation. Dashed lines correspond to high SS settings. (mean±SD, n=20), first published in Pharmaceutical Development and Technology [153] and used by courtesy of Taylor & Francis

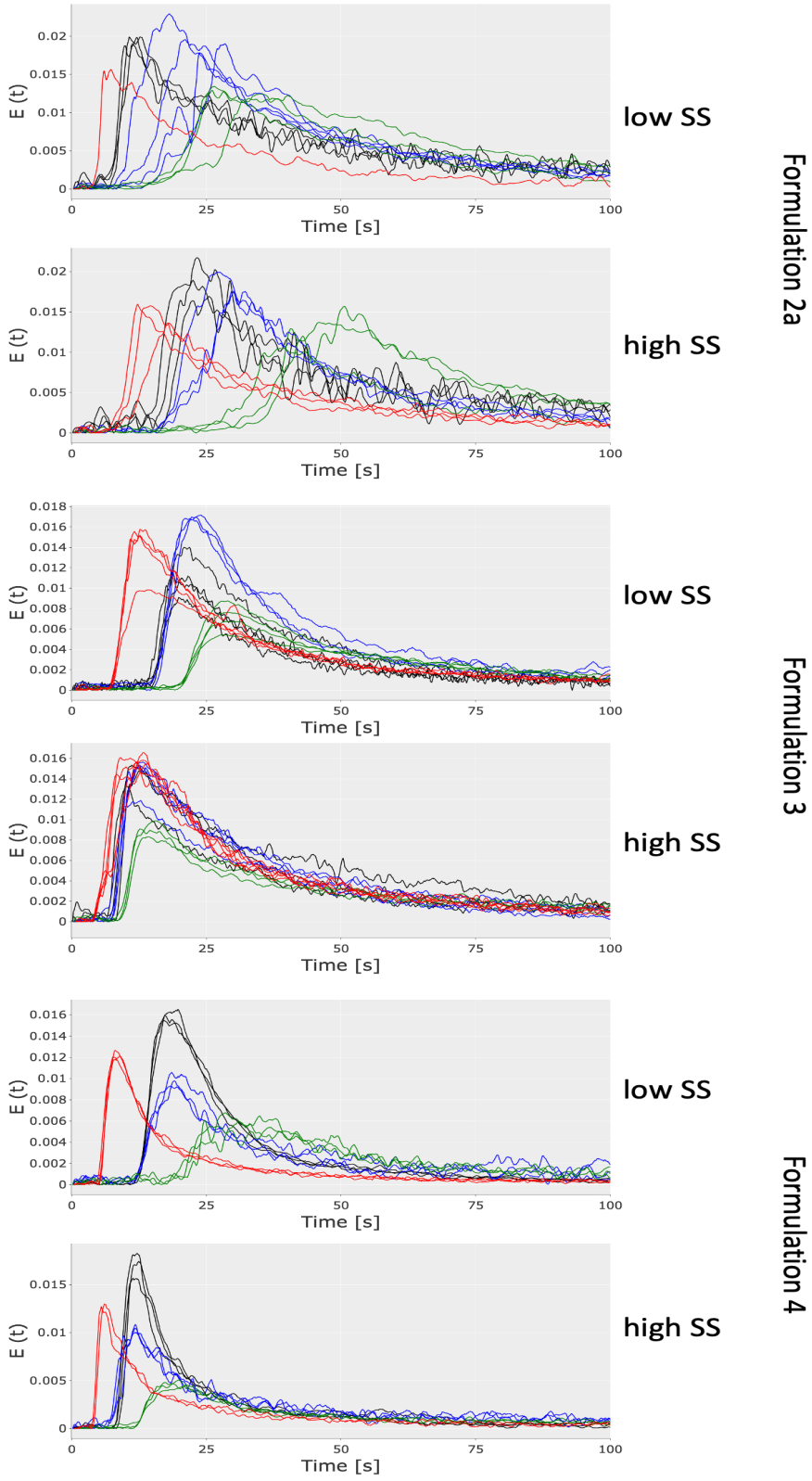

Figure 44 Overview of RTD measurements in 3.3.3 - Strategies and scales depicted in different colors (S1 – blue, S2 – green, S3 – red, R – grey) with black lines as reference for the small scale, first published in Pharmaceutical Development and Technology [153] and used by courtesy of Taylor & Francis

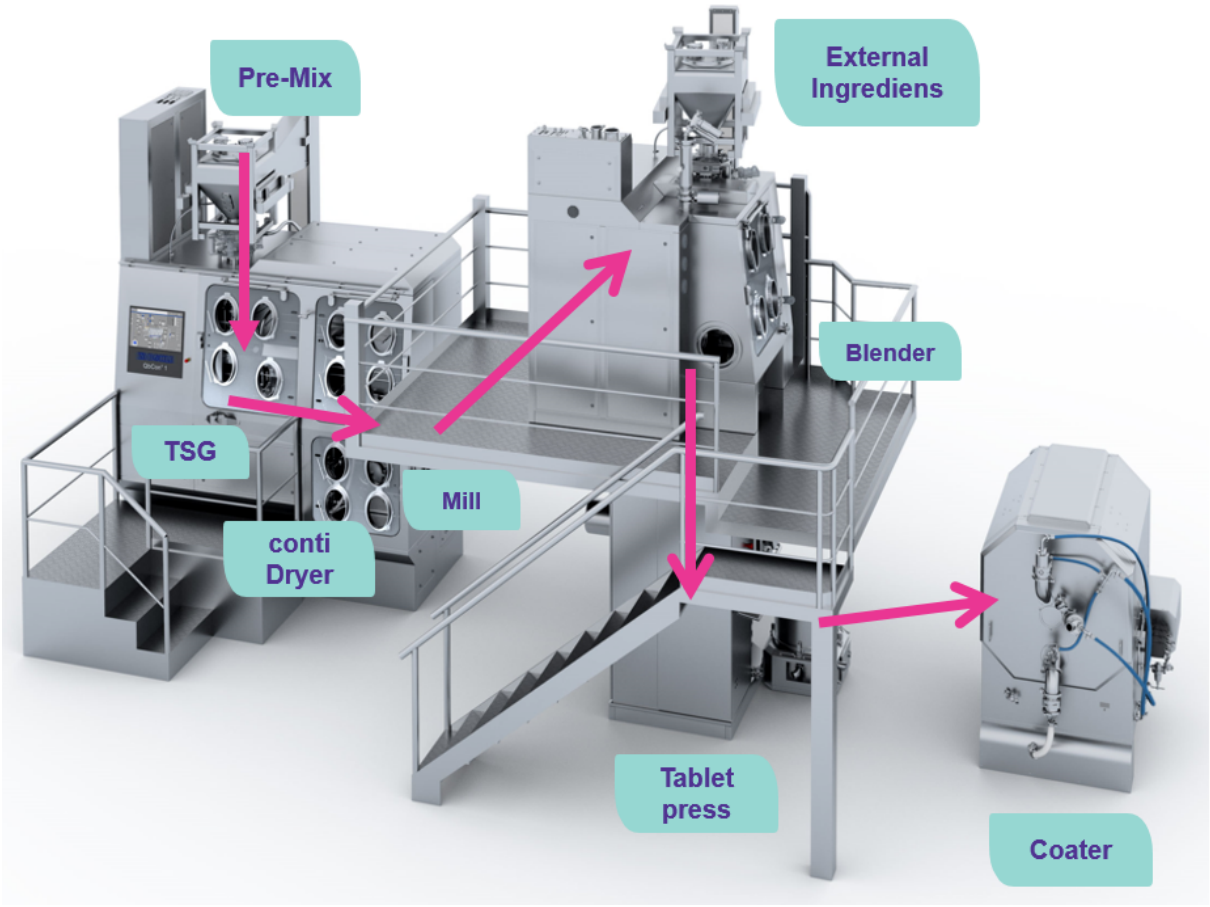

Figure 45 Design of a fully continuous QbCon© 1 line for clinical trial supply of highly potent APIs from powder blend to tablet, kindly provided by Merck Healthcare KGaA in Darmstadt

.

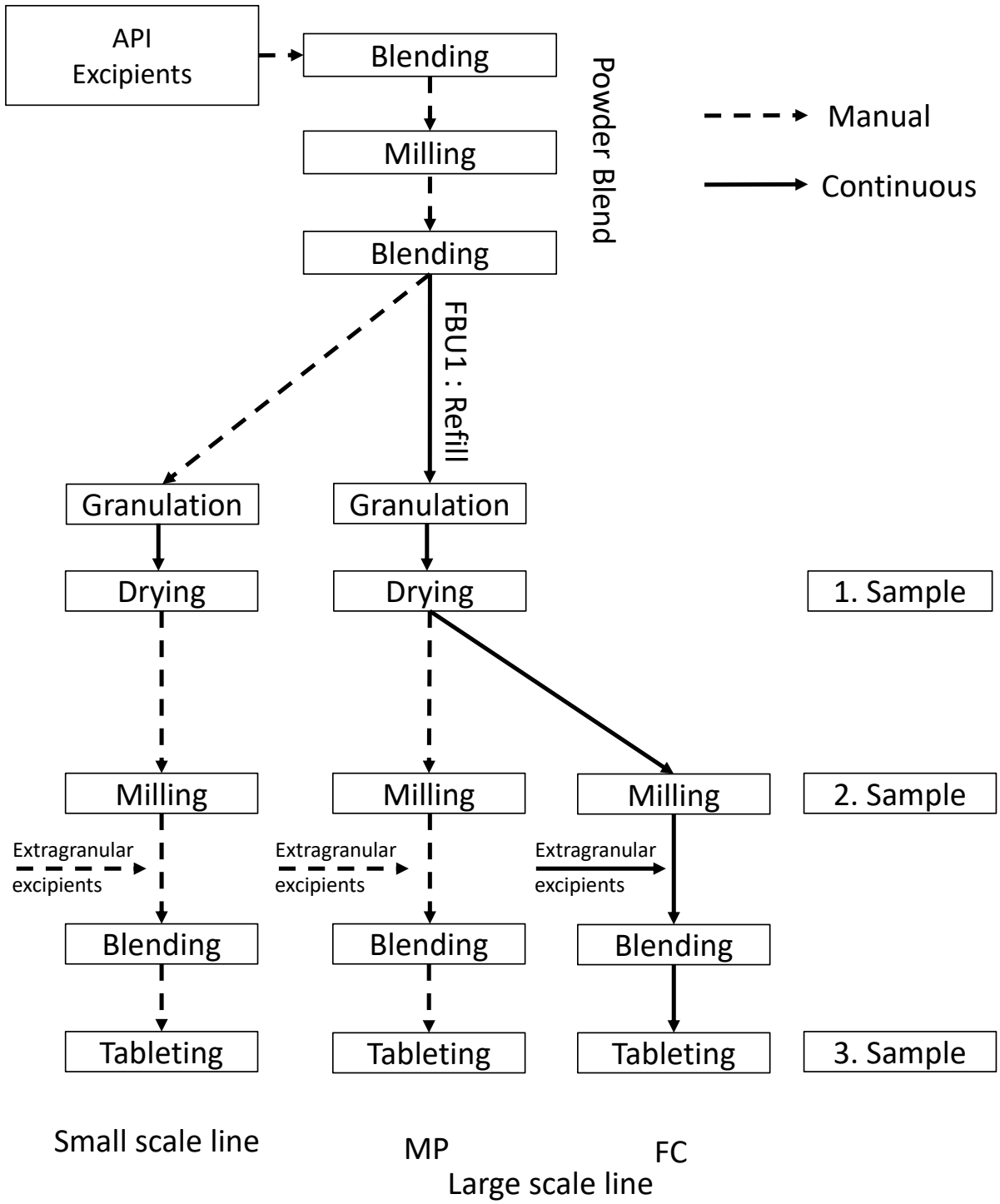

Figure 46 Overview for process flow during experiments on small scale and during manual processing (MP) mode and fully continuous (FC) mode on the large-scale line

7 References

[1] P. York, "The design of dosage forms", in *Aulton's Pharmaceutics the Design and Manufacture of Medicines*, 6th ed., Churchill Livingstone, London, 2013, 1–12.

[2] A. Fahr, "Voigt Pharmazeutische Technologie : Für Studium und Beruf", 11th ed. Deutscher Apotheker Verlag, Gerlingen, 2021. doi: 10.52777/9783769277487.

[3] L. L. Augsburger and S. W. Hoag, Eds., "Pharmaceutical Dosage Forms - Tablets", 3rd ed. CRC Press, Boca Raton, 2016. doi: 10.1201/b15115.

[4] Council of Europe, "European Pharmacopoeia", 10th ed. EDQM, Strasbourg, France, 2020.

[5] S. P. Chaudhari and P. S. Patil, "Pharmaceutical Excipients: A review", *Int J Adv Pharm Biol Chem* 2012, 21–34.

[6] M. Jivraj, L. G. Martini, and C. M. Thomson, "An overview of the different excipients useful for the direct compression of tablets", *Pharm. Sci. Technol. Today* 3, 2000, 58–63, doi: 10.1016/S1461-5347(99)00237-0.

[7] M. Sohail Arshad, S. Zafar, B. Yousef, Y. Alyassin, R. Ali, A. AlAsiri, M.-W. Chang, Z. Ahmad, A. Ali Elkordy, A. Faheem, and K. Pitt, "A review of emerging technologies enabling improved solid oral dosage form manufacturing and processing", *Adv. Drug Deliv. Rev.* 178, 2021, 113840, doi: 10.1016/j.addr.2021.113840.

[8] R. Shaikh, D. P. O'Brien, D. M. Croker, and G. M. Walker, "The development of a pharmaceutical oral solid dosage forms", in *Computer Aided Chemical Engineering*, 41, Elsevier, 2018, 27–65. doi: 10.1016/B978-0-444-63963-9.00002-6.

[9] G. L. Amidon, H. Lennernäs, V. P. Shah, and J. R. Crison, "A Theoretical Basis for a Biopharmaceutic Drug Classification: The Correlation of in Vitro Drug Product Dissolution and in Vivo Bioavailability", *Pharm. Res.* 12, 1995, 413–420, doi: 10.1023/A:1016212804288.

[10] M. Leane, K. Pitt, G. Reynolds, and The Manufacturing Classification System (MCS) Working Group, "A proposal for a drug product Manufacturing Classification System (MCS) for oral solid dosage forms", *Pharm. Dev. Technol.* 20, 2015, 12–21, doi: 10.3109/10837450.2014.954728.

[11] H. A. Lieberman, L. Lachman, and J. B. Schwartz, Eds., "Pharmaceutical dosage forms--tablets", 2nd ed., rev.Expanded. Dekker, New York, 1989.

[12] F. Stauffer, V. Vanhoorne, G. Pilcer, P.-F. Chavez, S. Rome, M. A. Schubert, L.

Aerts, and T. De Beer, "Raw material variability of an active pharmaceutical ingredient and its relevance for processability in secondary continuous pharmaceutical manufacturing", *Eur. J. Pharm. Biopharm.* 127, 2018, 92–103, doi: 10.1016/j.ejpb.2018.02.017.

[13] P. Kleinebudde, "Roll compaction/dry granulation: pharmaceutical applications", *Eur. J. Pharm. Biopharm.* 58, 2004, 317–326, doi: 10.1016/j.ejpb.2004.04.014.

[14] C. C. Sun and P. Kleinebudde, "Mini review: Mechanisms to the loss of tabletability by dry granulation", *Eur. J. Pharm. Biopharm.* 106, 2016, 9–14, doi: 10.1016/j.ejpb.2016.04.003.

[15] H. G. Kristensen and T. Schaefer, "Granulation: A Review on Pharmaceutical Wet-Granulation", *Drug Dev. Ind. Pharm.* 13, 1987, 803–872, doi: 10.3109/03639048709105217.

[16] A. Faure, P. York, and R. C. Rowe, "Process control and scale-up of pharmaceutical wet granulation processes: a review", *Eur. J. Pharm. Biopharm.* 52, 2001, 269–277, doi: 10.1016/S0939-6411(01)00184-9.

[17] E. Keleb, A. Vermeire, C. Vervaet, and J. P. Remon, "Twin screw granulation as a simple and efficient tool for continuous wet granulation", *Int. J. Pharm.* 273, 2004, 183–194, doi: 10.1016/j.ijpharm.2004.01.001.

[18] S. L. Lee, T. F. O'Connor, X. Yang, C. N. Cruz, S. Chatterjee, R. D. Madurawe, C. M. V. Moore, L. X. Yu, and J. Woodcock, "Modernizing Pharmaceutical Manufacturing: from Batch to Continuous Production", *J. Pharm. Innov.* 10, 2015, Art. 3, doi: 10.1007/s12247-015-9215-8.

[19] C. Vervaet and J. P. Remon, "Continuous granulation in the pharmaceutical industry", *Chem. Eng. Sci.* 60, 2005, 3949–3957, doi: 10.1016/j.ces.2005.02.028.

[20] H. Leuenberger, "New trends in the production of pharmaceutical granules: batch versus continuous processing", *Eur. J. Pharm. Biopharm.* 52, 2001, 289–296, doi: 10.1016/S0939-6411(01)00199-0.

[21] V. Vanhoorne and C. Vervaet, "Recent progress in continuous manufacturing of oral solid dosage forms", *Int. J. Pharm.* 579, 2020, 119194, doi: 10.1016/j.ijpharm.2020.119194.

[22] K. Matsunami, T. Miyano, H. Arai, H. Nakagawa, M. Hirao, and H. Sugiyama, "Decision Support Method for the Choice between Batch and Continuous Technologies in Solid Drug Product Manufacturing", *Ind. Eng. Chem. Res.* 57, 2018, 9798–9809, doi:

10.1021/acs.iecr.7b05230.

[23] K. Matsunami, S. Tanabe, H. Nakagawa, M. Hirao, and H. Sugiyama, "Economic Evaluation of Batch and Continuous Manufacturing Technologies for Solid Drug Products during Clinical Development", in *Computer Aided Chemical Engineering*, 44, Elsevier, 2018, 2131–2136. doi: 10.1016/B978-0-444-64241-7.50350-5.

[24] C. Badman, C. L. Cooney, A. Florence, K. Konstantinov, M. Krumme, S. Mascia, M. Nasr, and B. L. Trout, "Why We Need Continuous Pharmaceutical Manufacturing and How to Make It Happen", *J. Pharm. Sci.* 108, 2019, 3521–3523, doi: 10.1016/j.xphs.2019.07.016.

[25] S. D. Schaber, D. I. Gerogiorgis, R. Ramachandran, J. M. B. Evans, P. I. Barton, and B. L. Trout, "Economic Analysis of Integrated Continuous and Batch Pharmaceutical Manufacturing: A Case Study", *Ind. Eng. Chem. Res.* 50, 2011, 10083–10092, doi: 10.1021/ie2006752.

[26] C. V. Rossi, "A Comparative Investment Analysis of Batch Versus Continuous Pharmaceutical Manufacturing Technologies", *J. Pharm. Innov.* 17, 2022, 1373–1391, doi: 10.1007/s12247-021-09612-y.

[27] J. M. Juran, "Juran on quality by design: the new steps for planning quality into goods and services". Simon and Schuster, New York, 1992.

[28] International Council for Harmonisation of Technical Requirements for Pharmaceuticals for Human Use, "Pharmaceutical development Q8(R2)". Accessed: 2023. [Online]. Available: https://database.ich.org/sites/default/files/Q8%28R2%29%20Guideline.pdf

[29] International Council for Harmonisation of Technical Requirements for Pharmaceuticals for Human Use, "Quality Risk Management (Q9)". Accessed: 2023. [Online]. Available: https://database.ich.org/sites/default/files/ICH_Q9%28R1%29_Guideline_Step4_2023_0126_0.pdf

[30] International Council for Harmonisation of Technical Requirements for Pharmaceuticals for Human Use, "Pharmaceutical Quality Systems (Q10)". Accessed: 2023. [Online]. Available: https://database.ich.org/sites/default/files/Q10%20Guideline.pdf

[31] International Council for Harmonisation of Technical Requirements for Pharmaceuticals for Human Use, "Development and Manufacture of Drug Substance

(Q11)". Accessed: 2023. [Online]. Available: https://database.ich.org/sites/default/files/Q11_Q%26As_Q%26As.pdf

[32] S. Chatterjee, "FDA Perspective on Continuous Manufacturing", presented at the FPAC Annual Meeting, Baltimore, 2012, 34–42.

[33] J. Woodcock, "Modernizing pharmaceutical manufacturing–continuous manufacturing as a key enabler", in *Proceedings of the MIT-CMAC International Symposium on Continuous Manufacturing of Pharmaceuticals, Cambridge, MA, USA*, 2014.

[34] T. F. O'Connor, L. X. Yu, and S. L. Lee, "Emerging technology: A key enabler for modernizing pharmaceutical manufacturing and advancing product quality", *Int. J. Pharm.* 509, 2016, 492–498, doi: 10.1016/j.ijpharm.2016.05.058.

[35] M. M. Nasr, M. Krumme, Y. Matsuda, B. L. Trout, C. Badman, S. Mascia, C. L. Cooney, K. D. Jensen, A. Florence, C. Johnston, K. Konstantinov, and S. L. Lee, "Regulatory Perspectives on Continuous Pharmaceutical Manufacturing: Moving From Theory to Practice", *J. Pharm. Sci.* 106, 2017, 3199–3206, doi: 10.1016/j.xphs.2017.06.015.

[36] G. Allison, Y. T. Cain, C. Cooney, T. Garcia, T. G. Bizjak, O. Holte, N. Jagota, B. Komas, E. Korakianiti, D. Kourti, R. Madurawe, E. Morefield, F. Montgomery, M. Nasr, W. Randolph, J.-L. Robert, D. Rudd, and D. Zezza, "Regulatory and Quality Considerations for Continuous Manufacturing May 20–21, 2014 Continuous Manufacturing Symposium", *J. Pharm. Sci.* 104, 2015, 803–812, doi: 10.1002/jps.24324.

[37] International Council for Harmonisation of Technical Requirements for Pharmaceuticals for Human Use, "Continuous Manufacturing of Drug Substances and Drug Products (Q13)". Accessed: 2024. [Online]. Available: https://database.ich.org/sihttps://www.ema.europa.eu/en/documents/scientific-guideline/ich-guideline-q13-continuous-manufacturing-drug-substances-and-drug-products-step-5_en.pdf

[38] J. Markarian, "Breaking Through Barriers to Continuous Manufacturing", *Pharm. Technol.* 46, 2022, 16–20.

[39] E. J. Kim, J. H. Kim, M.-S. Kim, S. H. Jeong, and D. H. Choi, "Process Analytical Technology Tools for Monitoring Pharmaceutical Unit Operations: A Control Strategy for Continuous Process Verification", *Pharmaceutics* 13, 2021, 919, doi:

10.3390/pharmaceutics13060919.

[40] M. Fonteyne, J. Vercruysse, F. De Leersnyder, B. Van Snick, C. Vervaet, J. P. Remon, and T. De Beer, "Process Analytical Technology for continuous manufacturing of solid-dosage forms", *TrAC Trends Anal. Chem.* 67, 2015, 159–166, doi: 10.1016/j.trac.2015.01.011.

[41] P.-F. Chavez, F. Stauffer, F. Eeckman, N. Bostijn, D. Didion, C. Schaefer, H. Yang, Y. El Aalamat, X. Lories, M. Warman, B. Mathieu, and J. Mantanus, "Control strategy definition for a drug product continuous wet granulation process: Industrial case study", *Int. J. Pharm.* 624, 2022, 121970, doi: 10.1016/j.ijpharm.2022.121970.

[42] Y. Roggo, V. Pauli, M. Jelsch, L. Pellegatti, F. Elbaz, S. Ensslin, P. Kleinebudde, and M. Krumme, "Continuous manufacturing process monitoring of pharmaceutical solid dosage form: A case study", *J. Pharm. Biomed. Anal.* 2019, 112971, doi: 10.1016/j.jpba.2019.112971.

[43] L. Chablani, M. K. Taylor, A. Mehrotra, P. Rameas, and W. C. Stagner, "Inline Real-Time Near-Infrared Granule Moisture Measurements of a Continuous Granulation–Drying–Milling Process", *AAPS PharmSciTech* 12, 2011, 1050–1055, doi: 10.1208/s12249-011-9669-z.

[44] J. G. Rosas, P. Brush, B. Thompson, C. Miller, P. Overton, N. Tugby, D. Stoliarskaia, S. Hurley, M. Ramasamy, and S. L. Conway, "Implementation of a fully integrated CM direct compression and coating process at a commercial pharmaceutical facility – Part 2: PAT and RTD results for normal operational conditions batches", *Int. J. Pharm.* 636, 2023, 122814, doi: 10.1016/j.ijpharm.2023.122814.

[45] J. M. Vargas, S. Nielsen, V. Cárdenas, A. Gonzalez, E. Y. Aymat, E. Almodovar, G. Classe, Y. Colón, E. Sanchez, and R. J. Romañach, "Process analytical technology in continuous manufacturing of a commercial pharmaceutical product", *Int. J. Pharm.* 538, 2018, 167–178, doi: 10.1016/j.ijpharm.2018.01.003.

[46] M. Jelsch, Y. Roggo, P. Kleinebudde, and M. Krumme, "Model predictive control in pharmaceutical continuous manufacturing: A review from a user's perspective", *Eur. J. Pharm. Biopharm.* 159, 2021, 137–142, doi: 10.1016/j.ejpb.2021.01.003.

[47] C. M. V. Moore, "Regulatory Perspective on Real Time Release Testing (RTRT)", in *Proceedings of the AAPS Annual Meeting, Washington DC*, 2011, 32.

[48] P. Bawuah and J. A. Zeitler, "Advances in terahertz time-domain spectroscopy of pharmaceutical solids: A review", *TrAC Trends Anal. Chem.* 139, 2021, 116272, doi: 10.1016/j.trac.2021.116272.

[49] V. Kumar, M. K. Taylor, A. Mehrotra, and W. C. Stagner, "Real-Time Particle Size Analysis Using Focused Beam Reflectance Measurement as a Process Analytical Technology Tool for a Continuous Granulation–Drying–Milling Process", *AAPS PharmSciTech* 14, 2013, 523–530, doi: 10.1208/s12249-013-9934-4.

[50] W. Meng, A. D. Román-Ospino, S. S. Panikar, C. O'Callaghan, S. J. Gilliam, R. Ramachandran, and F. J. Muzzio, "Advanced process design and understanding of continuous twin-screw granulation via implementation of in-line process analytical technologies", *Adv. Powder Technol.* 30, 2019, 879–894, doi: 10.1016/j.apt.2019.01.017.

[51] M. Fonteyne, J. Arruabarrena, J. De Beer, M. Hellings, T. Van Den Kerkhof, A. Burggraeve, C. Vervaet, J. P. Remon, and T. De Beer, "NIR spectroscopic method for the in-line moisture assessment during drying in a six-segmented fluid bed dryer of a continuous tablet production line: Validation of quantifying abilities and uncertainty assessment", *J. Pharm. Biomed. Anal.* 100, 2014, 21–27, doi: 10.1016/j.jpba.2014.07.012.

[52] S. Mascia, P. L. Heider, H. Zhang, R. Lakerveld, B. Benyahia, P. I. Barton, R. D. Braatz, C. L. Cooney, J. M. B. Evans, T. F. Jamison, K. F. Jensen, A. S. Myerson, and B. L. Trout, "End-to-End Continuous Manufacturing of Pharmaceuticals: Integrated Synthesis, Purification, and Final Dosage Formation", *Angew. Chem.* 125, 2023, 12585–12589, doi: 10.1002/ange.201305429.

[53] L. Schenck, D. Erdemir, L. Saunders Gorka, J. M. Merritt, I. Marziano, R. Ho, M. Lee, J. Bullard, M. Boukerche, S. Ferguson, A. J. Florence, S. A. Khan, and C. C. Sun, "Recent Advances in Co-processed APIs and Proposals for Enabling Commercialization of These Transformative Technologies", *Mol. Pharm.* 17, 2020, 2232–2244, doi: 10.1021/acs.molpharmaceut.0c00198.

[54] B. Van Snick, J. Holman, V. Vanhoorne, A. Kumar, T. De Beer, J. P. Remon, and C. Vervaet, "Development of a continuous direct compression platform for low-dose drug products", *Int. J. Pharm.* 529, 2017, 329–346, doi: 10.1016/j.ijpharm.2017.07.003.

[55] O. N. Kavanagh, C. Wang, G. M. Walker, and C. C. Sun, "Modulation of the powder properties of lamotrigine by crystal forms", *Int. J. Pharm.* 595, 2021, 120274, doi: 10.1016/j.ijpharm.2021.120274.

[56] J. Rojas, I. Buckner, and V. Kumar, "Co-proccessed excipients with enhanced

direct compression functionality for improved tableting performance", *Drug Dev. Ind. Pharm.* 38, 2012, 1159–1170, doi: 10.3109/03639045.2011.645833.

[57] A. Schmidt, H. De Waard, P. Kleinebudde, and M. Krumme, "Continuous Single-Step Wet Granulation with Integrated in-Barrel-Drying", *Pharm. Res.* 35, 2018, 167, doi: 10.1007/s11095-018-2451-0.

[58] A. Domokos, B. Nagy, B. Szilágyi, G. Marosi, and Z. K. Nagy, "Integrated Continuous Pharmaceutical Technologies—A Review", *Org. Process Res. Dev.* 25, 2021, 721–739, doi: 10.1021/acs.oprd.0c00504.

[59] K. Kohlgrüber, "Co-rotating twin-screw extruder". Carl Hanser Verlag GmbH Co KG, Munich, 2012.

[60] N.-O. Lindberg, C. Tufvesson, and L. Olbjer, "Extrusion of an Effervescent Granulation with a Twin Screw Extruder, Baker Perkins MPF 50 D", *Drug Dev. Ind. Pharm.* 13, 1987, 1891–1913, doi: 10.3109/03639048709068698.

[61] R. Schroeder and K. Steffens, "A new system for continuous wet granulation", *Pharm. Ind.* 64, 2002, 283–288.

[62] T. C. Seem, N. A. Rowson, A. Ingram, Z. Huang, S. Yu, M. de Matas, I. Gabbott, and G. K. Reynolds, "Twin screw granulation - A literature review", *Powder Technol.* 276, 2015, 89–102, doi: 10.1016/j.powtec.2015.01.075.

[63] P. H. M. Janssen, S. S. Kulkarni, C. M. Torrecillas, F. Tegel, R. Weinekötter, B. Meir, and B. H. J. Dickhoff, "Effect of batch-to-batch variation of spray dried lactose on the performance of feeders", *Powder Technol.* 409, 2022, 117776, doi: 10.1016/j.powtec.2022.117776.

[64] R. Meier, M. Thommes, N. Rasenack, K.-P. Moll, M. Krumme, and P. Kleinebudde, "Granule size distributions after twin-screw granulation – Do not forget the feeding systems", *Eur. J. Pharm. Biopharm.* 106, 2016, 59–69, doi: 10.1016/j.ejpb.2016.05.011.

[65] W. E. Engisch and F. J. Muzzio, "Method for characterization of loss-in-weight feeder equipment", *Powder Technol.* 228, 2012, 395–403, doi: 10.1016/j.powtec.2012.05.058.

[66] W. E. Engisch and F. J. Muzzio, "Loss-in-Weight Feeding Trials Case Study: Pharmaceutical Formulation", *J. Pharm. Innov.* 10, 2015, 56–75, doi: 10.1007/s12247-014-9206-1.

[67] F. Stauffer, V. Vanhoorne, G. Pilcer, P.-F. Chavez, M. A. Schubert, C. Vervaet, and T. De Beer, "Managing active pharmaceutical ingredient raw material variability

during twin-screw blend feeding", *Eur. J. Pharm. Biopharm.* 135, 2019, 49–60, doi: 10.1016/j.ejpb.2018.12.012.

[68] W. Engisch and F. Muzzio, "Using Residence Time Distributions (RTDs) to Address the Traceability of Raw Materials in Continuous Pharmaceutical Manufacturing", *J. Pharm. Innov.* 11, 2016, 64–81, doi: 10.1007/s12247-015-9238-1.

[69] J. Hanson, "Control of a system of loss-in-weight feeders for drug product continuous manufacturing", *Powder Technol.* 331, 2018, 236–243, doi: 10.1016/j.powtec.2018.03.027.

[70] B. Van Snick, A. Kumar, M. Verstraeten, K. Pandelaere, J. Dhondt, G. Di Pretoro, T. De Beer, C. Vervaet, and V. Vanhoorne, "Impact of material properties and process variables on the residence time distribution in twin screw feeding equipment", *Int. J. Pharm.* 556, 2019, 200–216, doi: 10.1016/j.ijpharm.2018.11.076.

[71] T. Ervasti, H. Niinikoski, E. Mäki-Lohiluoma, H. Leppinen, J. Ketolainen, O. Korhonen, and S. Lakio, "The Comparison of Two Challenging Low Dose APIs in a Continuous Direct Compression Process", *Pharmaceutics* 12, 2020, 279, doi: 10.3390/pharmaceutics12030279.

[72] P. Toson and J. G. Khinast, "Particle-level residence time data in a twin-screw feeder", *Data Brief* 27, 2019, 104672, doi: 10.1016/j.dib.2019.104672.

[73] R. M. Dhenge, J. J. Cartwright, D. G. Doughty, M. J. Hounslow, and A. D. Salman, "Twin screw wet granulation: Effect of powder feed rate", *Adv. Powder Technol.* 22, 2011, 162–166, doi: 10.1016/j.apt.2010.09.004.

[74] J. Vercruysse, D. Córdoba Díaz, E. Peeters, M. Fonteyne, U. Delaet, I. Van Assche, T. De Beer, J. P. Remon, and C. Vervaet, "Continuous twin screw granulation: Influence of process variables on granule and tablet quality", *Eur. J. Pharm. Biopharm.* 82, 2012, 205–211, doi: 10.1016/j.ejpb.2012.05.010.

[75] R. Meier, K.-P. Moll, M. Krumme, and P. Kleinebudde, "Impact of fill-level in twin-screw granulation on critical quality attributes of granules and tablets", *Eur. J. Pharm. Biopharm.* 115, 2017, 102–112, doi: 10.1016/j.ejpb.2017.02.010.

[76] Pohl, Sebastian, "Transfer of twin-screw granulation processes and predictions of barrel fill", Düsseldorf, Heinrich Heine University, 2022.

[77] M. R. Thompson, "Twin screw granulation – review of current progress", *Drug Dev. Ind. Pharm.* 41, 2015, 1223–1231, doi: 10.3109/03639045.2014.983931.

[78] M. R. Thompson and J. Sun, "Wet Granulation in a Twin-Screw Extruder:

Implications of Screw Design", *J. Pharm. Sci.* 99, 2010, 2090–2103, doi: 10.1002/jps.21973.

[79] R. M. Dhenge, K. Washino, J. J. Cartwright, M. J. Hounslow, and A. D. Salman, "Twin screw granulation using conveying screws: Effects of viscosity of granulation liquids and flow of powders", *Powder Technol.* 238, 2013, 77–90, doi: 10.1016/j.powtec.2012.05.045.

[80] J. Menth, M. Maus, and K. G. Wagner, "Continuous twin screw granulation and fluid bed drying: A mechanistic scaling approach focusing optimal tablet properties", *Int. J. Pharm.* 586, 2020, 119509, doi: 10.1016/j.ijpharm.2020.119509.

[81] J. Li, S. U. Pradhan, and C. R. Wassgren, "Granule transformation in a twin screw granulator: Effects of conveying, kneading, and distributive mixing elements", *Powder Technol.* 346, 2019, 363–372, doi: 10.1016/j.powtec.2018.11.099.

[82] D. Djuric and P. Kleinebudde, "Impact of screw elements on continuous granulation with a twin-screw extruder", *J. Pharm. Sci.* 97, 2008, 4934–4942, doi: 10.1002/jps.21339.

[83] J. Vercruysse, A. Burggraeve, M. Fonteyne, P. Cappuyns, U. Delaet, I. Van Assche, T. De Beer, J. P. Remon, and C. Vervaet, "Impact of screw configuration on the particle size distribution of granules produced by twin screw granulation", *Int. J. Pharm.* 479, 2015, 171–180, doi: 10.1016/j.ijpharm.2014.12.071.

[84] C. Portier, K. Pandelaere, U. Delaet, T. Vigh, G. Di Pretoro, T. De Beer, C. Vervaet, and V. Vanhoorne, "Continuous twin screw granulation: a complex interplay between formulation properties, process settings and screw design", *Int. J. Pharm.* 2020, 119004, doi: 10.1016/j.ijpharm.2019.119004.

[85] A. S. El Hagrasy and J. D. Litster, "Granulation rate processes in the kneading elements of a twin screw granulator", *AIChE J.* 59, 2013, 4100–4115, doi: 10.1002/aic.14180.

[86] R. Sayin, A. S. El Hagrasy, and J. D. Litster, "Distributive mixing elements: Towards improved granule attributes from a twin screw granulation process", *Chem. Eng. Sci.* 125, 2015, 165–175, doi: 10.1016/j.ces.2014.06.040.

[87] D. Djuric, B. Vanmelkebeke, P. Kleinebudde, J. Remon, and C. Vervaet, "Comparison of two twin-screw extruders for continuous granulation", *Eur. J. Pharm. Biopharm.* 71, 2009, 155–160, doi: 10.1016/j.ejpb.2008.06.033.

[88] A. Kumar, J. Vercruysse, M. Toiviainen, P.-E. Panouillot, M. Juuti, V. Vanhoorne, C. Vervaet, J. P. Remon, K. V. Gernaey, T. De Beer, and I. Nopens,

"Mixing and transport during pharmaceutical twin-screw wet granulation: Experimental analysis via chemical imaging", *Eur. J. Pharm. Biopharm.* 87, 2014, 279–289, doi: 10.1016/j.ejpb.2014.04.004.

[89] H. Liu, S. C. Galbraith, B. Ricart, C. Stanton, B. Smith-Goettler, L. Verdi, T. O'Connor, S. Lee, and S. Yoon, "Optimization of critical quality attributes in continuous twin-screw wet granulation via design space validated with pilot scale experimental data", *Int. J. Pharm.* 525, 2017, 249–263, doi: 10.1016/j.ijpharm.2017.04.055.

[90] A. Kumar, G. M. Ganjyal, D. D. Jones, and M. A. Hanna, "Digital image processing for measurement of residence time distribution in a laboratory extruder", *J. Food Eng.* 75, 2006, 237–244, doi: 10.1016/j.jfoodeng.2005.04.025.

[91] J. Vercruysse, M. Toiviainen, M. Fonteyne, N. Helkimo, J. Ketolainen, M. Juuti, U. Delaet, I. Van Assche, J. P. Remon, C. Vervaet, and T. De Beer, "Visualization and understanding of the granulation liquid mixing and distribution during continuous twin screw granulation using NIR chemical imaging", *Eur. J. Pharm. Biopharm.* 86, 2014, 383–392, doi: 10.1016/j.ejpb.2013.10.012.

[92] A. S. El Hagrasy, J. R. Hennenkamp, M. D. Burke, J. J. Cartwright, and J. D. Litster, "Twin screw wet granulation: Influence of formulation parameters on granule properties and growth behavior", *Powder Technol.* 238, 2013, 108–115, doi: 10.1016/j.powtec.2012.04.035.

[93] R. M. Dhenge, J. J. Cartwright, M. J. Hounslow, and A. D. Salman, "Twin screw wet granulation: Effects of properties of granulation liquid", *Powder Technol.* 229, 2012, 126–136, doi: 10.1016/j.powtec.2012.06.019.

[94] L. Vandevivere, P. Denduyver, C. Portier, O. Häusler, T. De Beer, C. Vervaet, and V. Vanhoorne, "Influence of binder attributes on binder effectiveness in a continuous twin screw wet granulation process via wet and dry binder addition", *Int. J. Pharm.* 585, 2020, 119466, doi: 10.1016/j.ijpharm.2020.119466.

[95] L. Vandevivere, E. Van Wijmeersch, O. Häusler, T. De Beer, C. Vervaet, and V. Vanhoorne, "The effect of screw configuration and formulation variables on liquid requirements and granule quality in a continuous twin screw wet granulation process", *J. Drug Deliv. Sci. Technol.* 68, 2022, 103042, doi: 10.1016/j.jddst.2021.103042.

[96] R. M. Dhenge, J. J. Cartwright, M. J. Hounslow, and A. D. Salman, "Twin screw granulation: Steps in granule growth", *Int. J. Pharm.* 438, 2012, 20–32, doi: 10.1016/j.ijpharm.2012.08.049.

[97] A. Ito and P. Kleinebudde, "Influence of granulation temperature on particle size distribution of granules in twin-screw granulation (TSG)", *Pharm. Dev. Technol.* 24, 2019, 874–882, doi: 10.1080/10837450.2019.1615089.

[98] V. Vanhoorne, B. Vanbillemont, J. Vercruysse, F. De Leersnyder, P. Gomes, T. D. Beer, J. P. Remon, and C. Vervaet, "Development of a controlled release formulation by continuous twin screw granulation: Influence of process and formulation parameters", *Int. J. Pharm.* 505, 2016, doi: 10.1016/j.ijpharm.2016.03.058.

[99] Y. Liu, M. R. Thompson, K. P. O'Donnell, and N. S. Grasman, "Effect of temperature on the wetting behavior of hydroxypropyl methylcellulose in a twin-screw granulator", *Powder Technol.* 302, 2016, 63–74, doi: 10.1016/j.powtec.2016.08.032.

[100] A. K. Meena, D. Desai, and A. T. M. Serajuddin, "Development and Optimization of a Wet Granulation Process at Elevated Temperature for a Poorly Compactible Drug Using Twin Screw Extruder for Continuous Manufacturing", *J. Pharm. Sci.* 106, 2017, 589–600, doi: 10.1016/j.xphs.2016.10.020.

[101] A. Haser, N. Kittikunakorn, E. Dippold, J. C. DiNunzio, and W. Blincoe, "Continuous Twin-Screw wet granulation process with In-Barrel drying and NIR setup for Real-Time Moisture Monitoring", *Int. J. Pharm.* 630, 2023, 122377, doi: 10.1016/j.ijpharm.2022.122377.

[102] K. Kiricenko and P. Kleinebudde, "Drying behavior of a horizontal vibrated fluidized bed dryer for continuous manufacturing", *Pharm. Dev. Technol.* 2023, 1–12, doi: 10.1080/10837450.2023.2205932.

[103] R. Meier, D. Emanuele, and P. Harbaum, "Important elements in continuous granule drying processes: Experiences from lab and production scale.", *TechnoPharm* 10, 2020, 92–101.

[104] R. Meier and D. Emanuele, "Kontinuierliche Feuchtgranulierung und Wirbelschichttrocknung: Experimentelle Untersuchung eines neuartigen, revolutionaeren Systems", *TechnoPharm* 8, 2018, 124.

[105] G. Fülöp, A. Domokos, D. Galata, E. Szabó, M. Gyürkés, B. Szabó, A. Farkas, L. Madarász, B. Démuth, T. Lendér, T. Nagy, D. Kovács-Kiss, F. Van Der Gucht, G. Marosi, and Z. K. Nagy, "Integrated twin-screw wet granulation, continuous vibrational fluid drying and milling: A fully continuous powder to granule line", *Int. J. Pharm.* 594, 2021, 120126, doi: 10.1016/j.ijpharm.2020.120126.

[106] J. N. Michaels, L. Farber, G. S. Wong, K. Hapgood, S. J. Heidel, J. Farabaugh, J.-H. Chou, and G. I. Tardos, "Steady states in granulation of pharmaceutical powders

with application to scale-up", *Powder Technol.* 189, 2009, 295–303, doi: 10.1016/j.powtec.2008.04.028.

[107] K. M. Kyttä, S. Lakio, H. Wikström, A. Sulemanji, M. Fransson, J. Ketolainen, and P. Tajarobi, "Comparison between twin-screw and high-shear granulation - The effect of filler and active pharmaceutical ingredient on the granule and tablet properties", *Powder Technol.* 376, 2020, 187–198, doi: 10.1016/j.powtec.2020.08.030.

[108] A. Megarry, A. Taylor, A. Gholami, H. Wikström, and P. Tajarobi, "Twin-screw granulation and high-shear granulation: The influence of mannitol grade on granule and tablet properties", *Int. J. Pharm.* 590, 2020, 119890, doi: 10.1016/j.ijpharm.2020.119890.

[109] Y. Miyazaki, V. Lenhart, and P. Kleinebudde, "Switch of tablet manufacturing from high shear granulation to twin-screw granulation using quality by design approach", *Int. J. Pharm.* 579, 2020, 119139, doi: 10.1016/j.ijpharm.2020.119139.

[110] P. Beer, D. Wilson, Z. Huang, and M. De Matas, "Transfer from High-Shear Batch to Continuous Twin Screw Wet Granulation: A Case Study in Understanding the Relationship Between Process Parameters and Product Quality Attributes", *J. Pharm. Sci.* 103, 2014, 3075–3082, doi: 10.1002/jps.24078.

[111] K. T. Lee, A. Ingram, and N. A. Rowson, "Comparison of granule properties produced using Twin Screw Extruder and High Shear Mixer: A step towards understanding the mechanism of twin screw wet granulation", *Powder Technol.* 238, 2013, 91–98, doi: 10.1016/j.powtec.2012.05.031.

[112] E. I. Keleb, A. Vermeire, C. Vervaet, and J. P. Remon, "Extrusion Granulation and High Shear Granulation of Different Grades of Lactose and Highly Dosed Drugs: A Comparative Study", *Drug Dev. Ind. Pharm.* 30, 2004, 679–691, doi: 10.1081/DDC-120039338.

[113] J. G. Osorio, R. Sayin, A. V. Kalbag, J. D. Litster, L. Martinez-Marcos, D. A. Lamprou, and G. W. Halbert, "Scaling of continuous twin screw wet granulation", *AIChE J.* 63, 2017, 921–932, doi: 10.1002/aic.15459.

[114] B. Liu, J. Wang, J. Zeng, L. Zhao, Y. Wang, Y. Feng, and R. Du, "A review of high shear wet granulation for better process understanding, control and product development", *Powder Technol.* 381, 2021, 204–223, doi: 10.1016/j.powtec.2020.11.051.

[115] G. I. Tardos, K. P. Hapgood, O. O. Ipadeola, and J. N. Michaels, "Stress

measurements in high-shear granulators using calibrated “test” particles: application to scale-up", *Powder Technol.* 140, 2004, 217–227, doi: 10.1016/j.powtec.2004.01.015.

[116] J. Tao, P. Pandey, D. S. Bindra, J. Z. Gao, and A. S. Narang, "Evaluating Scale-Up Rules of a High-Shear Wet Granulation Process", *J. Pharm. Sci.* 104, 2015, 2323–2333, doi: 10.1002/jps.24504.

[117] G. Horsthuis, J. Vanlaarhoven, R. Vanrooij, and H. Vromans, "Studies on upscaling parameters of the Gral high shear granulation process", *Int. J. Pharm.* 92, 1993, 143–150, doi: 10.1016/0378-5173(93)90273-I.

[118] J. D. Litster, K. P. Hapgood, J. N. Michaels, A. Sims, M. Roberts, and S. K. Kameneni, "Scale-up of mixer granulators for effective liquid distribution", *Powder Technol.* 124, 2002, 272–280, doi: 10.1016/S0032-5910(02)00023-2.

[119] A. Hassanpour, C. C. Kwan, B. H. Ng, N. Rahmanian, Y. L. Ding, S. J. Antony, X. D. Jia, and M. Ghadiri, "Effect of granulation scale-up on the strength of granules", *Powder Technol.* 189, 2009, 304–312, doi: 10.1016/j.powtec.2008.04.023.

[120] A. Faure, I. M. Grimsey, R. C. Rowe, P. York, and M. J. Cliff, "Applicability of a scale-up methodology for wet granulation processes in Collette Gral high shear mixer-granulators", *Eur. J. Pharm. Sci.* 8, 1999, 85–93, doi: 10.1016/S0928-0987(98)00063-3.

[121] H. Leuenberger, B. Luy, and J. Studer, "New development in the control of a moist agglomeration and pelletization process", *STP Pharma* 6, 1990, 303–309.

[122] H. Leuenberger, M. Puchkov, E. Krausbauer, and G. Betz, "Manufacturing pharmaceutical granules: Is the granulation end-point a myth?", *Powder Technol.* 189, 2009, 141–148, doi: 10.1016/j.powtec.2008.04.005.

[123] A. Kumar, K. V. Gernaey, T. D. Beer, and I. Nopens, "Model-based analysis of high shear wet granulation from batch to continuous processes in pharmaceutical production – A critical review", *Eur. J. Pharm. Biopharm.* 85, 2013, 814–832, doi: 10.1016/j.ejpb.2013.09.013.

[124] K. Kolter, M. Karl, A. Gryczke, and B. Ludwigshafen am Rhein, "Hot-melt extrusion with BASF pharma polymers: extrusion compendium". BASF, 2012.

[125] M. Franke, T. Riedel, R. Meier, C. Schmidt, and P. Kleinebudde, "Comparison of scale-up strategies in twin-screw wet granulation", *Int. J. Pharm.* 2023, 123052, doi: 10.1016/j.ijpharm.2023.123052.

[126] S. Bandari, D. Nyavanandi, V. R. Kallakunta, K. Y. Janga, S. Sarabu, A.

Butreddy, and M. A. Repka, "Continuous twin screw granulation – An advanced alternative granulation technology for use in the pharmaceutical industry", *Int. J. Pharm.* 580, 2020, 119215, doi: 10.1016/j.ijpharm.2020.119215.

[127] R. M. Dhenge, R. S. Fyles, J. J. Cartwright, D. G. Doughty, M. J. Hounslow, and A. D. Salman, "Twin screw wet granulation: Granule properties", *Chem. Eng. J.* 164, 2010, 322–329, doi: 10.1016/j.cej.2010.05.023.

[128] K.-M. Hwang, C.-H. Cho, S.-D. Yoo, K.-I. Cha, and E.-S. Park, "Continuous twin screw granulation: Impact of the starting material properties and various process parameters", *Powder Technol.* 356, 2019, 847–857, doi: 10.1016/j.powtec.2019.08.062.

[129] R. Sayin, L. Martinez-Marcos, J. G. Osorio, P. Cruise, I. Jones, G. W. Halbert, D. A. Lamprou, and J. D. Litster, "Investigation of an 11 mm diameter twin screw granulator: Screw element performance and in-line monitoring via image analysis", *Int. J. Pharm.* 496, 2015, 24–32, doi: 10.1016/j.ijpharm.2015.09.024.

[130] A. Kumar, J. Dhondt, J. Vercruysse, F. De Leersnyder, V. Vanhoorne, C. Vervaet, J. P. Remon, K. V. Gernaey, T. De Beer, and I. Nopens, "Development of a process map: A step towards a regime map for steady-state high shear wet twin screw granulation", *Powder Technol.* 300, 2016, 73–82, doi: 10.1016/j.powtec.2015.11.067.

[131] B. Van Melkebeke, C. Vervaet, and J. P. Remon, "Validation of a continuous granulation process using a twin-screw extruder", *Int. J. Pharm.* 356, 2008, 224–230, doi: 10.1016/j.ijpharm.2008.01.012.

[132] C. Portier, K. Pandelaere, U. Delaet, T. Vigh, A. Kumar, G. Di Pretoro, T. De Beer, C. Vervaet, and V. Vanhoorne, "Continuous twin screw granulation: Influence of process and formulation variables on granule quality attributes of model formulations", *Int. J. Pharm.* 576, 2020, 118981, doi: 10.1016/j.ijpharm.2019.118981.

[133] M. F. Saleh, R. M. Dhenge, J. J. Cartwright, M. J. Hounslow, and A. D. Salman, "Twin screw wet granulation: Effect of process and formulation variables on powder caking during production", *Int. J. Pharm.* 496, 2015, 571–582, doi: 10.1016/j.ijpharm.2015.10.069.

[134] S. Lute, R. Dhenge, and A. Salman, "Twin Screw Granulation: An Investigation of the Effect of Barrel Fill Level", *Pharmaceutics* 10, 2018, 67, doi: 10.3390/pharmaceutics10020067.

[135] A. Kumar, J. Vercruysse, V. Vanhoorne, M. Toiviainen, P.-E. Panouillot, M.

Juuti, C. Vervaet, J. P. Remon, K. V. Gernaey, T. D. Beer, and I. Nopens, "Conceptual framework for model-based analysis of residence time distribution in twin-screw granulation", *Eur. J. Pharm. Sci.* 71, 2015, 25–34, doi: 10.1016/j.ejps.2015.02.004.

[136] "MODDE® 12 User Guide". Accessed: 2023. [Online]. Available: https://www.sartorius.com/download/544636/modde-12-user-guide-en-b-00090-sartorius-data.pdf

[137] T. Köhler and H. Schubert, "Influence of the Particle Size Distribution on the flow behaviour of fine powders", *Part. Part. Syst. Charact.* 8, 1991, 101–104, doi: 10.1002/ppsc.19910080119.

[138] S. M. Iveson, J. D. Litster, K. Hapgood, and B. J. Ennis, "Nucleation, growth and breakage phenomena in agitated wet granulation processes: a review", *Powder Technol.* 117, 2001, Art. 1–2, doi: 10.1016/S0032-5910(01)00313-8.

[139] S. V. Lute, R. M. Dhenge, M. J. Hounslow, and A. D. Salman, "Twin screw granulation: Understanding the mechanism of granule formation along the barrel length", *Chem. Eng. Res. Des.* 110, 2016, 43–53, doi: 10.1016/j.cherd.2016.03.008.

[140] L. G. Wang, S. U. Pradhan, C. Wassgren, D. Barrasso, D. Slade, and J. D. Litster, "A breakage kernel for use in population balance modelling of twin screw granulation", *Powder Technol.* 363, 2020, 525–540, doi: 10.1016/j.powtec.2020.01.024.

[141] L. G. Wang, J. P. Morrissey, D. Barrasso, D. Slade, S. Clifford, G. Reynolds, J. Y. Ooi, and J. D. Litster, "Model driven design for twin screw granulation using mechanistic-based population balance model", *Int. J. Pharm.* 607, 2021, 120939, doi: 10.1016/j.ijpharm.2021.120939.

[142] R. Meier, K.-P. Moll, M. Krumme, and P. Kleinebudde, "Simplified, High Drug-Loaded Formulations Containing Hydrochlorothiazide for Twin-Screw Granulation", *Chem. Ing. Tech.* 89, 2017, 1025–1033, doi: 10.1002/cite.201600134.

[143] D. Djuric and P. Kleinebudde, "Continuous granulation with a twin-screw extruder: Impact of material throughput", *Pharm. Dev. Technol.* 15, 2010, 518–525, doi: 10.3109/10837450903397578.

[144] R. M. Dhenge, R. S. Fyles, J. J. Cartwright, D. G. Doughty, M. J. Hounslow, and A. D. Salman, "Twin screw wet granulation: Granule properties", *Chem. Eng. J.* 164, 2010, doi: 10.1016/j.cej.2010.05.023.

[145] L. J. Gorringe, G. S. Kee, M. F. Saleh, N. H. Fa, and R. G. Elkes, "Use of the channel fill level in defining a design space for twin screw wet granulation", *Int. J.*

Pharm. 519, 2017, 165–177, doi: 10.1016/j.ijpharm.2017.01.029.

[146] N. A. M. Tamimi and P. Ellis, "Drug Development: From Concept to Marketing!", *Nephron Clin. Pract.* 113, 2009, 125–131, doi: 10.1159/000232592.

[147] G. I. Taylor, "Diffusion and Mass Transport in Tubes", *Proc. Phys. Soc. Sect. B* 67, 1954, 857–869, doi: 10.1088/0370-1301/67/12/301.

[148] L. Kotamarthy and R. Ramachandran, "Mechanistic understanding of the effects of process and design parameters on the mixing dynamics in continuous twin-screw granulation", *Powder Technol.* 390, 2021, 73–85, doi: 10.1016/j.powtec.2021.05.071.

[149] E. Reitz, H. Podhaisky, D. Ely, and M. Thommes, "Residence time modeling of hot melt extrusion processes", *Eur. J. Pharm. Biopharm.* 85, 2013, Art. 3, doi: 10.1016/j.ejpb.2013.07.019.

[150] A. C. Shah and A. R. Mlodozeniec, "Mechanism of Surface Lubrication: Influence of Duration of Lubricant-Excipient Mixing on Processing Characteristics of Powders and Properties of Compressed Tablets", *J. Pharm. Sci.* 66, 1977, 1377–1382, doi: 10.1002/jps.2600661006.

[151] J.-I. Kikuta and N. Kitamori, "Effect of Mixing Time on the Lubricating Properties of Magnesium Stearate and the Final Characteristics of the Compressed Tablets", *Drug Dev. Ind. Pharm.* 20, 1994, 343–355, doi: 10.3109/03639049409050187.

[152] V. Mazel and P. Tchoreloff, "Lamination of Pharmaceutical Tablets: Classification and Influence of Process Parameters", *J. Pharm. Sci.* 111, 2022, doi: 10.1016/j.xphs.2021.10.025.

[153] M. Franke, T. Riedel, R. Meier, C. Schmidt, and P. Kleinebudde, "Scale-up in Twin-screw wet granulation: Impact of formulation properties", *Pharm. Dev. Technol.* 28, 2023, 948–961, doi: 10.1080/10837450.2023.2276791.

[154] N. Willecke, A. Szepes, M. Wunderlich, J. P. Remon, C. Vervaet, and T. De Beer, "A novel approach to support formulation design on twin screw wet granulation technology: Understanding the impact of overarching excipient properties on drug product quality attributes", *Int. J. Pharm.* 545, 2018, 128–143, doi: 10.1016/j.ijpharm.2018.04.017.

[155] R. Meier, M. Thommes, N. Rasenack, M. Krumme, K.-P. Moll, and P. Kleinebudde, "Simplified formulations with high drug loads for continuous twin-screw granulation", *Int. J. Pharm.* 496, 2015, 12–23, doi: 10.1016/j.ijpharm.2015.05.060.

[156] M. R. Thompson and K. P. O'Donnell, "“Rolling” phenomenon in twin screw

granulation with controlled-release excipients", *Drug Dev. Ind. Pharm.* 41, 2015, 482–492, doi: 10.3109/03639045.2013.879723.

[157] A. W. Jenike, "Storage and flow of solids", Bulletin 123, Engineering Experiment Station, University of Utah, 1964. doi: 10.2172/5240257.

[158] T. Kojima and J. A. Elliott, "Effect of silica nanoparticles on the bulk flow properties of fine cohesive powders", *Chem. Eng. Sci.* 101, 2013, 315–328, doi: 10.1016/j.ces.2013.06.056.

[159] S. Yu, G. K. Reynolds, Z. Huang, M. De Matas, and A. D. Salman, "Granulation of increasingly hydrophobic formulations using a twin screw granulator", *Int. J. Pharm.* 475, 2014, 82–96, doi: 10.1016/j.ijpharm.2014.08.015.

[160] H. Li, M. R. Thompson, and K. P. O'Donnell, "Examining drug hydrophobicity in continuous wet granulation within a twin screw extruder", *Int. J. Pharm.* 496, 2015, 3–11, doi: 10.1016/j.ijpharm.2015.07.070.

[161] A. N. Chandran, S. S. Rao, and Y. B. G. Varma, "Fluidized bed drying of solids", *AIChE J.* 36, 1990, 29–38, doi: 10.1002/aic.690360106.

[162] B. Kozanoglu, J. Martinez, S. Alvarez, J. A. Guerrero-Beltrán, and J. Welti-Chanes, "Influence of Particle Size on Vacuum–Fluidized Bed Drying", *Dry. Technol.* 30, 2012, 138–145, doi: 10.1080/07373937.2011.628427.

[163] C. Portier, C. De Vriendt, T. Vigh, G. Di Pretoro, T. De Beer, C. Vervaet, and V. Vanhoorne, "Continuous twin screw granulation: Robustness of lactose/MCC-based formulations", *Int. J. Pharm.* 588, 2020, 119756, doi: 10.1016/j.ijpharm.2020.119756.

[164] S. Lakio, P. Tajarobi, H. Wikström, M. Fransson, J. Arnehed, T. Ervasti, S.-P. Simonaho, J. Ketolainen, S. Folestad, and S. Abrahmsén-Alami, "Achieving a robust drug release from extended release tablets using an integrated continuous mixing and direct compression line", *Int. J. Pharm.* 511, 2016, 659–668, doi: 10.1016/j.ijpharm.2016.07.052.

[165] J. Siepmann, K. Podual, M. Sriwongjanya, N. A. Peppas, and R. Bodmeier, "A New Model Describing the Swelling and Drug Release Kinetics from Hydroxypropyl Methylcellulose Tablets", *J. Pharm. Sci.* 88, 1999, 65–72, doi: 10.1021/js9802291.

[166] A. Vanarase, R. Aslam, S. Oka, and F. Muzzio, "Effects of mill design and process parameters in milling dry extrudates", *Powder Technol.* 278, 2015, 84–93, doi: 10.1016/j.powtec.2015.02.021.

[167] J. J. A. M. Verheezen, K. Van Der Voort Maarschalk, F. Faassen, and H. Vromans, "Milling of agglomerates in an impact mill", *Int. J. Pharm.* 278, 2004, 165–

172, doi: 10.1016/j.ijpharm.2004.03.006.

[168] L. Schenck and R. Plank, "Impact milling of pharmaceutical agglomerates in the wet and dry states", *Int. J. Pharm.* 348, 2008, 18–26, doi: 10.1016/j.ijpharm.2007.07.029.

[169] L. Kotamarthy, N. Metta, and R. Ramachandran, "Understanding the Effect of Granulation and Milling Process Parameters on the Quality Attributes of Milled Granules", *Processes* 8, 2020, 683, doi: 10.3390/pr8060683.

[170] J. J. Motzi and N. R. Anderson, "The Quantitative Evaluation of a Granulation Milling Process II. Effect of Ouput Screen Size, Mill Speed and Impeller Shape", *Drug Dev. Ind. Pharm.* 10, 1984, 713–728, doi: 10.3109/03639048409040779.

[171] A. Mckenna and D. F. Mccafferty, "Effect of particle size on the compaction mechanism and tensile strength of tablets", *J. Pharm. Pharmacol.* 34, 2011, 347–351, doi: 10.1111/j.2042-7158.1982.tb04727.x.

[172] G. Ragnarsson and J. Sjögren, "Force-displacement measurements in tableting", *J. Pharm. Pharmacol.* 37, 2011, 145–150, doi: 10.1111/j.2042-7158.1985.tb05029.x.

[173] C. Sun and M. W. Himmelspach, "Reduced tabletability of roller compacted granules as a result of granule size enlargement", *J. Pharm. Sci.* 95, 2006, 200–206, doi: 10.1002/jps.20531.

[174] E. Shotton and D. Ganderton, "The Strength of Compressed Tablets", *J. Pharm. Pharmacol.* 13, 1961, 144T-152T, doi: 10.1111/j.2042-7158.1961.tb10506.x.

[175] C. E. Ruegger and M. Çelick, "The Effect of Compression and Decompression Speed on the Mechanical Strength of Compacts", *Pharm. Dev. Technol.* 5, 2000, 485–494, doi: 10.1081/PDT-100102032.

[176] R. Ishino, H. Yoshino, Y. Hirakawa, and K. Noda, "Influence of tabletting speed on compactibility and compressibility of two direct compressible powders under high speed compression.", *Chem. Pharm. Bull. (Tokyo)* 38 7, 1990, 1987–92.

[177] C. K. Tye, C. Sun, and G. E. Amidon, "Evaluation of the effects of tableting speed on the relationships between compaction pressure, tablet tensile strength, and tablet solid fraction", *J. Pharm. Sci.* 94, 2005, 465–472, doi: 10.1002/jps.20262.

[178] G. Alderborn and C. Ahlneck, "Moisture adsorption and tabletting. III. Effect on tablet strenght-post compaction storage time profiles", *Int. J. Pharm.* 73, 1991, 249–258, doi: 10.1016/0378-5173(91)90417-M.

[179] M. Eriksson and G. Alderborn, "Mechanisms for post-compaction changes in tensile strength of sodium chloride compacts prepared from particles of different dimensions", *Int. J. Pharm.* 109, 1994, 59–72, doi: 10.1016/0378-5173(94)90121-X.

[180] C. Ahlneck and G. Alderborn, "Moisture adsorption and tabletting. I. Effect on volume reduction properties and tablet strength for some crystalline materials", *Int. J. Pharm.* 54, 1989, 131–141, doi: 10.1016/0378-5173(89)90332-3.

[181] A. Hartung, M. Knoell, U. Schmidt, and P. Langguth, "Role of continuous moisture profile monitoring by inline NIR spectroscopy during fluid bed granulation of an Enalapril formulation", *Drug Dev. Ind. Pharm.* 37, 2011, 274–280, doi: 10.3109/03639045.2010.509725.

[182] I. P. Gabbott, F. Al Husban, and G. K. Reynolds, "The combined effect of wet granulation process parameters and dried granule moisture content on tablet quality attributes", *Eur. J. Pharm. Biopharm.* 106, 2016, 70–78, doi: 10.1016/j.ejpb.2016.03.022.

[183] O.-R. Arndt and P. Kleinebudde, "Roll Compaction and Tableting of High Loaded Metformin Formulations Using Efficient Binders", *AAPS PharmSciTech* 19, 2018, 2068–2076, doi: 10.1208/s12249-018-1012-5.

[184] N. O. Sierra-Vega, A. Román-Ospino, J. Scicolone, F. J. Muzzio, R. J. Romañach, and R. Méndez, "Assessment of blend uniformity in a continuous tablet manufacturing process", *Int. J. Pharm.* 560, 2019, 322–333, doi: 10.1016/j.ijpharm.2019.01.073.

[185] A. U. Vanarase, M. Alcalà, J. I. Jerez Rozo, F. J. Muzzio, and R. J. Romañach, "Real-time monitoring of drug concentration in a continuous powder mixing process using NIR spectroscopy", *Chem. Eng. Sci.* 65, 2010, 5728–5733, doi: 10.1016/j.ces.2010.01.036.

[186] A. S. El Hagrasy, P. Cruise, I. Jones, and J. D. Litster, "In-line Size Monitoring of a Twin Screw Granulation Process Using High-Speed Imaging", *J. Pharm. Innov.* 8, 2013, 90–98, doi: 10.1007/s12247-013-9149-y.

[187] A. Kumar, J. Dhondt, F. De Leersnyder, J. Vercruysse, V. Vanhoorne, C. Vervaet, J. P. Remon, K. V. Gernaey, T. De Beer, and I. Nopens, "Evaluation of an in-line particle imaging tool for monitoring twin-screw granulation performance", *Powder Technol.* 285, 2015, 80–87, doi: 10.1016/j.powtec.2015.05.031.

[188] K. T. Lee, A. Ingram, and N. A. Rowson, "Twin screw wet granulation: The study of a continuous twin screw granulator using Positron Emission Particle Tracking

(PEPT) technique", *Eur. J. Pharm. Biopharm.* 81, 2012, 666–673, doi: 10.1016/j.ejpb.2012.04.011.

[189] A. Kumar, M. Alakarjula, V. Vanhoorne, M. Toiviainen, F. De Leersnyder, J. Vercruysse, M. Juuti, J. Ketolainen, C. Vervaet, J. P. Remon, K. V. Gernaey, T. De Beer, and I. Nopens, "Linking granulation performance with residence time and granulation liquid distributions in twin-screw granulation: An experimental investigation", *Eur. J. Pharm. Sci.* 90, 2016, 25–37, doi: 10.1016/j.ejps.2015.12.021.

[190] A. U. Vanarase, M. Järvinen, J. Paaso, and F. J. Muzzio, "Development of a methodology to estimate error in the on-line measurements of blend uniformity in a continuous powder mixing process", *Powder Technol.* 241, 2013, 263–271, doi: 10.1016/j.powtec.2013.02.012.

[191] L. Martínez, A. Peinado, L. Liesum, and G. Betz, "Use of near-infrared spectroscopy to quantify drug content on a continuous blending process: Influence of mass flow and rotation speed variations", *Eur. J. Pharm. Biopharm.* 84, 2013, 606–615, doi: 10.1016/j.ejpb.2013.01.016.

[192] Y. Roggo, M. Jelsch, P. Heger, S. Ensslin, and M. Krumme, "Deep learning for continuous manufacturing of pharmaceutical solid dosage form", *Eur. J. Pharm. Biopharm.* 153, 2020, 95–105, doi: 10.1016/j.ejpb.2020.06.002.

[193] B. Nagy, D. L. Galata, A. Farkas, and Z. K. Nagy, "Application of Artificial Neural Networks in the Process Analytical Technology of Pharmaceutical Manufacturing—a Review", *AAPS J.* 24, 2022, 74, doi: 10.1208/s12248-022-00706-0.

[194] H. Lou, B. Lian, and M. J. Hageman, "Applications of Machine Learning in Solid Oral Dosage Form Development", *J. Pharm. Sci.* 110, 2021, 3150–3165, doi: 10.1016/j.xphs.2021.04.013.

[195] D. Markl, M. Warman, M. Dumarey, E.-L. Bergman, S. Folestad, Z. Shi, L. F. Manley, D. J. Goodwin, and J. A. Zeitler, "Review of real-time release testing of pharmaceutical tablets: State-of-the art, challenges and future perspective", *Int. J. Pharm.* 582, 2020, 119353, doi: 10.1016/j.ijpharm.2020.119353.

[196] S. Sacher, J. Poms, J. Rehrl, and J. G. Khinast, "PAT implementation for advanced process control in solid dosage manufacturing – A practical guide", *Int. J. Pharm.* 613, 2022, 121408, doi: 10.1016/j.ijpharm.2021.121408.

[197] E. Reitz, H. Podhaisky, D. Ely, and M. Thommes, "Residence time modeling of hot melt extrusion processes", *Eur. J. Pharm. Biopharm.* 85, 2013, 1200–1205, doi:

10.1016/j.ejpb.2013.07.019.

[198] J. Vercruysse, U. Delaet, I. Van Assche, P. Cappuyns, F. Arata, G. Caporicci, T. De Beer, J. P. Remon, and C. Vervaet, "Stability and repeatability of a continuous twin screw granulation and drying system", *Eur. J. Pharm. Biopharm.* 85, 2013, 1031–1038, doi: 10.1016/j.ejpb.2013.05.002.

[199] Y. Rubner, C. Tomasi, and L. J. Guibas, "The Earth Mover's Distance as a Metric for Image Retrieval", *International Journal of Computer Vision* 2000, 99–121.

[200] Zhenghua Yu and G. Herman, "On the Earth Mover'S Distance as a Histogram Similarity Metric for Image Retrieval", in *2005 IEEE International Conference on Multimedia and Expo*, IEEE, Amsterdam, The Netherlands, 2005, 686–689. doi: 10.1109/ICME.2005.1521516.

[201] Qi Zhao, Zhi Yang, and Hai Tao, "Differential Earth Mover's Distance with Its Applications to Visual Tracking", *IEEE Trans. Pattern Anal. Mach. Intell.* 32, 2010, 274–287, doi: 10.1109/TPAMI.2008.299.

[202] M. Hu, X. Jiang, M. Absar, S. Choi, D. Kozak, M. Shen, Y.-T. Weng, L. Zhao, and R. Lionberger, "Equivalence Testing of Complex Particle Size Distribution Profiles Based on Earth Mover's Distance", *AAPS J.* 20, 2018, Art. 3, doi: 10.1208/s12248-018-0212-y.

[203] "The Earth Mover's Distance". The University of Edinburgh, School of Informatics. Accessed: 2023. [Online]. Available: https://homepages.inf.ed.ac.uk/rbf/CVonline/LOCAL_COPIES/RUBNER/emd.htm

[204] Granutools, "Granutools | GranuPack", Granutools. Accessed: 2023. [Online]. Available: https://www.granutools.com/en/granupack

[205] M. J. Adams, M. A. Mullier, and J. P. K. Seville, "Agglomerate strength measurement using a uniaxial confined compression test", *Powder Technol.* 78, 1994, 5–13, doi: 10.1016/0032-5910(93)02777-8.

[206] O.-R. Arndt, R. Baggio, A. K. Adam, J. Harting, E. Franceschinis, and P. Kleinebudde, "Impact of Different Dry and Wet Granulation Techniques on Granule and Tablet Properties: A Comparative Study", *J. Pharm. Sci.* 107, 2018, 3143–3152, doi: 10.1016/j.xphs.2018.09.006.

[207] J. T. Fell and J. M. Newton, "Determination of Tablet Strength by the Diametral-Compression Test", *J. Pharm. Sci.* 59, 1970, 688–691, doi: 10.1002/jps.2600590523.

[208] K. G. Pitt, J. M. Newton, and P. Stanley, "Tensile fracture of doubly-convex cylindrical discs under diametral loading", *J. Mater. Sci.* 23, 1988, 2723–2728, doi:

10.1007/BF00547442.

Danksagung

An erster Stelle möchte ich mich bei meinem Doktorvater, Prof. Dr. Dr. Peter Kleinebudde, bedanken, der mich mit seiner ehrlichen und offenen Art herzlich in seinen Arbeitskreis aufgenommen hat und trotz der großen Entfernung und seiner zahlreichen anderen Doktoranden und Aufgaben als Dekan immer noch Zeit für mich und meine Angelegenheiten gefunden hat. Seine professionelle Betreuung und die allzeit konstruktiven Ratschläge haben mir sehr bei meiner Arbeit geholfen und sie enorm bereichert (und unterdessen hoffentlich endlich auch dazu geführt hat, dass mir nun nicht mehr der Unterschied zwischen *sieving* und *milling* verloren geht). Vielen Dank - ich hätte mir keinen besseren Betreuer wünschen können!

Weiterhin danke ich Prof. Dr. Jörg Breitkreutz für seine praktischen Ratschläge und Beiträge während meiner Doktorandenvorträge in Düsseldorf, sowie die Bereitschaft trotz seiner zahlreichen anderen Aufgaben und Verantwortlichkeiten, als Zweitgutachter für meine Thesis zu fungieren.

Der Inhalt dieser Dissertation entstand aus einer Kooperation zwischen der Firma Merck Healthcare KGaA, der L.B. Bohle Maschinen und Verfahren GmbH und der Heinrich-Heine-Universität in Düsseldorf. Entsprechend möchte ich mich auch noch einmal bei allen Kooperationspartnern explizit für die umfangreiche Unterstützung bei der Durchführung meiner Arbeit bedanken. Durch die vielen Kooperationspartner hatte ich außerdem das große Vergnügen mit zahlreichen wundervollen und brillanten Menschen aus allen drei Institutionen zusammenzuarbeiten und auszutauschen und möchte mich bei all den Menschen bedanken, die mich über die Zeit meiner Promotion begleitet und mir geholfen haben! Ich hoffe trotz der Fülle an Menschen, niemanden vergessen zu haben.

Dr. Carsten Schmidt danke ich für die Gelegenheit, die er mir bei Merck mit der Aufnahme in die Kooperation gegeben hat, für die zahlreichen fachlichen Diskussionen und seine Ratschläge und Ideen.

Dr. Thomas Riedel, der als mein direkter Betreuer bei Merck jederzeit ein offenes Ohr für mich hatte, mir hilfreiche Tipps für meine Dissertation gegeben hat und trotz zweier Neuzugänge und einer weiteren Doktorandin immer noch Zeit dafür gefunden hat meine Arbeiten zu korrigieren und sich meiner Probleme anzunehmen.

Ein weiterer besonderer Dank gilt allen Doktoranden aus unserer Doktorandenrunde bei Merck in Darmstadt. Insbesondere gilt hier ein riesiges Dankeschön an Dr. Melinda Kern, die mir nicht nur organisatorisch bei Merck mit vielen Anliegen geholfen hat, sondern auch noch ihre Freizeit für das Korrekturlesen dieser Arbeit geopfert hat und

dabei geduldig auch das hundertste Leerzeichen zwischen Zahl und Einheit korrigiert hat. Aber auch die Möglichkeit sich mit anderen „Leidensgefährten“ beim gemeinsamen Doktorandenfrühstück, beim gemeinsamen Abendessen oder auch einfach mal im Flur oder Technikum auszutauschen, hat essenziell zur erfolgreichen Entstehung dieser Arbeit beigetragen. Neben der moralischen und freundschaftlichen Unterstützung außerdem explizit noch einmal ein großen Dankeschön an Nicole Hofmann, Dr. Katharina Krollik und Florian Johann, die mir außerdem mit allen Fragen rund um das Labor bei DDI geholfen haben, Lena Mareczek für den kontinuierlichen Austausch an der Styl‘One, Lara Rosenberger für deine gelassene Art und die hilfreichen Tipps im Umgang mit der Steuererklärung, sowie Nadine Gottschalk, die mir auch bei jeglichen organisatorischen Fragen sowohl bei Merck als auch der Uni Düsseldorf jederzeit helfen konnte.

Ich danke Dr. Stefan Busche, Ingo Kaminski und Franziska Kuhn, denen so schnell im Umgang mit CM und PAT niemand etwas vormacht und die mich sowohl fachlich als auch persönlich an vielen Punkten unterstützt und zu meiner persönlichen Entwicklung enorm beigetragen haben.

Meinen Bürokollegen Michael Back und Alexander Sander danke ich für die tolle Zeit und die zahlreichen privaten Anekdoten, die hilfreichen Ratschläge, die auf jahrzehntelanger Erfahrung fußen und die Geduld im Umgang mit meiner Pfandflaschensammlung auf dem Schreibtisch.

Zusätzlich aus unserer Mittagsrunde danke ich Matthias Schäfer, Marcel Krüger und Dr. Raphael Wiedey für den Erfahrungsaustausch, die vielen unterhaltsamen Mittagsrunden und auch für die Einweisungen an verschiedene Geräte im Technikum.

Der „Digital Guild“ und ihren Mitgliedern danke ich für die Aufnahme und die tolle Möglichkeit sich hier zu verschiedenen Themengebieten weiterzubilden, um gemeinsam die Digitalisierung voranzubringen! Hier möchte ich gerne noch Dr. Andreas Lehmann und Dr. Johannes Wittmann hervorheben, die mich mit Rat und Tat zum Thema Statistik und in der Fehlersuche meiner Skripte unterstützt haben.

Dr. Caroline Riehl, Martina Jeschke und Oliver Laukhardt danke ich für die Einweisung in verschiedene Gerätschaften in Technikum und Labor und die schnelle Hilfe bei jeglichen Rückfragen zu den Methoden und Geräten.

Bei Karina Schmutzler (unterdessen Merck Life Sciences) danke ich für die schnelle Unterstützung bei der Suche nach alternativen Freisetzungstestern, während unsere

in Reparatur waren und für die unkomplizierte Möglichkeit meine Tabletten dann in ihrer Abteilung zu vermessen.
Von der Firma Bohle möchte ich mich insbesondere bei Dr. Robin Meier bedanken für seine offene Art, die vielen hilfreichen Ratschläge und die Möglichkeit meine Versuche in Ennigerloh durchzuführen – ich habe mich bei euch immer sehr willkommen gefühlt und konnte mit jedem relevanten Thema zu dir kommen, um mir hilfreichen Input zu holen!
Außerdem möchte ich mich bei Dr. Andreas Altmayer bedanken, der den kontinuierlichen Trockner bei Bohle versteht, wie kein Zweiter und jederzeit geholfen hat, wenn ich mit Fragen zu ihm kam.
Wer mit L.B. Bohle und der QbCon zu tun hat, wird an Daniel Emanuele, Philipp Harbaum und Andreas Teske nicht vorbeikommen. Ich danke Euch vielmals für die vielen Stunden, die Ihr damit verbracht habt, Geräte für mich vorzubereiten und Versuche mit mir durchzuführen, um dann im Anschluss gemeinsam wieder alles aufwändig zu reinigen. Außerdem ein großer Dank für eure offen herzliche rheinländische Art und dafür, dass ich unterdessen schon, wenn ich nur kurz an euch denke, schon Philipp & Daniel ein lautes „OHHHHHH MARCELLO-MARCELLO-MARCELLO“ singen höre.
Zudem möchte ich Daniel Bexte für die viele Unterstützung zu allen Fragen rund um das Technikum und den Umgang mit verschiedenen Gerätschaften, sowie Charlotte Ribeiro Maier, die mich immer, wenn es gerade zeitlich knapp wurde mit zwei helfenden Händen unterstützt hat, danken!
Jochen Stauvermann danke ich für die schnelle und unkomplizierte Hilfe bei allen kurzfristigen elektrischen Anpassungen oder Herausforderungen, Damian Mika und Martin Kehrt für die schnelle Hilfe bei allen softwareseitigen Änderungen und Rückfragen.
An der Heinrich-Heine Universität gilt mein Dank außerdem allen Doktoranden, die mich herzlich in ihre Gruppe aufgenommen haben und die während der jährlichen Vorträge immer sehr konstruktive und hilfreiche Rückmeldungen gegeben haben. Ganz besonders möchte ich hier noch kurz folgende Menschen hervorheben:
Dr. Tobias Auel und Jennifer Kuck für die Einweisung in verschiedene Gerätschaften in Düsseldorf, Stefan Klinken für die Unterstützung bei der Skripterstellung zur Bestimmung der EMD und Katharina Kiricenko und Christofer Mentrup dafür, dass Sie

jederzeit für mich erreichbar waren, wenn ich auf dem kurzen Wege etwas Organisatorisches in Düsseldorf klären wollte.
Zuletzt möchte ich mich noch ganz besonders bei den Menschen bedanken, die mich hauptsächlich persönlich in dem Projekt „Promotion“ begleitet haben:
Meiner erweiterten Familie und meinen Freunden, die oft und viel zu meiner Motivation und meinem persönlichen Glück beigetragen haben und insbesondere dem aktuell wichtigsten Menschen in meinem Leben: Meiner Partnerin Elisabeth, die mit mir in den letzten 10 Jahren durch alle Höhen und Tiefen gemeinsam durchgegangen ist und die mich immer wieder dazu bringt über mich hinauszuwachsen. Vielen Dank für deine Geduld, deine Liebe und deine bedingungslose Unterstützung!

Eidesstattliche Erklärung

Ich versichere an Eides Statt, dass die Dissertation von mir selbständig und ohne unzulässige fremde Hilfe unter Beachtung der „Grundsätze zur Sicherung guter wissenschaftlicher Praxis an der Heinrich-Heine-Universität Düsseldorf“ erstellt worden ist.

Marcel Franke